Salt Bayou Watershed Restoration Efficacy Research - Phase I Final Research Report (August 2016 to May 2018 Activity).

Subrecipient: Lamar University (GLO Contact: 18-092-000-A603)

Author and PI: Matthew P. Hoch, Ph.D.

Date: 30 July 2019

Executive Summary:

This research addresses two major goals of the Salt Bayou Watershed Restoration Plan, namely modification of freshwater-seawater hydrodynamics to reduce salinity and the restoration of marsh using dredge materials as a sediment subsidy. Installation of a baffle structure at the Keith Lake Fish Pass (KLFP) in summer 2016 is intended to reduce seawater input to Salt Bayou Estuary, which encompassing Shell, Johnson, and Keith Lakes. Inverted siphons currently under construction in summer 2019 are designed to increase freshwater inflow. The resulting change in salinity may have impacts on the fundamental biogeochemical parameters and communities of plankton and microphytobenthos of this shallow well mixed estuary. The first aim of this research (Tasks 1-2) was to establish a biological oceanographic baseline of the estuary. Marsh vegetation in the watershed has experienced progressive die-back in recent decades in areas of increased inundation. Application of dredge material, as terrace structures or broadly dispersed to elevate the sediment surface, has been used to reduce open water areas and restore marsh vegetation health. However, an understanding of sediment geochemistry and microbiology that contributes to both the die-back and restoration of vegetation and ecological function is limited. The second aim of this research (Tasks 3-4) was to compare marsh sediment geochemistry and microbial communities at natural marsh sites of contrasting ecological stability and at restored sites.

Tasks 1-2 involved a thorough monitoring of physicochemical conditions and communities of planktonic and microphytobenthic microbes (algal and heterotrophic prokaryotes) in the Salt Bayou Estuary using continuous monitoring by water quality sonde and quarterly sampling of six survey sites from summer 2016 to summer 2018. The original contract was for analysis of just four quarterly samplings (fall 2017 to summer 2018), but a budget reallocation has permitted analyses of planktonic and microphytobenthic communities from prior quarterly samplings of the estuary supported through Lamar University resources since summer 2016. Reported here are all physicochemical parameters and analyses of microbial communities, based on photopigments and targeted metagenomic sequencing of small subunit (SSU) rDNA, for nine consecutive quarterly samplings of Salt Bayou Estuary. Likewise, continuous monitoring of temperature, salinity and depth had been performed between Keith and Johnson Lakes since summer 2016, and these data are included in this report in addition to that for the contracted period.

Continuous monitoring of water quality parameters was performed at a site between Johnson and Keith Lakes (KJ-site) and within the Keith Lake Fish Pass (KLFP) during the contract period (Feb 2018 to May 2019). Since summer 2016 an YSI 600SL series sonde was deployed at the KJ-site to measure depth, salinity and water temperature at the KJ-site. Since February 2018 a new, CMP purchased, YSI EXO2 sonde was deployed at the KJ-site to measure depth, salinity, temperature, chlorophyll, cyanobacterial phycoerythrin,

fluorescent dissolved organic matter (fDOM), pH, dissolved oxygen, redox and turbidity. At the Slat Bayou Watershed Restoration Workgroup in January 2018, it was decided to begin additional continuous monitoring at the KJFP using the YSI 600SL sonde. Salinity is the most important parameter measured by both sondes, because the target for hydrological restoration effectiveness is a salinity < 10 psu for 80 % of the year.

Common parameters (salinity, temperature and depth) at the KJ and KLFP sites correlated strongly, with mean (± SD) salinity at the JK-site of 7.75 ± 5.6 psu and 8.10 ± 5.58 psu at the KLFP-site for 389 days from Feb 2018 to May 2019. The target for hydrological restoration effectiveness is a salinity < 10 psu for 80 % of the year. The sites were under the target salinity of 10 psu for 75 % and 71 % of readings for this period at these respective sites. Prior to this contractual study period, the mean (± SD) salinity at the KJ-site from Aug 2016 through Dec 2017 was 10.15 ± 4.1 psu, and only 47% of readings were below 10 psu. Cumulative rainfall during each study period and the mean monthly cumulative rainfalls were similar, but the precipitation was dominated by episodic events, including Hurricane Harvey in the earlier study period. The strong correlations for these common parameters between these two sonde sites, and lack any significant difference of any monthly mean, suggests that just one of these sites is needed future monitoring efforts.

Additional biogeochemical and biological parameters have been measured by YSI EXO2 sonde from Feb-Nov 2018 at the KJ-sonde site. A significant correlation between phycoerythrin (PE) and chlorophyll (Chl*a*) suggests that cyanobacteria are important component of the phytoplankton community throughout the year at this site, although to a lesser extent in fall when the monthly mean PE:Chl*a* ratio was lowest. This conclusion is corroborated by the predominance of zeaxanthin content, an important cyanobacterial photopigment and *Synechococcus* SSU rDNA sequences in the phytoplankton community. Turbidity was most variable and appears to correlate with windy periods, and resulting wind-wave resuspension of benthic sediments. Dissolved oxygen (DO) concentration correlated inversely with that of water temperature, as to be expected. With the exception of storm events, for most of the year the diel pattern in DO correlated with pH, as expected due to net photosynthesis and respiration. Fluorescent dissolved organic carbon (fDOM) inversely correlated with salinity, suggesting a terrestrial source in freshwater runoff.

Nine quarterly surveys throughout Salt Bayou estuary (six sites) have been performed, beginning in Aug 2016 and ending in Aug 2018. Surveys include sonde profiles of water quality physicochemical parameters (water temperature, DO, salinity, pH), water samples were analyzed for dissolved inorganic nitrogen (DIN species), soluble reactive phosphates (SRP), dissolved organic carbon (DOC), total suspended sediment (TSS), photopigment concentrations, and microbial community relative abundance based on SSU rDNA analysis. Sediment cores were also collected and the surface microphytobenthic layer

(top 2 mm) was analyzed for both photopigment concentrations and microbial community relative abundances. Phytoplankton biomass, as chlorophyll *a*, did not follow distinct seasonality. Frequency of precipitation and wind patterns appear to have major influences on primary producer biomass in this ecosystem by causing salinity variation and turbidity events throughout the year. Based on low (< 11) DIN:SRP ratios, the primary production is assumed to be N-limited based on Redfield ratio (N:P = 16), yet phytoplankton biomass correlates with SRP. Some of the major phytoplankton classed determined by CHEMTAX modelling of photopigment concentrations also correlated positively with SRP and inversely with salinity.

Cyanobacteria, Diatoms and Chlorophytes dominated the phytoplankton communities; whereas Diatoms dominate the microphytobenthos. There is a potential for *Karenia* red tide blooms, given the ample gyroxanthin content in the phytoplankton, yet *Karenia* was extremely rare based on SSU rDNA analysis. Salinity was important in partly controlling phytoplankton community structure, but not so much for the microphytobenthos community. There appeared to be a pattern of greater chlorophyll content in microphytobenthose at shallow upper estuary site-1 and the deeper site-6 in proximity to the KLFP; these sites had often had the greatest amount of surface solar irradiance reaching the bottom. Phytoplankton chlorophyll positively correlated with bacterial abundance.

Freshwater runoff contributes to higher DOC concentrations and reduced salinity, and both parameters were important drivers of bacterioplankton biomass, as well as their community structure. Dominant orders of bacterioplankton were typical of other estuaries with both marine and riverine taxa. Like with microphytobenthos, the surface benthic prokaryote community structure was more resilient to salinity and other changes in water column conditions than bacterioplankton. With increased freshwater into the estuary from marshes north of the intercoastal waterway (ICWW), via inverted siphons being constructed summer 2019, there is expected to be a change in phytoplankton and bacterioplankton community structure. Although hypoxic conditions were rarely detected in this shallow well mixes estuary, the increased flow could supply more nutrients and DOC to the estuary and drive greater microbial biomass and respiratory demand of dissolved oxygen. Monitoring near the siphons outfall, or even in the retention waters north of the ICWW, is recommended in future monitoring of inverted siphon inflow impacts.

Task 3-4 focused on coastal marsh health and effectiveness of beneficial use of dredge material restoration in the Salt Bayou Watershed, specifically in TPWD, J.D. Murphree Wildlife Management Area. Nine sites were surveyed quarterly in 2018. Three sites were chosen for their obvious inundated condition (standing water at mean high tide conditions), fragments vegetation dominated by *Spartina patens* (clumps of grasses with “potholes” of open water), and dead vegetation during the summer growing season; named “unstable” sites. Three sites of

healthy *Spartina patens* growth, mostly contiguous consolidated sediment surface, and not inundated at mean high tide; named "stable" sites. Three sites had experienced BUDM restoration, either as terraces of more contiguous coverage; named "restored sites".

Task 3 focused on assessing the porewater and sediment geochemistry. The inundated sediments at unstable marsh sites, presumably due to subsidence and low sediment accretion rates, had sediment geochemistry and microbiology most distinct from the BUDM restored sites. These unstable sites had sediments that were mostly water, most negative redox, high organic content, and high porewater concentrations of sulfide and ammonium relative to stable and restored sites. There was little seasonal variation in these conditions at unstable, in contrast stable and restored sites. The R1 site was restored more recently (2011) than the other two restored sites (2005). R1 had some geochemical conditions more aligned with stable sites, and based on molecular analysis of this site in 2011 pre-restoration and post-restoration in 2018 there had not been as much change as compared to other restored sites. The S3 site had some geochemical conditions more similar to unstable sites and the other two stable sites, suggesting it is in decline. The phytotoxic sulfide level in porewaters at unstable sites was not correlated to salinity, which has been a target parameter for Salt Bayou Watershed restoration. Iron biogeochemistry needs consideration in understand levels of sulfide accumulation, as sites in fall 2018 with greatest dissolved iron in porewaters had no detectable sulfide.

Task 4 focused on sediment microbial community composition for all prokaryotes based on small subunit (SSU) rDNA sequencing and specifically sulfate reducing prokaryotes based on the dissimilatory sulfite reductase subunit B gene (*dsr*B) sequencing. Both the total microbial community and specifically SRB communities revealed dominant taxa that were distinct in their relative abundance for specific site types. Unstable sites had microbial communities with greater proportions of hydrogenotrophic methanogenic orders of Archaea than SRB orders, in contrast to stable and restored sites. Methanogen dominance at unstable sites may have implications for the ability of marsh in this state of health to sequester and store carbon versus carbon loss, including that in the form of methane. The specific genus of SRB, *Desulfatiglans* and the Chloroflexis order Dehalococcoidales both dominated at unstable sites and both can use organohalide reduction metabolism based on H_2. The presence of hydrogenotrophic taxa dominating at unstable site suggests a vigorous fermentative community of cellulose decomposers supplying H_2. Other SRB genera were distinctly greater in abundance at restored sites. There were also IRB genera whose abundance was distinct among site types, specifically *Geobacter* at restored sites. Conclusively, microbial community analysis based on DNA is effective in distinguishing differences in marsh health at natural sites and restored sites, but RNA based analysis contributed little additional information.

Future monitoring of natural marsh health and restoration effectiveness, should continue using most methods and parameters, but there is some rationale for changing sampling frequency and number of sites. When seasonal differences were observed in geochemical and microbiology parameters they most distinguishable between winter, a period of vegetation senescence and net decomposition, and summer during peak vegetation growth. More sites of different states of health and periods post restoration are needed to increase the rigor of assessment for prioritizing areas in most need of restoration, as well as, restoration effectiveness.

Sampling during two versus all four seasons would allow future monitoring at double the sites at similar cost. Additional costs savings would be to keep microbial community analysis based on DNA, as RNA analysis appears to be an unnecessary added cost. Sediment porewater dissolved iron needs to be added to the routine analyses. Collectively, vegetation health, marsh elevation change, and biogeochemistry, makes for the best assessment of marsh health and restoration effectiveness. To be able to correlate all parameters across the landscape, and model specific parameters assessable to the landscape, i.e. broader geospatial scales, may allow modeling and mapping other parameters. High resolution remote sensing of vegetation health and elevation, coupled with ground truthing and sediment biogeochemistry (geochemistry and microbiology) measurements is proposed for mapping a comprehensive marsh health index.

Task 5 involved Lamar University (LU) students in educational outreach, research training and conference presentations, and outreach to stakeholders of Salt Bayou Watershed. In total, twenty-three Lamar University undergraduate students in the BS Biology and BS Environmental Science majors, and one MS Biology graduate student have been involved in collecting and analyzing samples since the start of Salt Bayou Watershed Restoration monitoring research and educational outreach. Prior to contract start, students held workshops with Central High School, Beaumont Independent School District, and made visits to Lamar State Community College and Lee College environmental science classes. During the contracts a number of circumstances limited the educational outreach activities to five community and LU campus events. Educational outreach activities focused on topics of watershed function, plankton ecology, and molecular microbial ecology approaches relevant to the project research. Student research posters of the preliminary results were also available to discuss at these outreach events. Another component of the educational task was training students in research methods in the field and laboratory, which was extensive, and bringing data analyses to the level of conference poster presentations. A total of six different research posters were presented at peer reviewed conferences, including the Gulf Estuary Research Society meeting in November 2017. Outreach to local Salt Bayou Watershed stakeholders was also performed twice, once at project initiation in January 2018 and at contract end in July 2019. This was in the form of presentations by the PI to the Salt Bayou Watershed Restoration Workgroup, chaired by Dr. Michael Reszutek (TPWD, J.D. Murphree W. M. A.) and including stakeholders from U.S.FWS, TPDW Fisheries Unit, Ducks Unlimited, Jefferson County Government, and Community. Presentation are include in the deliverables for this task.

Table of Contents:

Task 1 - Monitor Physicochemical and Biological Conditions of Johnson and Keith Lakes:

Continuous Monitoring Salinity, Water Temperature, and Depth:

Continuous monitoring of depth, water temperature and salinity was monitored at a site between Keith and Johnson Lakes (KJ-sonde) since Aug 2016, and additional continuous monitoring was begun at the Keith Lake Fish Pass (KLFP-sonde) in Feb 2018. Monitoring ended at both sonde sites in May 2019. There is a gap in the KJ-sonde data set between Dec 2017 and Feb 2018 due to deployment problem with the YSI 600SL sonde initially used at the KJ-sonde site, the purchase of a new YSI EXO2 sonde on this contract, and redesign of the mooring at that site. Since mid-Feb 2018 the YSI EXO2 sonde was deployed at the KJ-sonde site and the YSI 600SL sonde at the KLFP-sonde site at mean depth of about 0.8 m depth in about 1.2 m deep water columns (Fig. 1; Table 1). Deployment periods ranged between 28-43

Table 1. Mean (± SD) sampling site location and bottom depth for six quarterly survey sites (n = 9) and for the KJ (n = 856) and KLFP (n = 434) sonde sites.

Site	Latitude (°N)	Longitude (°W)	Depth (m)
1	29.78805 (± 0.00038)	-94.01136 (± 0.00050)	0.49 (± 0.10)
2	29.75979 (± 0.00110)	-94.02286 (± 0.00054)	0.98 (± 0.13)
3	29.74657 (± 0.00054)	-94.00102 (± 0.00059)	0.95 (± 0.09)
4	29.75437 (± 0.00047)	-93.97145 (± 0.00046)	1.27 (± 0.16)
5	29.76021 (± 0.00049)	-93.94401 (± 0.00084)	1.04 (± 0.10)
6	29.76920 (± 0.00089)	-93.95160 (± 0.00164)	1.51 (± 0.81)
KJ-sonde	29.75640	-93.97276	1.15 (± 0.19)
KLFP-sonde	29.77043	-93.95013	1.20 (± 0.15)

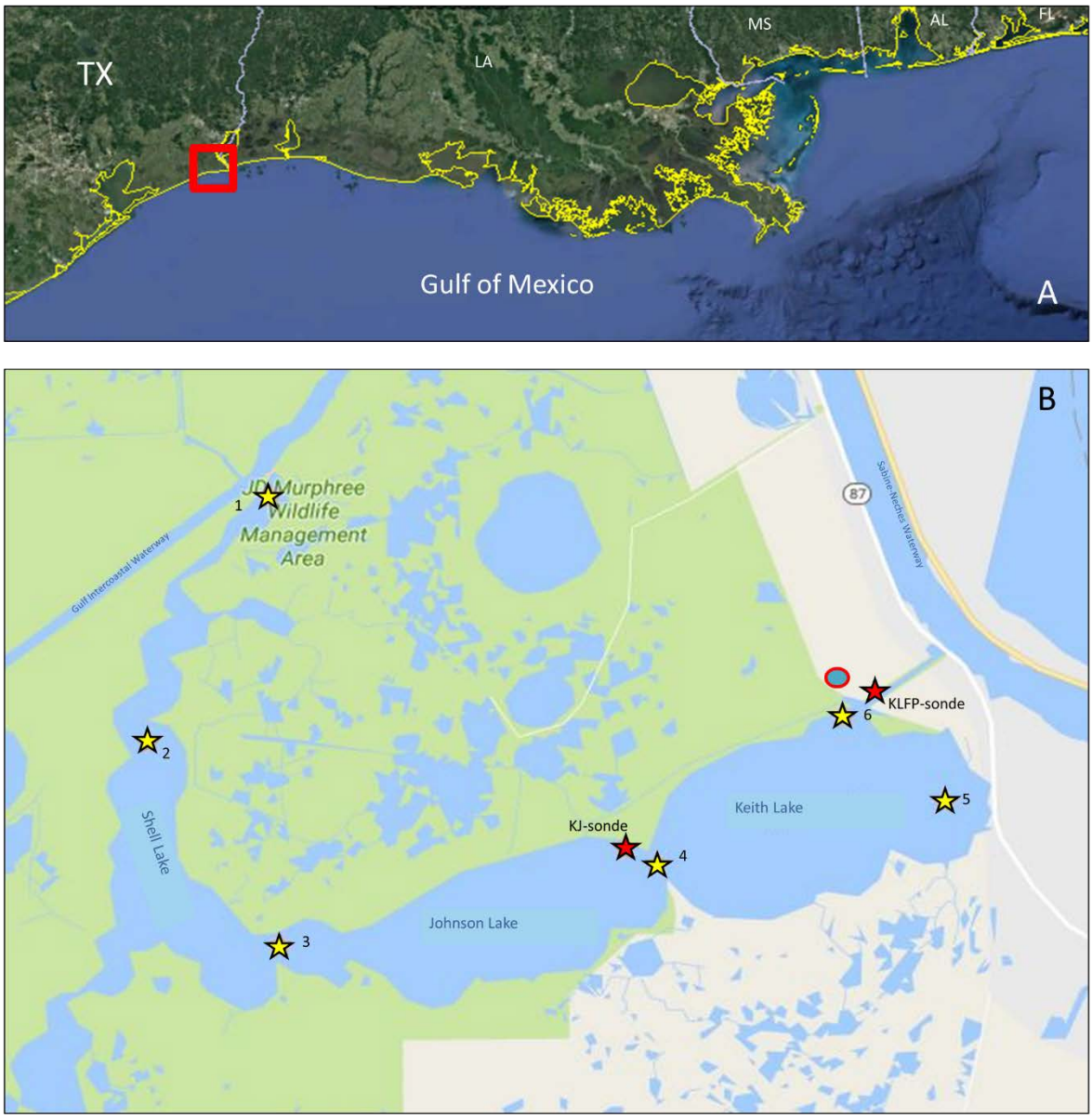

Figure 1. Map of Northern Gulf of Mexico (A) with location of Salt Bayou Watershed in red box. Map of Salt Bayou Watershed Estuary (B) with site for six benthic–pelagic surveys (☆), sonde continuous monitoring of water quality (★), and rainfall (⬭).

days with 1-10 day maintenance interval prior to redeployment. Rainfall data was downloaded from the Texas Drainage District 6 site 7300 Keith Lake @ Highway 87 at Junior's, now located at the TPWD, Keith Lake Boat Ramp (Fig. 1), and mean day and night air temperature and wind speeds were calculated from hourly data downloaded from the DD6 site 5900 Taylors Bayou Saltwater Barrier 8 Gate.

Continuous monitoring of salinity, water temperature, and depth was performed at the KJ-sonde covered nearly a three year period, revealing varaibility interannual, seasonally, and in magnitude of meteorological events, i.e. storms (Fig. 2 & 3). Monthly means for all three parameters at (Fig. 4) the KLFP-sonde site strongly correlate ($P<0.001$) with those at the KJ-sonde site from Feb 2018 to May 2019 ($n = 16$) deployments, with regression slopes not significantly different from unity and R^2 values of 0.93, 0.99, and 0.93 for salinity, water temperature and depth, respectively. Monthly means for these parameters were never significantly different between the two sites for any month, suggesting just one sonde location is needed in future surveys.

Although water temperature had a distinct seasonal pattern, depth and salinity is more variable due to metereological conditions. Heavy and episodic precipitations events throughout the year (Fig 2 & 3) are often preceded by atmospheric pressure changes and strong southern winds, which appear to drive coastal storm surge or a localized seiche that increases depth and salinity prior to the rainfall decreasing salinity for a prolonged period following the storm. Depth also increased with rainfall for some storm events. This pattern is clear for Hurricane Harvey (late Aug 2017), but also observed for other storms (Fig 2B & 3C; red arrows). During these storm events salinity can rise by 5-12 psu and then fall by 10-25 psu.

For all sonde deployment between Aug 2016 through Dec 2017, the mean (± SD) salinity at the KJ-site was 10.15 ± 4.1 psu, and only 47% of readings were below 10 psu. However, for sonde deployments from Feb 2018 to May 2019, the mean (± SD) salinity at the JK-site was 7.75 ± 5.6 psu and 8.10 ± 5.58 psu at the KLFP-site. The target for hydrological restoration effectiveness is a salinity < 10 psu for 80 % of the year. The sites were under the target salinity of 10 psu for 75 % and 71 % of readings for this period at these respective sites. Although the cumulative rainfall for these two study periods were very similar, 305 and 292 cm, respectively, there were differences magnitude and frequency of precipitation event, which may help explain salinity differences. The earlier period had more episodic heavy storm events; whereas the later period had more frequent lower magnitude events during the last 8 months. Generally, the higher salinity months were during warmest months, and there was a moderate positive correlation ($R^2 = 0.34$) between temperature and salinity (Table 2). Overall mean (± SD) salinity was 9.5 ± 4.8 psu and < 10 psu for 55% of readings.

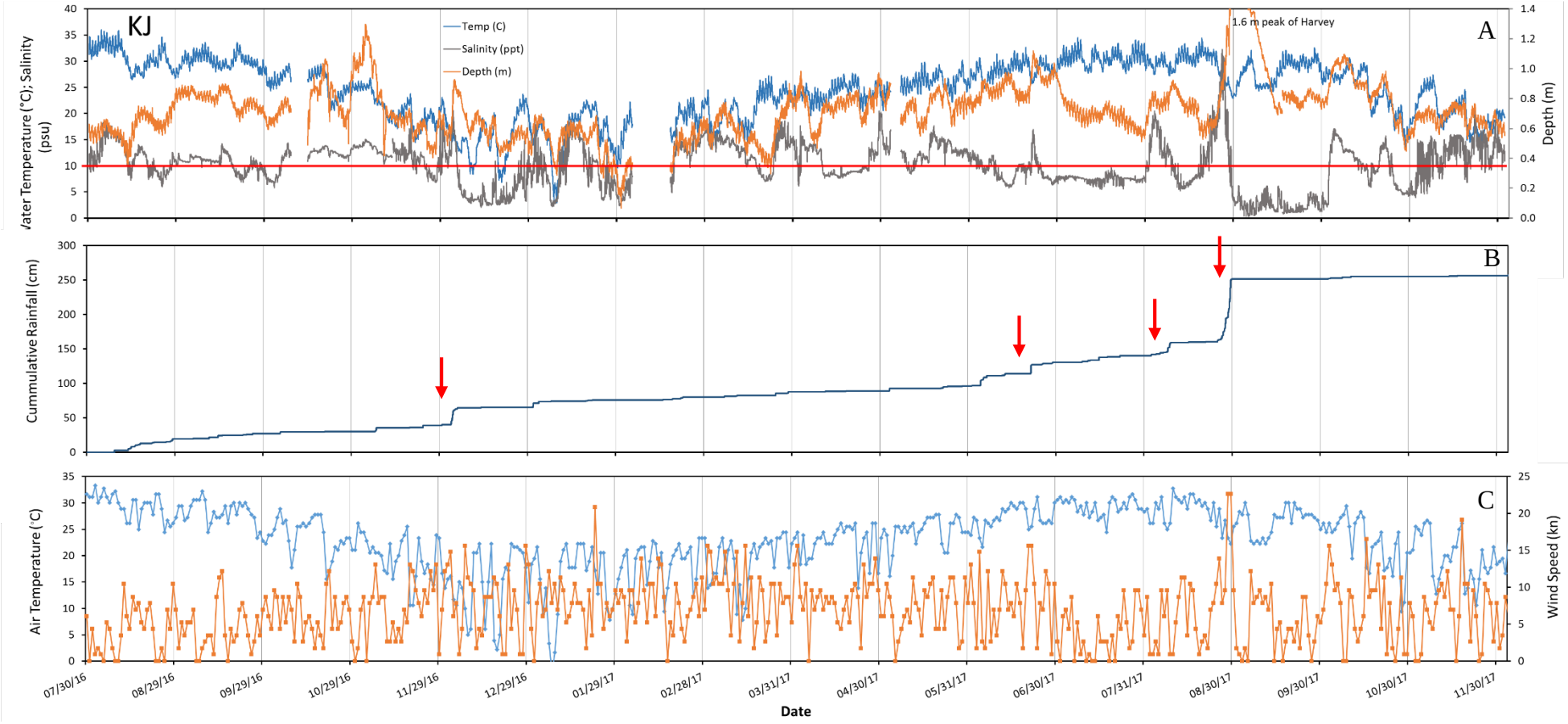

Figure 2. KJ-Site sonde measurements of water temperature, depth, and salinity from July 30, 2016, to Nov 30, 2017 (red line salinity threshold of 10 psu), and cumulative rainfall (B; red arrows indicate storms) and daily air temperature and wind speed (C).

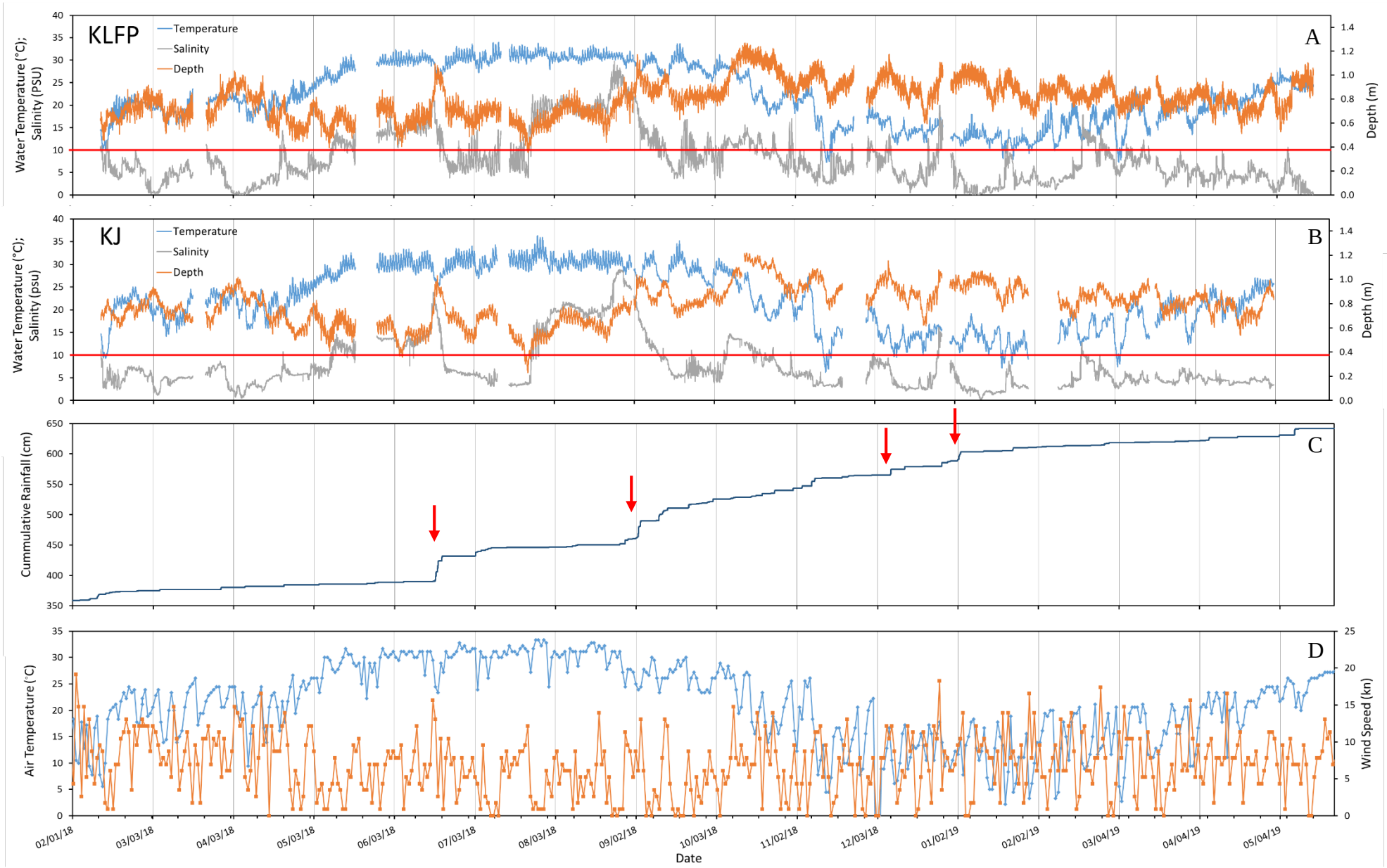

Figure 3. **S**onde measurements of water temperature, depth, and salinity at KLFP (A) and KJ (B) sites from Feb 1, 2018 to May 12, 2019 (red line salinity threshold of 10 psu), and cumulative rainfall (C; red arrow indicate storms) and daily air temperature and wind speed (D).

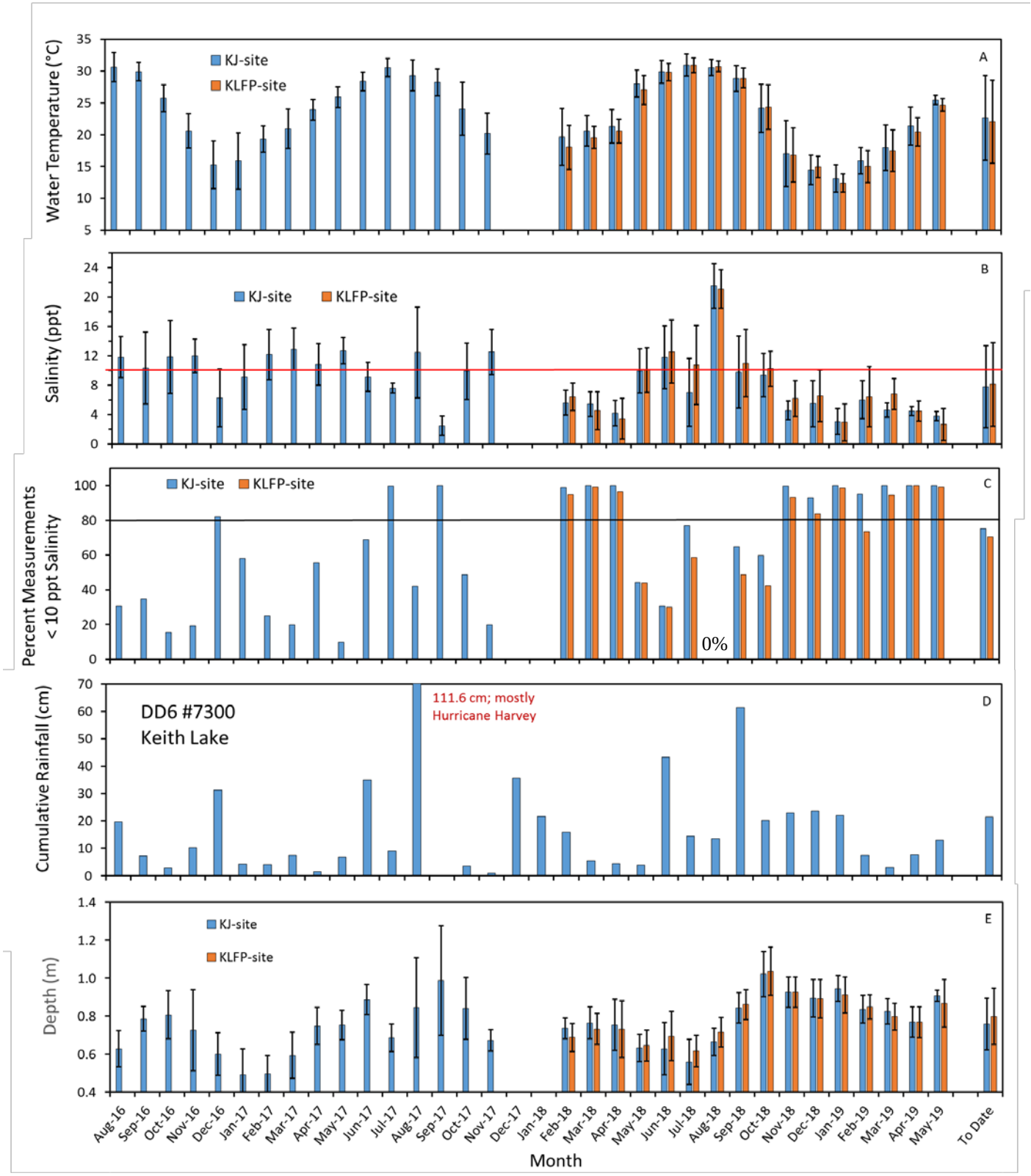

Figure 4. Monthly mean water temperature (A), salinity (B;red line marks 10 psu), percent sonde readings with salinity less than 10 psu (C; black line marks 80%), cumulative rainfall (D), and depth (E) at the KJ and KLFP sites from August 2016 to mid-May 2019 and over this study period (no data for Nov and Dec 2017). Error bars are ± SD

Continuously Monitoring of Turbidity and Photopigments:

The YSI EXO2 sonde was deployed at the KJ-sonde site from Feb 2018 to May 2019 monitored turbidity the phytoplankton photopigments, chlorophyll *a* (Chl*a*) and phycoerythrin (PE). Chlorophyll a is present in all cyanobacteria and eukaryotic phytoplankton; whereas, PE is unique to cyanobacteria, particularly marine taxa. Turbidity is influenced by not just living particulates, but by detrital and mineral particulates, including those resuspended from benthic sediments due to wind-waves. Data for Chl*a*, PE, and turbidity (Fig. 4A & 4B) were filtered for intermittent "spiked" values > 60 µg/L for both photopigments and >250 NTU for turbidity. However during periods in late May 2018 and late Aug into early Sept 2018, both photopigment measurements experienced excessive erratic spiking (Fig. 4C), and these values were discarded and not used in averaging monthly mean values. There were ***Gobiidae*** fish among the YSI EXO2 probes when the sonde was retrieved in July 2018 and early September 2018, so these fish or some other organisms may contribute to spiking values of the optical probes.

Both photopigments followed the same trends, often with distinct diel pattern (Fig. 5), and were strongly correlated (R2 = 0.50; Table 2). Chlorophyll values were generally lower in magnitude than phycoerythrin, and mean monthly values were not significantly different (Fig. 6). The lowest mean monthly Chl*a* concentrations were during spring (Mar-May) in both 2018 and 2019. Likewise the spring quarterly surveys in 2017 and 2018 had the lowest concentrations of extractable Chl*a* measured fluorometrically and by HPLC (Table 3). The monthly mean ratio of PE:Chl*a* was constant at about 1.3 from Feb to August 2018, and then decreased to 0.7 through fall 2018 (Fig. 6). This suggests that cyanobacteria are an important component of the phytoplankton community, but to a less degree in fall 2018. This is confirmed with both SSU rDNA sequences and HPLC photopigment analyses for plankton samples from quarterly samplings (see below).

Turbidity did had very weak but significant ($R^2 < 0.06$; $P < 0.05$) correlation with photopigment (Table 2), and did not follow a predictable diel patterns as with photopigments (Fig. 5). Peaks in turbidity are likely due to wind-wave resuspension of sediments in this shallow (Table 1) estuary, given the frequency and amplitude of wind velocities (Fig. 2C & 3D). Mean monthly turbidity values (Fig. 6) were not significantly different among months, although fall 2018 monthly means and variance were less than during months of other seasons. Detailed consideration of both wind speed and direction, suggest calmer periods coincide with winds speeds below about 7 kn and when direction from the north. Greater speeds and direction from the east, south, and west are associated with turbidity peaks. How these wind-wave sediment resuspension events impact the overall primary productivity and community structure of primary producers is unclear. However, it is not surprising that there are numerous similar algal taxa in both the phytoplankton and microphytobenthos (see below).

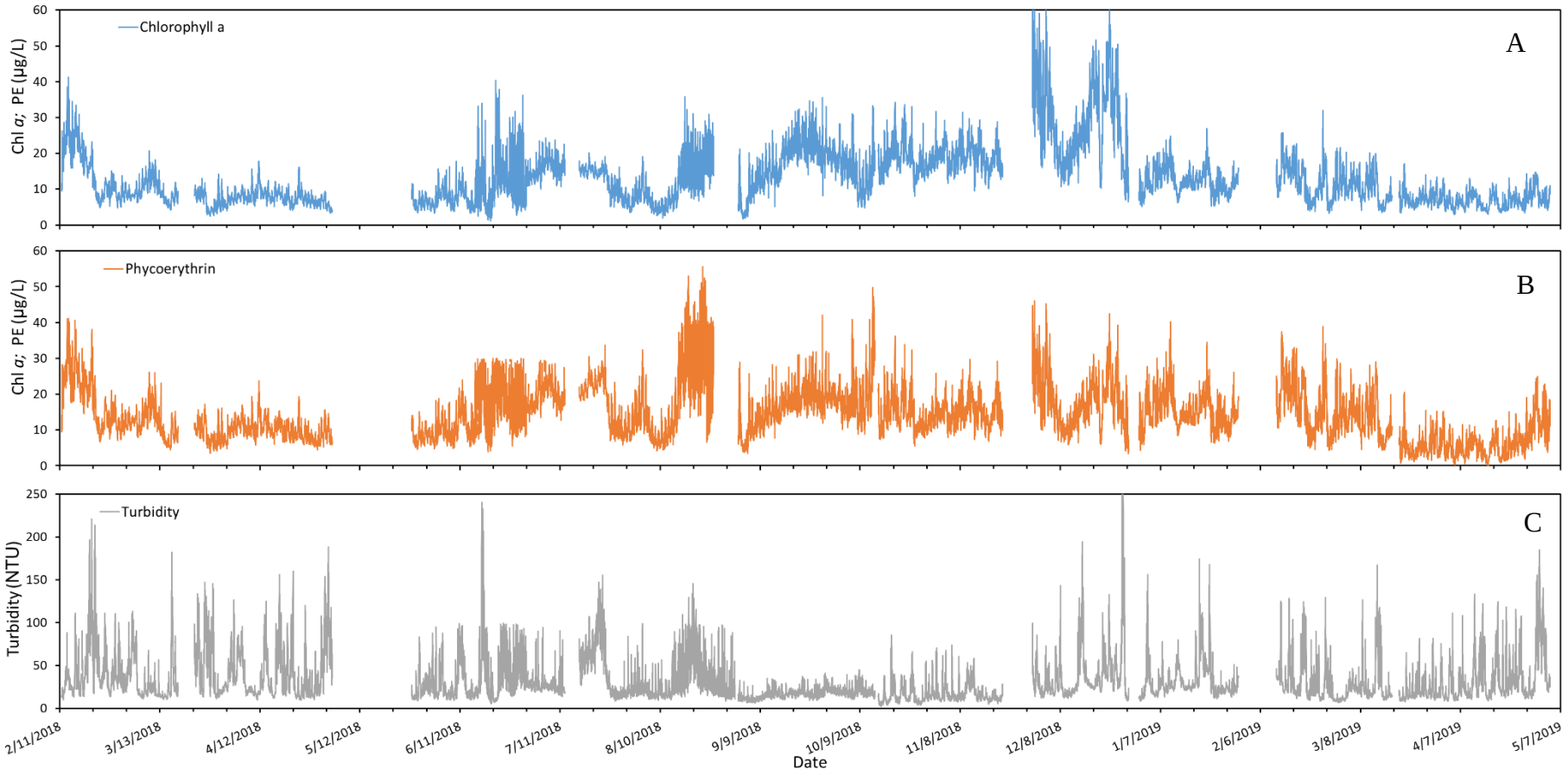

Figure 5. Continuous monitoring of chlorophyll *a*, phycoerythrin (PE), and turbidity by YSI EXO2 sonde at KJ-site Feb 2018 to early-May 2019. Gaps due to maintenance periods and periods of probe interference.

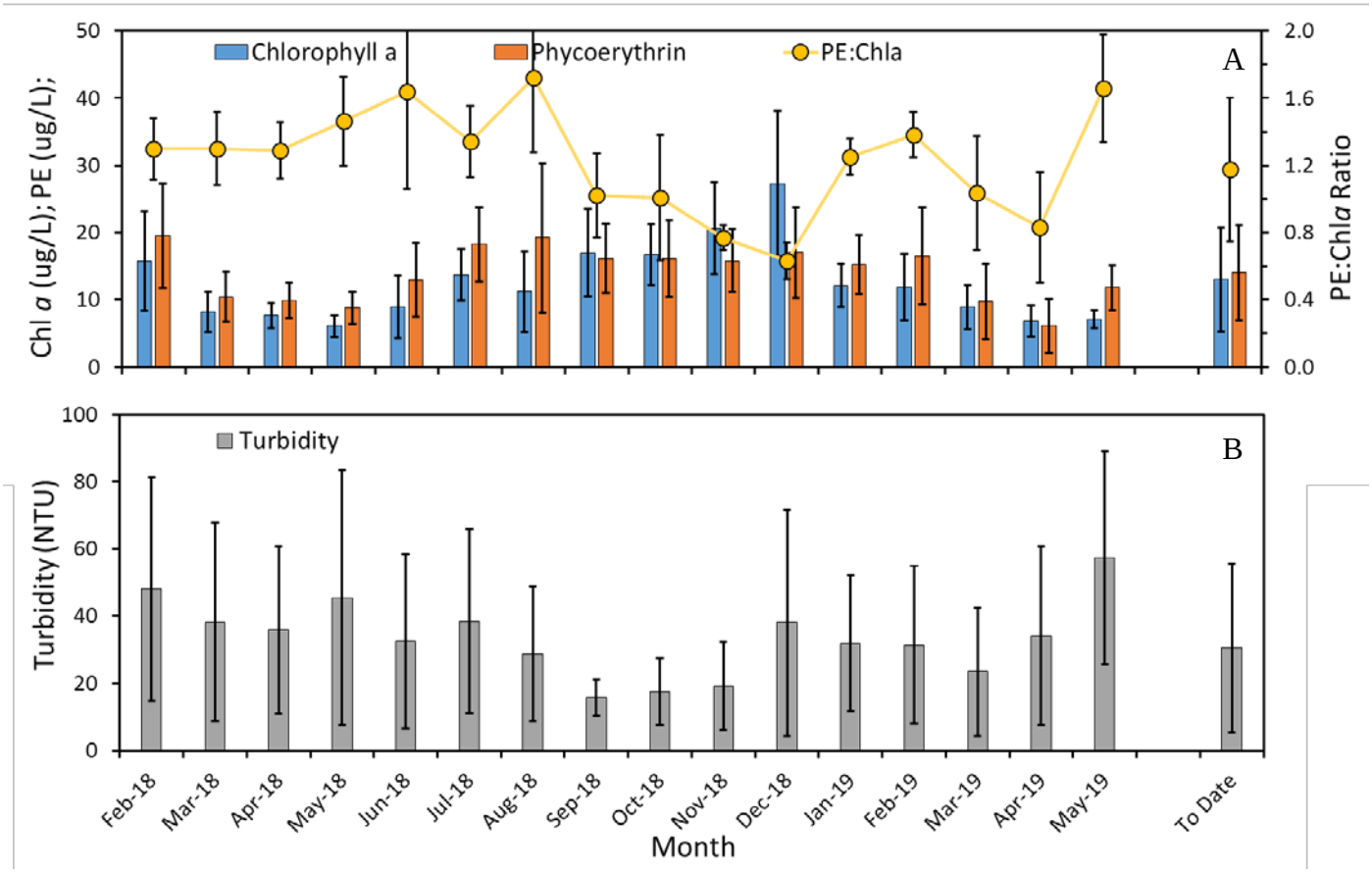

Figure 6. Monthly mean chlorophyll (Chl), phycoerythrin (PE), and CLa:PE ratio (A) and turbidity (B) for continuous monitoring at the KJ-site from Feb 2018 to early May 2019. Error bars as ± SD.

Continuous Monitoring Chemistry:

The YSI EXO2 sonde deployed from Feb 2018 to May 2019 at the KJ-sonde site monitored dissolved oxygen (DO), percent DO saturation, pH, fluorescent dissolved organic matter (fDOM), and oxidation-reduction potential (ORP). (Fig. 7). Both DO and percent DO saturation covaried with pH and ORP over diel cycles, except for during storms and high turbidity events (Fig. 7). Mean (± SD) monthly DO concentration (Fig 8A) was least in the warmest month, Aug 2018, 6.01 ± 0.08 mg DO L^{-1}) and greatest in Dec 2018 (11.86 ± 1.09 mg DO L^{-1}). Water temperature had a strong negative correlation with DO (R^2 = 0.65; Table 2), and salinity had a weak negative correlation (R^2 = 0.28). Also, DO had a weak positive correlated

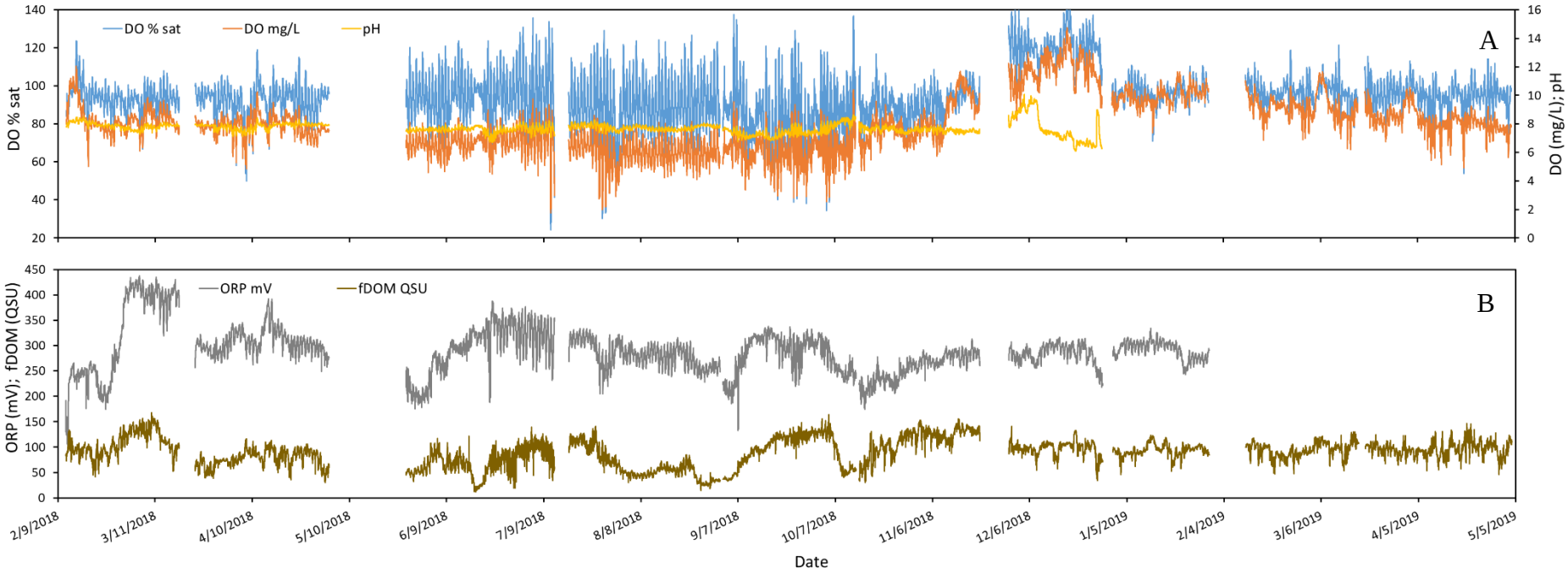

Figure 7 *(above)*. Continuous monitoring for dissolved oxygen (DO) and pH (A), redox potential (ORP), and fluorescent dissolved organic matter (fDOM; B) by YSI EXO2 sonde at the KJ-site for deployments from Feb 2018 to May 2019. Error bars are ± SD.

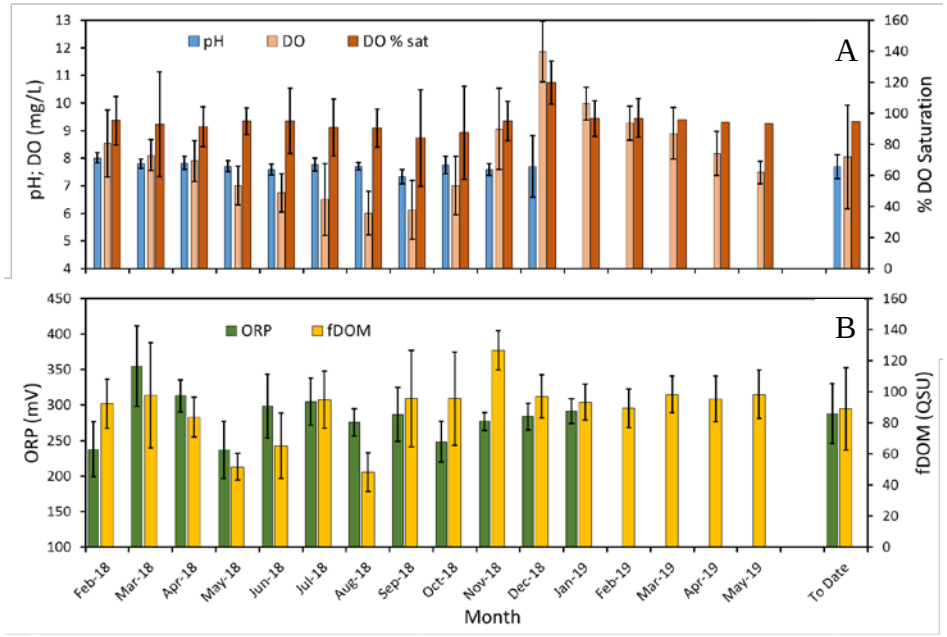

Figure 8 *(left)*. Monthly mean pH, DO (A), ORP and fDOM (B) for the study period. Error bars are ± 95% confidence intervals. No pH data for Feb to May 2019 due to probe failure. Error bars are ± SD.

with Chl*a* content (R2 = 0.16) but not with PE (Table 2). Percent DO saturation strongly correlated with DO but not with temperature or salinity, as would be expected given the biological influences (photosynthesis and respiration) on percent DO saturation in a eutrophic system like Salt Bayou Estuary. Unfortunately, all pH and ORP data was lost after Jan 2019 due to a probe failure. Mean monthly ORP values were not significantly different from the study period mean (± SD) of 288 ± 42 mV (Fig. 8B), as expected for this well oxygenated system. No other parameter significantly correlated with ORP. The concentration of fDOM Mean monthly fDOM concentration ranged from 48 to 126 QSU, with a study period mean (± SD) of 89 ± 26 QSU (Fig. 8B). The concentration of fDOM negatively correlated with salinity (R^2 = 0.48), which supports a terrestrial source of fDOM in freshwater runoff.

Table 2. Pearson correlation coefficient matrix for continuous monitoring of physicochemical and biological parameters at the KJ-site from Aug 2016 through early May 2019.

	Temp	Salinity	Depth	Chla	PE	Turbidity	DO
Salinity	0.58	1.00					
Depth	-0.53	-0.21	1.00				
Chla	-0.17	-0.16	0.21	1.00			
PE	0.10	0.08	-0.03	0.71	1.00		
Turbidity	0.01	-0.13	-0.20	0.04	0.25	1.00	
DO	-0.81	-0.53	0.37	0.40	0.08	0.12	1.00
fDOM	-0.40	-0.69	0.17	0.30	-0.01	-0.27	0.28

Percent variance explained = 10-30 %; 30-50 %; ; >50%.
Not signifcant relationships are grey.

Continuous Monitoring Overall Principle Components Analysis:

Principle components analysis of all YSI EXO2 sonde parameters, except for pH and ORP, was performed on data from all deployments from Feb 2018 to May 2019 (Fig. 9). PC1 explained 37.8% of dataset variance, with the most important factors being temperature, salinity, and DO, and to a lesser extent depth and fDOM. PC2 explained 21.6 % of dataset variance, with PE and Chl*a* being the most important factors, and to a lesser extent turbidity. PC 3, not plotted, explained 15% of dataset variance and most important factor was turbidity. The biplots presented, in two month increments from Feb 2018 to May 2019 (Fig. 9), illustrate seasonal trends with temperature, salinity, DO and fDOM, which were noted above. Cooler months had higher DO bus lower salinity with more fDOM, in contrast to warm periods. Blooms of phytoplankton biomass, based on PE and Chl*a* occurred throughout the year, best especially high blooms occurred in Aug and Dec, 2018.

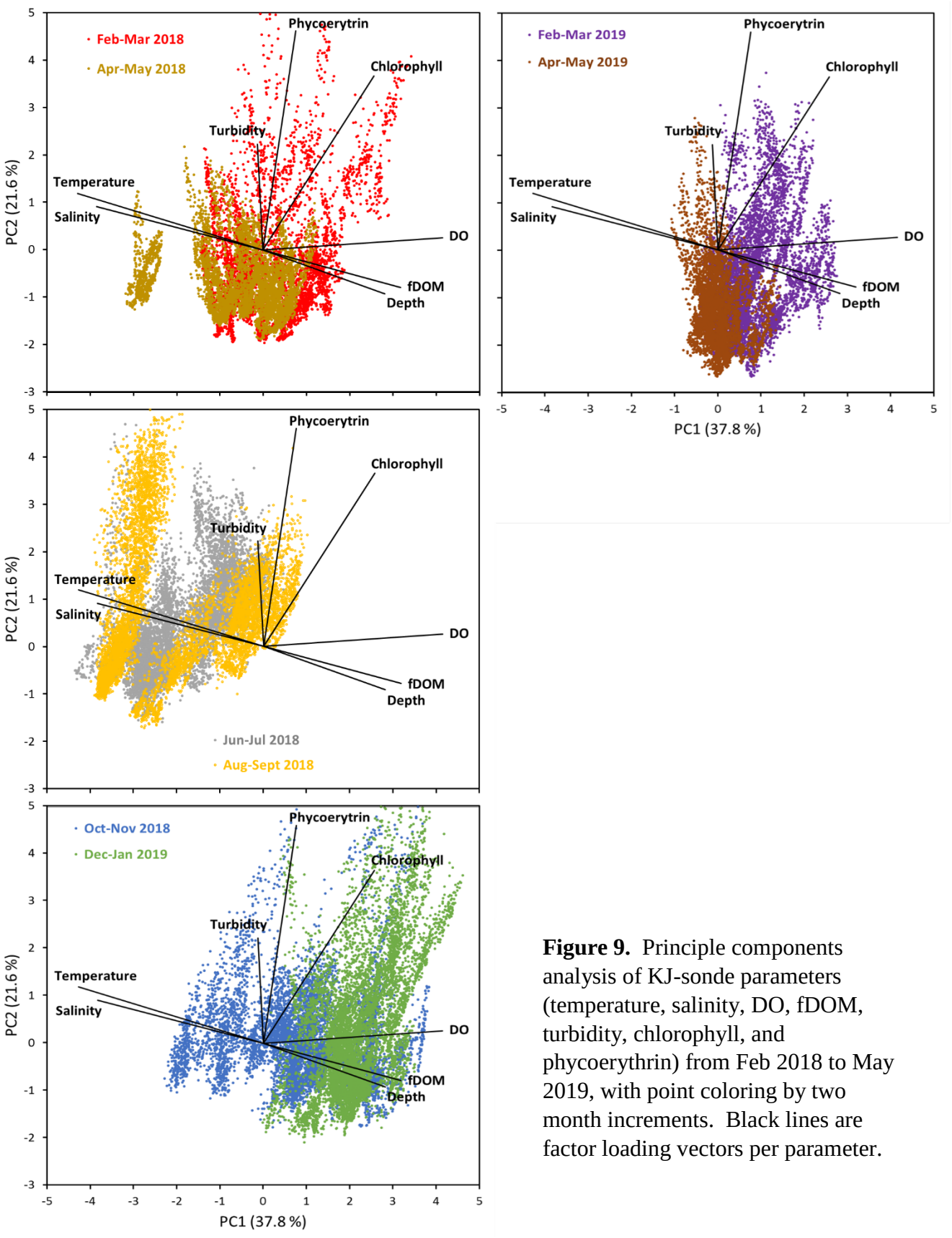

Figure 9. Principle components analysis of KJ-sonde parameters (temperature, salinity, DO, fDOM, turbidity, chlorophyll, and phycoerythrin) from Feb 2018 to May 2019, with point coloring by two month increments. Black lines are factor loading vectors per parameter.

Task 2 - Define Benthic-Pelagic Primary and Secondary Producer Communities:

Quarterly Sampling of Salt Bayou Estuary Physicochemical and Biological Parameters:

Nine quarterly samplings of physicochemical and biological oceanographic parameters at six sites along the longitudinal axis of the Salt Bayou Estuary (Fig. 1) were performed from July 2016 (Su16) to Aug 2018. At each site, depth profiles of water temperature, salinity, pH, DO, and percent DO saturation were performed with an YSI EXO1 sonde, and values from the surface 0.5 m were used to compare to seawater sample parameters for all sampling dates but for winter 2017 when only the sampling depth was measured. Depth profiles of downwelling photosynthetically reactive radiation (PAR) was measured with a LI-COR LI-192 Underwater Quantum Sensor, and used to calculate light attenuation coefficients (k). Seawater samples were collected from a depth of 0.3-0.4 m from the surface in acid washed, 5 L polycarbonate Nalgene Biotainer bottles. Seawater was stored on ice until returned to the laboratory to prepare filtrate for analysis of macronutrients (ammonium, nitrite, nitrate, phosphate, and silicate) and dissolved organic carbon (DOC), and to prepare particulates on glass fiber (GF/F) filters for extractable Chl*a*, and total suspended solids (TSS). Samples were also collected for photopigment analysis and SSU rDNA sequence analysis (see Task 2 below). A subsample of unfiltered seawater was preserved with 0.2 % paraformaldehyde for epifluorescence microscopy determination of bacterial abundance. All quarterly survey data is presented in Tables 3 and 4.

The strong relationships among physicochemical parameters for KJ-sonde site continuous monitoring data were also seen for quarterly survey results across the estuary (Table 5). It is noteworthy that quarterly survey results at site 4 (adjacent to the KJ-sonde site; Fig 1) had similar seasonal trends for temperature and salinity as for the KJ-sonde continuous monitoring at similar months. Both salinity and temperature values between site 4 and KJ-sonde were strongly correlated, R^2 of 0.819 and 0.818, respectively. Quarterly DO concentration negatively correlated with temperature ($R^2 = 0.45$). DOC concentrations, like sonde fDOM, had a strong negative correlation with salinity ($R^2 = 0.67$), and to a weaker degree with site location ($R^2 = 0.32$) location; both relationships suggest a terrestrial DOC source from freshwater runoff.

Depth profiles of YSI EXO1 sonde parameters most often support a well-mixed water column at all sites (Appendix A). Other important relationships were observed for physicochemical parameters along the estuary and seasons surveyed (Table 5). However, one unanticipated result was the weak positive correlation between salinity site number ($R^2 = 0.21$). Close comparison of salinity values at sites 4, 5 and 6 (Table 3), and in light of the similarity between KJ-sonde and KLFP-sonde results (see above), suggests that strong tidal currents connect sites 4 and 6 and isolate site 5. Site five is displaced to the south of the main sampling site longitudinal axis (Fig. 1). It is adjacent to marsh tidal creeks on the

Table 3. Physicochemical and biological oceanographic parameters measured for quarterly sampling of the six sites in Salt Bayou Estuary from summer 2016 through summer 2018.

Date	sites	Salinity (ppt)	Temperature (°C)	Dissolved Oxygen Saturation (%DO)	Dissolved Oxygen (mg DO/L)	pH	Total Suspended Solids TSS (mg/L)	Light Attenuation k (1/m)	HPLC Chl *a* (µg/L)	Fluorometer Chl *a* (µg/L)	Pheophytin (µg/L)	Bacteria (cellsx10^6/ml)
6/30/2016	7/16 KJS-1	2.89	29.47	56.9	4.27	7.13	52.9	5.0	18.51	25.5	4.36	30.0
	7/16 KJS-2	2.70	30.25	59.0	4.37	7.59	47.0	4.9	12.86	14.4	10.17	26.3
	7/16 KJS-3	2.46	30.98	65.3	4.79	7.76	115.5	7.2	19.14	23.0	14.94	29.5
	7/16 KJS-4	2.72	31.38	72.7	5.29	7.97	105.9	7.6	23.29	21.3	12.59	30.4
	7/16 KJS-5	4.12	31.82	84.5	6.05	7.87	66.2	6.0	16.44	15.9	8.05	17.4
	7/16 KJS-6	5.74	30.95	40.2	2.89	7.63	36.9	2.8	6.09	8.0	3.31	11.6
10/1/2016	10/16 KJS-1	5.28	23.7	116.7	9.6	8.0	51.1	2.6	17.16	21.5	1.26	25.1
	10/16 KJS-2	5.77	24.4	124.1	10.0	8.1	62.3	2.5	14.98	18.7	2.00	19.9
	10/16 KJS-3	5.35	24.7	117.1	9.4	8.1	66.2	3.2	16.18	17.9	12.59	21.6
	10/16 KJS-4	8.32	25.1	130.2	10.2	8.2	61.4	3.2	14.22	14.1	9.20	20.7
	10/16 KJS-5	9.95	25.3	138.6	10.8	8.3	60.2	3.5	13.01	11.5	7.61	14.5
	10/16 KJS-6	9.70	26.2	130.2	10.0	8.2	55.0	2.0	9.71	12.3	6.20	15.4
2/19/2017	2/17 KJS-1	4.4	20.5	78.8	6.95	8.04	54.0	6.1	26.09	36.1	7.4	28.0
	2/17 KJS-2	4.2	20.2	89.7	7.92	8.08	77.1	5.9	13.72	15.0	2.6	24.6
	2/17 KJS-3	8.0	20.8	84.1	7.15	7.85	241.2	15.6	13.13	17.1	7.5	17.9
	2/17 KJS-4	14.2	21.0	92.3	7.62	8.06	136.7	7.0	12.89	11.4	7.8	17.9
	2/17 KJS-5	18.9	21.0	93.0	7.41	8.2	105.2	3.8	9.28	8.3	5.4	17.7
	2/17 KJS-6	13.1	18.8	89.5	7.55	8.16	66.2	1.6	1.87	3.6	0.6	13.3
5/9/2017	5/17 KJS-1	11.86	25.2	98.6	7.57	7.67	62.0	6.62	8.31	8.6	3.6	25.2
	5/17 KJS-2	11.67	25.2	95.7	7.36	7.63	123.3	8.76	9.05	8.4	1.5	19.6
	5/17 KJS-3	12.84	25.9	101.6	7.66	7.71	94.7	4.80	9.76	7.7	3.4	19.7
	5/17 KJS-4	9.70	26.1	110.1	8.43	7.85	40.0	3.32	9.73	9.2	5.5	17.7
	5/17 KJS-5	14.10	26.8	109.3	8.06	7.83	69.3	3.21	7.18	7.8	1.9	16.3
	5/17 KJS-6	6.87	24.4	85.9	6.88	7.46	34.3	2.59	3.62	5.0	3.0	15.0
7/20/2017	7/17 KJS-1	5.40	30.7	76.2	5.53	7.80	55.5	5.90	18.33	17.9	3.3	24.6
	7/17 KJS-2	7.40	32.0	87.2	6.12	7.82	43.1	3.73	7.89	8.1	5.1	18.5
	7/17 KJS-3	7.43	32.1	93.2	6.53	7.83	43.5	3.53	8.94	9.4	5.5	17.1
	7/17 KJS-4	8.14	32.0	111.4	7.79	8.11	42.0	4.14	9.67	9.2	4.9	16.0
	7/17 KJS-5	9.32	32.3	121.1	8.37	8.18	45.0	3.33	7.88	9.5	4.5	16.7
	7/17 KJS-6	10.24	31.8	80.3	5.57	7.71	49.8	2.69	10.41	13.6	6.3	14.4

Table 3. *(continued)*

Date	sites	Salinity (ppt)	Temperature (°C)	Dissolved Oxygen Saturation (%DO)	Dissolved Oxygen (mg DO/L)	pH	Total Suspended Solids TSS (mg/L)	Light Attenuation k (1/m)	HPLC Chl *a* (µg/L)	Fluorometer Chl *a* (µg/L)	Pheophytin (µg/L)	Bacteria (cellsx10^6/ml)
11/12/2017	11/17 KJS-1	4.08	18.3	105.5	9.68	7.98	62.0	3.83	10.39	13.3	1.1	24.8
	11/17 KJS-2	5.09	18.5	105.2	9.58	7.92	34.7	2.97	11.84	10.6	1.3	18.6
	11/17 KJS-3	9.62	18.8	109.0	9.58	7.87	72.9	3.31	10.99	7.7	4.7	18.1
	11/17 KJS-4	13.81	20.0	119.0	9.98	7.93	74.9	2.62	8.69	7.6	4.4	14.2
	11/17 KJS-5	16.36	20.6	119.9	9.78	7.97	75.9	2.27	7.41	5.9	3.3	13.2
	11/17 KJS-6	16.64	21.4	124.9	10.02	8.02	71.3	1.86	5.14	8.3	3.9	9.7
2/17/2018	2/18 KJS-1	2.49	21.4	88.4	7.71	8.04	36.6	5.87	12.94	19.6	3.9	23.3
	2/18 KJS-2	2.44	21.7	94.6	8.19	8.11	57.1	6.21	10.95	15.1	2.6	18.1
	2/18 KJS-3	2.02	21.9	99.8	8.64	8.23	88.4	11.50	16.09	18.6	8.1	19.1
	2/18 KJS-4	4.10	21.6	101.4	8.72	8.25	95.0	7.16	10.19	13.1	9.3	16.6
	2/18 KJS-5	8.23	22.0	108.3	9.03	8.30	72.2	3.81	9.27	10.9	7.4	19.3
	2/18 KJS-6	5.97	21.9	111.7	9.45	8.37	73.0	5.09	13.13	18.5	4.7	16.5
5/10/2018	5/18 KJS-1	5.65	27.54	74.3	5.46	7.65	88.7	6.85	10.70	13.8	6.40	20.0
	5/18 KJS-2	5.58	27.70	85.0	6.09	7.54	70.9	3.23	6.77	7.0	1.21	15.3
	5/18 KJS-3	6.58	28.55	86.4	6.08	7.51	62.8	2.52	3.93	6.7	2.88	14.5
	5/18 KJS-4	6.56	28.60	80.0	5.53	7.54	52.0	3.31	5.48	5.9	5.23	18.6
	5/18 KJS-5	8.54	29.12	86.6	5.97	7.56	51.5	3.73	6.08	8.7	2.22	20.1
	5/18 KJS-6	12.17	26.09	84.4	5.63	7.70	38.6	1.79	3.36	4.4	2.43	12.5
8/4/2018	8/18 KJS-1	8.11	29.1	74.3	5.46	7.65	87.2	7.12	15.75	15.3	6.29	30.2
	8/18 KJS-2	13.93	28.7	85.0	6.09	7.54	83.8	3.31	12.43	8.8	7.96	24.1
	8/18 KJS-3	17.73	28.5	86.4	6.08	7.51	110.0	6.58	12.61	9.9	6.78	13.7
	8/18 KJS-4	20.42	28.7	80.0	5.53	7.54	89.6	3.46	3.67	4.8	3.93	7.6
	8/18 KJS-5	20.22	28.9	86.6	5.97	7.56	90.0	2.71	7.01	8.9	8.00	10.5
	8/18 KJS-6	21.84	30.3	84.4	5.63	7.70	83.8	2.09	2.07	3.2	1.39	8.3

Table 4. Nutrients and DOC concentrations measured for quarterly sampling of the six sites in Salt Bayou Estuary from summer 2016 through summer 2018.

Date	sites	NH4+ (µM N)	NO2- (µM N)	NO3- (µM N)	DIN (µM N)	PO_4^{2-} (µM P)	DIN:SRP	SIO2- (µM Si)	DOC (µM C)
6/30/2016	7/16 KJS-1	0.82	0.08	0.07	0.97	3.09	0.31	117.6	370.8
	7/16 KJS-2	0.67	0.14	0.02	0.84	5.03	0.17	164.2	373.4
	7/16 KJS-3	1.66	0.13	0.00	1.79	5.54	0.32	172.8	416.9
	7/16 KJS-4	1.65	0.10	0.08	1.84	4.88	0.38	178.9	385.1
	7/16 KJS-5	2.94	0.08	0.09	3.11	2.03	1.53	167.2	289.4
	7/16 KJS-6	5.19	0.54	1.00	6.72	1.13	5.97	155.3	193.7
10/1/2016	10/16 KJS-1	0.93	0.09	0.07	1.09	4.00	0.27	268.5	402.3
	10/16 KJS-2	1.52	0.09	0.05	1.65	3.68	0.45	245.6	356.6
	10/16 KJS-3	1.23	0.08	0.08	1.39	6.56	0.21	226.3	336.5
	10/16 KJS-4	0.54	0.05	0.09	0.67	3.50	0.19	189.3	260.6
	10/16 KJS-5	0.45	0.03	0.06	0.54	1.20	0.45	133.2	165.9
	10/16 KJS-6	0.40	0.07	0.05	0.51	2.32	0.22	164.0	216.1
2/19/2017	2/17 KJS-1	0.24	0.049	0.03	0.33	0.80	0.41	109.9	249.7
	2/17 KJS-2	0.16	0.035	0.11	0.30	2.49	0.12	135.7	221.3
	2/17 KJS-3	0.27	0.043	0.16	0.48	1.61	0.30	131.9	158.2
	2/17 KJS-4	0.06	0.268	0.69	1.02	1.14	0.89	221.5	105.1
	2/17 KJS-5	1.31	0.249	0.02	1.57	0.87	1.82	90.9	75.0
	2/17 KJS-6	4.67	0.260	5.32	10.25	0.90	11.37	162.4	123.5
5/9/2017	5/17 KJS-1	0.59	0.016	0.16	0.77	0.97	0.80	120.2	162.6
	5/17 KJS-2	0.19	0.024	0.04	0.25	0.73	0.34	108.7	159.2
	5/17 KJS-3	0.27	0.057	0.01	0.33	0.91	0.36	103.7	130.4
	5/17 KJS-4	0.28	0.217	1.51	2.01	0.61	3.32	75.6	138.0
	5/17 KJS-5	0.15	0.019	2.16	2.33	0.40	5.80	41.9	117.3
	5/17 KJS-6	4.58	0.612	2.11	7.30	0.87	8.43	16.1	148.7
7/20/2017	7/17 KJS-1	0.09	0.12	0.28	0.49	3.07	0.16	152.5	303.9
	7/17 KJS-2	0.19	0.09	0.59	0.87	0.80	1.09	163.4	233.3
	7/17 KJS-3	0.20	0.07	0.51	0.77	1.85	0.42	170.7	238.9
	7/17 KJS-4	0.23	0.07	0.31	0.60	1.66	0.36	165.7	217.1
	7/17 KJS-5	0.25	0.06	0.18	0.49	1.06	0.47	149.5	177.3
	7/17 KJS-6	0.49	2.43	0.30	3.22	1.39	2.31	108.5	145.3

Table 4. *(continued)*

Date	sites	NH4+ (µM N)	NO2- (µM N)	NO3- (µM N)	DIN (µM N)	PO_4^{2-} (µM P)	DIN:SRP	SIO2- (µM Si)	DOC (µM C)
11/12/2017	11/17 KJS-1	0.33	0.05	0.35	0.73	2.12	0.35	168.8	275.9
	11/17 KJS-2	0.31	0.05	0.29	0.64	2.09	0.31	172.5	264.4
	11/17 KJS-3	0.45	0.05	0.41	0.91	1.78	0.51	127.3	171.0
	11/17 KJS-4	0.24	0.00	1.10	1.34	0.78	1.72	45.7	119.0
	11/17 KJS-5	0.42	0.12	0.82	1.37	0.76	1.80	46.2	122.8
	11/17 KJS-6	0.40	0.13	0.98	1.51	0.56	2.72	34.4	82.2
2/17/2018	2/18 KJS-1	0.41	0.06	0.33	0.80	0.36	2.23	29.4	232.9
	2/18 KJS-2	0.36	0.08	0.32	0.76	0.75	1.00	33.4	229.6
	2/18 KJS-3	0.36	0.10	0.25	0.71	1.56	0.46	21.1	298.4
	2/18 KJS-4	0.35	0.04	0.34	0.74	0.93	0.79	44.5	187.5
	2/18 KJS-5	0.27	0.00	0.40	0.67	0.46	1.47	43.0	134.2
	2/18 KJS-6	0.40	0.03	0.29	0.72	0.61	1.18	48.2	161.3
5/10/2018	5/18 KJS-1	0.63	0.04	0.46	1.13	1.10	1.03	90.1	282.1
	5/18 KJS-2	0.52	0.03	0.22	0.76	1.42	0.53	123.8	231.3
	5/18 KJS-3	0.45	0.00	0.20	0.65	1.20	0.54	125.7	215.7
	5/18 KJS-4	0.48	0.01	0.45	0.94	0.97	0.97	124.4	177.2
	5/18 KJS-5	0.48	0.01	0.30	0.79	0.59	1.33	118.7	135.2
	5/18 KJS-6	2.74	0.56	2.36	5.66	1.00	5.66	80.2	99.8
8/4/2018	8/18 KJS-1	0.52	0.02	0.96	1.50	2.99	0.50	164.5	259.3
	8/18 KJS-2	0.45	0.00	0.64	1.09	1.31	0.83	125.7	133.7
	8/18 KJS-3	0.44	0.00	0.88	1.31	0.84	1.57	93.8	89.3
	8/18 KJS-4	4.23	0.21	0.92	5.36	1.14	4.70	74.1	65.0
	8/18 KJS-5	0.64	0.13	0.45	1.22	0.67	1.83	87.6	70.9
	8/18 KJS-6	4.43	0.74	0.57	5.74	1.08	5.29	62.9	53.9

Table 5. Pearson correlation (R) matrix for all physicochemical and biological oceanographic parameters in Salt Bayou Estuary from summer 2016 through summer 2018. Orange highlights indicate significant correlations from P<0.001 (darkest) to P<0.05 (lightest).

	Salinity	Temp	%DO	DO	pH	TSS	Light-k	Chla	Pheo	Bacteria	NH4	NO2	NO3	SRP	DIN:SRP	SIO2	DOC
Salinity	1.00																
Temp	-0.01	1.00															
%DO	0.19	-0.42	1.00														
DO	0.05	-0.67	0.94	1.00													
pH	-0.14	-0.49	0.65	0.73	1.00												
TSS	0.23	-0.19	-0.10	-0.04	0.01	1.00											
Light k	-0.32	-0.09	-0.27	-0.15	0.04	0.71	1.00										
Chla	-0.55	-0.02	-0.09	0.03	0.21	0.16	0.48	1.00									
Pheo	-0.21	0.23	-0.12	-0.13	0.15	0.31	0.36	0.54	1.00								
Bacteria	-0.62	0.03	-0.25	-0.14	-0.04	0.02	0.39	0.76	0.33	1.00							
NH4	0.19	0.16	-0.37	-0.37	-0.21	-0.11	-0.27	-0.35	-0.15	-0.35	1.00						
NO2	0.16	0.22	-0.22	-0.26	-0.15	-0.14	-0.21	-0.19	-0.04	-0.27	0.30	1.00					
NO3	0.31	-0.17	-0.06	-0.05	-0.04	-0.13	-0.31	-0.49	-0.32	-0.36	0.50	0.14	1.00				
SRP	-0.45	0.21	-0.10	-0.07	0.02	0.02	0.09	0.58	0.50	0.57	0.02	-0.07	-0.30	1.00			
DIN:SRP	0.37	-0.06	-0.18	-0.19	-0.13	-0.18	-0.37	-0.58	-0.36	-0.51	0.77	0.34	0.88	-0.36	1.00		
SIO2	-0.27	0.23	0.00	-0.03	0.05	-0.01	-0.06	0.37	0.17	0.39	-0.02	-0.09	-0.20	0.67	-0.33	1.00	
DOC	-0.82	0.18	-0.17	-0.09	0.04	-0.16	0.23	0.70	0.33	0.73	-0.13	-0.20	-0.39	0.79	-0.46	0.56	1.00
Site	0.46	0.07	0.20	0.08	0.21	-0.05	-0.39	-0.51	0.02	-0.70	0.43	0.39	0.39	-0.31	0.56	-0.29	-0.57

p < 0.001
p < 0.01
p < 0.05

southern shore of Keith Lake and their runoff, as supported by often having lower salinity than both sites 4 and 5. Another positive correlation in the quarterly survey data set was for the light attenuation coefficient (k) and TSS (R^2 = 0.50), with most turbid waters at site 3. Soluble reactive phosphorous (SRP; assumes to be phosphate) had strong positive correlations with silicate and DOC (R^2 values of 0.44 and 0.63, respectively), and weak negative correlation with salinity (R^2 = 0.20).

Ammonium, the dominant dissolved inorganic nitrogen (DIN) species throughout all sites and seasons, but for 3 samples (Table 4), representing 56 ± 25 % (mean ± SD; n = 54; P<0.005 for 2-tails t-Test) of DIN concentration. Nitrate and nitrite represented 35 ± 24 % and 9.1 ± 11 % of DIN concentration, respectively, and nitrate concentration greater than nitrite 76% of all samples throughout the study. Ammonium concentrations were typically greatest at site 6, although site 4 and 5 also had elevated ammonium relative to other site in some seasonal samplings (Table 4). Ammonium and nitrate weakly correlated and explained most variation in the DIN:SRP ratio (Table 5). The DIN:SRP was very low relative to the Redfield N:P ratio of 16 throughout all sites and seasons, with a mean (± 95 % CI) of 1.6 ± 0.61 (Table 5), suggesting nitrogen limiting conditions for phytoplankton and possibly bacterioplankton.

The seasonal pattern of Chl *a* content seen in KJ-sonde continuous monitoring results was not apparent for quarterly surveys, but generally the Chl *a* content decreased with salinity (R^2 = 0.30). For most survey dates, Chl *a* content was greatest at site 1, the shallowest site, and least at site 6, nearest the KLFP (Fig. 10A). Chlorophyll *a* content generally decreased toward KLFP and as salinity and DIN:SRP ratio increased (Table 5). This trend was observed for most

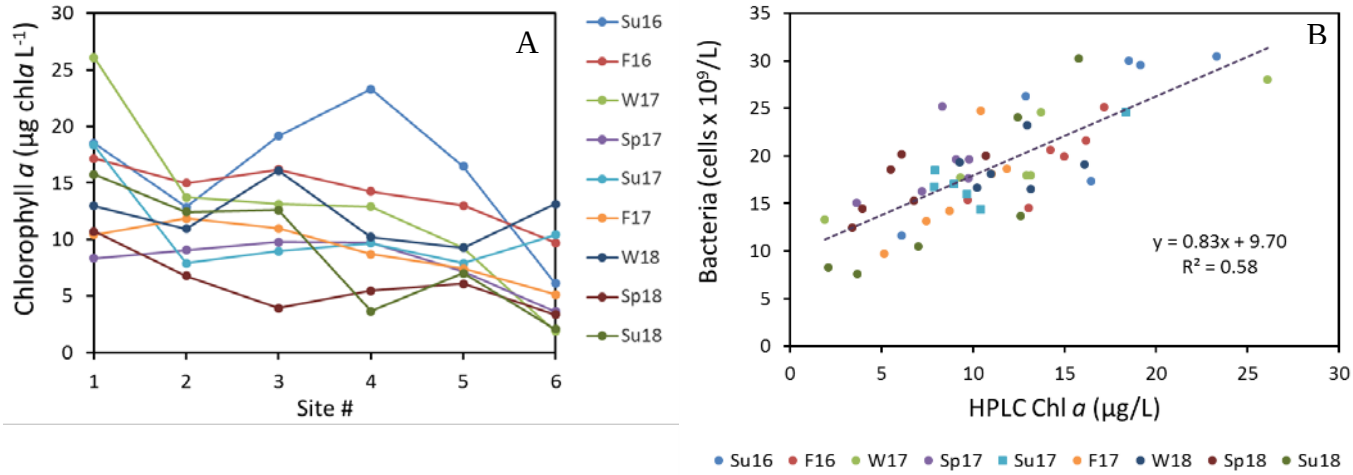

Figure 10. Longitudinal profile of HPLC chlorophyll *a* content during quarterly surveys in Salt Bayou Estuary from fall 2017 to summer 18 (A), and the regression analysis of bacterial abundance to chlorophyll *a* content (B).

seasonal surveys (Fig. 10A). Chl *a* weakly correlated with increasing light attenuation (R^2 = 0.23). Chl *a* content also correlated with DOC concentration (R^2 = 0.48). Bacterioplankton abundance strongly correlated with increasing phytoplankton biomass, as Chl *a* (R2 = 0.58; Fig. 10B), increasing DOC concentration (R^2 = 0.53), and to a lesser degree, decreasing salinity (R^2 = 0.39) and increasing SRP (R^2 = 0.33; Table 5).

Principle component analysis of all quarterly surveys reveals those physicochemical and biological parameters that drive seasonal differences throughout the Salt Bayou (Fig. 11). PC1 and PC2 explained 33 % and 19 % of variance, respectively. PC1 was driven by salinity, nutrients, DOC, biological biomass, and site location. PC2 was driven by temperature, DO and pH, and most reflect seasonal differences. In spring and summer the estuary was more similar with warmer water temperature and lower DO and pH than during fall and winter. The upper portion of the estuary (site 1-3) were generally of lower salinity and DIN:SRP ratio values, but greater DOC concentration, bacterial abundance and Chl *a* than the lower, Keith Lake portion of the estuary (sites 4-6).

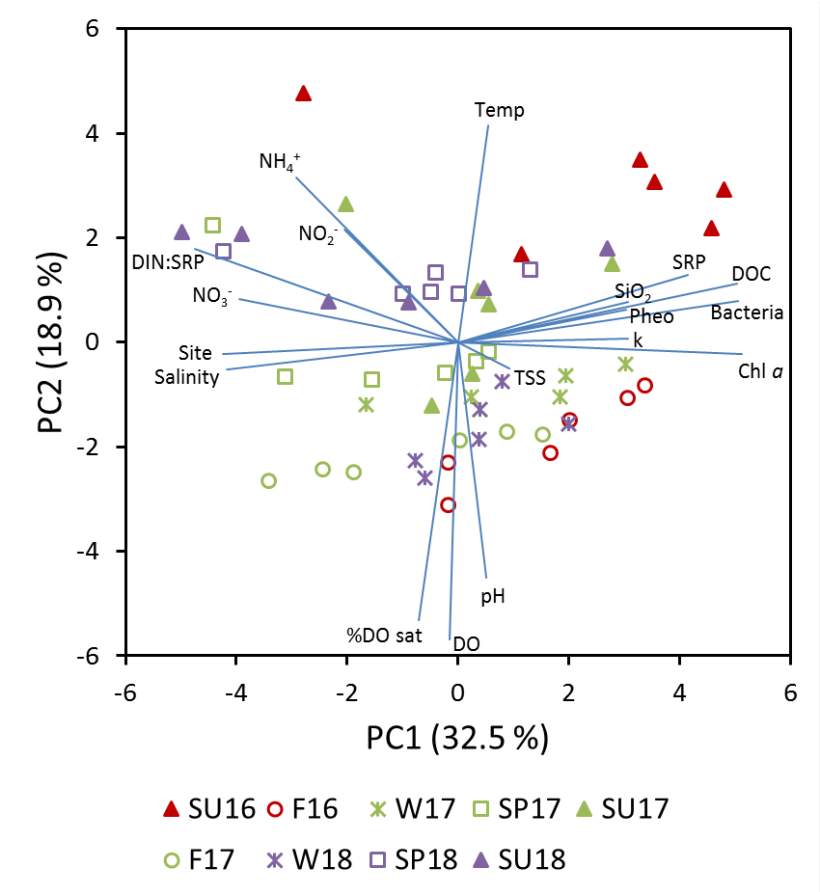

Figure 11. Principle component analyses of physicochemical and biological oceanographic parameters analyzed for quarterly samples of Salt Bayou Estuary from summer 2016 through summer 2018. Blue lines are factor loading vectors for each parameter.

Quarterly Sampling of Salt Bayou Estuary Primary Producer Communities:

In addition to the physicochemical and biological oceanographic parameters reported above, plankton and surface sediments were also collected at the six sites during quarterly surveys for photopigment and SSU rDNA sequencing analyses. These analyses defined the composition of benthic and pelagic communities of primary producers (phytoplankton and microphytobenthos) and secondary producers (bacterioplankton and surface benthic bacteria). Seawater particulates were filtered onto Supor membranes (< 0.22 um; Pall Corporation, Port Washington, NY) for nucleic acid extractions used in SSU rDNA sequencing on an Illumina MiSeq, and onto Whatman GF/F glass fiber filters (GE Life Sciences, Pittsburgh, PA) for photopigment composition analysis by HPLC with fluorometric detection. To analyze microphytobenthos and benthic surface bacteria, sediment cores were collected in 2" diameter, 20" length, polycarbonate core liners, either manually or with a K-B Corer (Wildco, Yulee, FL). The top 2 mm of mostly golden brown unconsolidated sediment was collected into a 50 ml conical tube, and stored on ice until processed in the laboratory. Surface sediment was centrifuged (10 min, 10,000 cfu) and the pellet homogenized before weighing for both photopigment analysis and nucleic acid extractions used in SSU rDNA sequencing by Illumina MiSeq platform. An operational taxonomic units (OTUs) was defined as a sequence similarity cluster of ≥ 95% similarity. Picking OTUs and identifications were performed in QIIME.

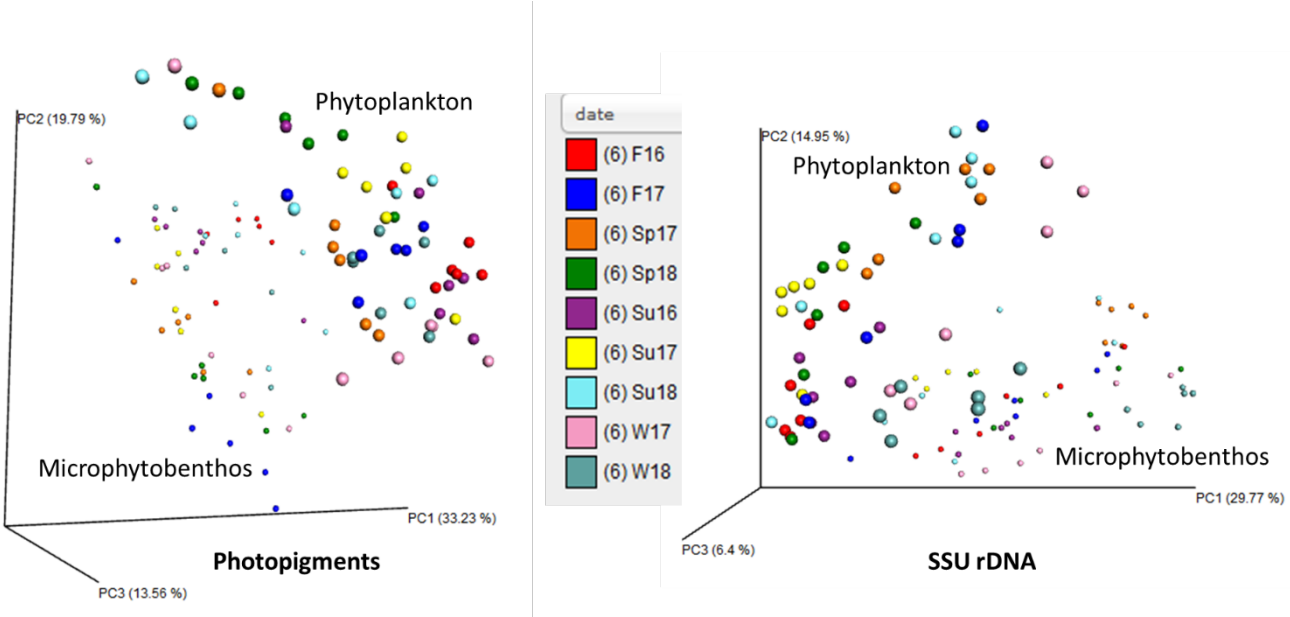

Figure 12. Principle coordinates analysis of Bray-Curtis dissimilarities of photopigments (left) and all phytoplankton taxa SSU rDNA sequences (right) for all sites and samples from quarterly sampling of phytoplankton and microphytobenthos from summer 2016 through summer 2018.

Primary producer studied in quarterly sampling of Salt Bayou Estuary included phytoplankton and microphytobenthos. The composition of these two communities were distinctly different based on principle coordinates analysis of Bray-Curtis of both photopigment profiles and SSU rDNA sequences of cyanobacteria and eukaryotic algal taxa (Fig. 12). Bray-Curtis matrices for the two methods were significantly correlated (Mantel test; $R^2 = 0.47$; $P < 0.01$). Concentrations of specific photopigments are in Appendix B. Principle component analysis of Bray-Curtis dissimilarities for photopigment profiles of all sites and quarterly sampling dates was performed for phytoplankton and microphytobenthos; all chlorophyll a isomers were excluded from these analyses (Fig. 13). For phytoplankton, the first two PCs explained 62% of variance and was driven mostly by gyroxanthin, zeaxanthin, antheraxanthin, fucoxanthin, chlorophyll c1c2, and α carotene (Fig 13A). Spring phytoplankton communities, due to their tighter clustering in the PCA biplot, were most similar between years and among sites; whereas, other seasons were more dissimilar and with greater site-to-site differences.

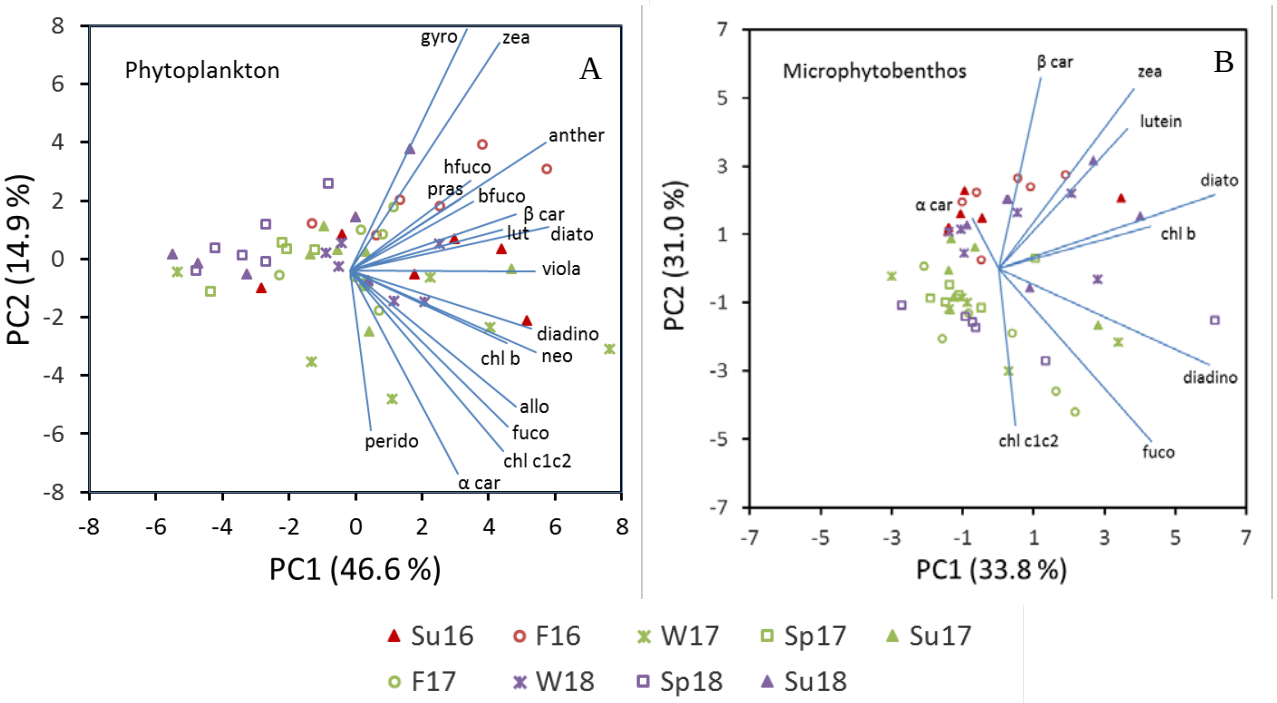

Figure 13. Principle components analysis of photopigments for all sampling dates and sites from quarterly sampling of phytoplankton (A) and microphytobenthos (B) from summer 2016 through summer 2018. Photopigments include are gyroxanthin-diester (gyro), zeaxanthin (zea), antherazanthin (anther), prasinoxanthin (pras), lutein (lut), diatoxanthin (diato), diadinoxanthin (diadino), violaxanthin (viola), 9' cis-neoxanthin (neo), alloxanthin (allo), peridinin (perid), fucoxanthin (fuco), 19' hexanoloxyfucoxanthin (hfuco), 19' butanoyloxyfucoxanthin (bfuco), chlorophyll c1c2 (chl c1c2), chlorophyll b (chl b), α carotene (α car), and β carotene (β car).

There was a far greater diversity of photopigments detected in the phytoplankton as compared to the microphytobenthos, suggesting a more complex community of primary producers in the plankton. For microphytobenthos, the first two PCs explained 64% of variance and was driven mostly by zeaxanthin, fucoxanthin, diatoxanthin, diadinxanthin, and β carotene (Fig 13B).. Microphytobenthos communities differ by date along the concentration gradients of zeaxanthin, lutein and β carotene, with lower content in winter, spring, fall 2017 and spring 2018 and greater content in summers, fall 2016 and winter 2018. For most dates, the sites differences followed concentration gradients of fucoxanthin and diadinoxanthin.

Specific photopigments are signatures for major algal classes, due to being unique to the class or greater content relative to chlorophyll a than other classes, including: fucoxanthin for diatoms; zeaxanthin for cyanobacteria, gyroxanthin diester for *Karenia* dinoflagellates, peridinin for other dinoflagellates, prasinoxanthin for prasinophytes, alloxanthin for cryptophytes, lutein for chlorophytes. Many classes may have the same photopigements but in different amounts relative to chlorophyll a. The CHEMTAX model estimates community composition of major classes based on the known classes in an ecosystem, determined by microscopy or molecular methods, and the pigment to chlorophyll a ratios for the pigment of these taxa. Based on the relative abundances of SSU rDNA sequences identified as cyanobacteria and eukaryotic algal classes, and the presence of class-specific photopigments present in the phytoplankton and microphytobenthos, an initial set of ratios based on literature values was used in CHEMTAX modeling (Table 6). Not all photopigments detected were used in CHEMTAX modelling of algal classes due to their common occurrence of similar content in multiple classes.

Cyanobacteria, chlorophytes diatoms, and *Karenia* dinoflagellates, and cryptophytes were more abundant in the phytoplankton community than euglenoids, prasinophytes, and other dinoflagellates (Fig. 14). All five more dominant classes correlated with total chl *a* (R^2 values of 0.52, 0.64, 0.37, 0.30, and 0.54, respectively; $P < 0.001$). There is no obvious seasonal trend in phytoplankton community composition, and no class correlated with temperature throughout all sampling dates ($P > 0.05$). Cyanobacteria positively correlated with chlorophytes ($R^2 = 0.36$) and *Karenia* ($R^2 = 0.75$), and cryptophytes positively correlated with diatoms ($R^2 = 0.33$). Both cyanobacteria and chlorophytes were negatively correlated with salinity (R^2 values of 0.34 and 0.53, respectively), and often more dominant in the upper estuary (sites 1-3). *Karenia* was also more abundant in the upper estuary. Cyanobacteria and *Karenia* positively correlated with SRP (R^2 values of 0.51 and 0.35, respectively), and cyanobacteria negatively correlated with nitrate and the DIN:SRP ratio (R^2 values of 0.33 and 0.43, respectively). Given the low DIN:SRP ratios contribute to N-limitation, the latter is not unexpected given ability of cyanobacteria to fix N_2 and better compete with eukaryotic algal classes.

Diatoms dominated (45-95 %) the microphytobenthos on most estuary survey dates, and cyanobacteria were 20-45 % of the community on four survey dates, Su16, F16, W18, and Su18 (Fig. 15). Both chlorophytes and euglenoids were < 15% of total chlorophyll *a* throughout all sites and survey dates. As with phytoplankton, there was no consistent seasonal pattern in microphytobenthic community composition. Total chlorophyll *a* content was 1.5-23.5 $\mu g\ g^{-1}$, with the greatest content most often observed at site 1 and site 6. These two sites frequently had

Table 6. The initial photopigment-to-chlorophyll *a* ratios for phytoplankton classes included in the CHEMTAX model. Photopigment abbreviations are defined in the legend of Figure 14.

Pigment_Class	perid	ButFuc	fuco	h_fuco	neo	pras	viola	anther	allo	lut	zea	gyro	Chl_b
Cyanobacteria	---	---	---	---	---	---	---	---	---	---	0.906	---	---
Euglenophytes	---	---	---	---	0.067	---	0.007	---	---	---	0.048	---	0.239
Chlorophytes	---	---	---	---	0.050	---	0.053	0.011	---	0.176	0.009	---	0.228
Dinoflagellates	0.786	---	---	---	---	---	---	---	---	---	---	---	---
Cryptophytes	---	---	---	---	---	---	---	---	0.266	---	---	---	---
Diatoms	---	---	0.464	---	---	---	---	---	---	---	---	---	---
Karenia	---	0.027	0.305	0.029	---	---	---	---	---	---	---	0.142	---
Prasinophytes	---	---	---	---	0.133	0.432	0.070	0.037	---	0.016	0.079	---	0.911

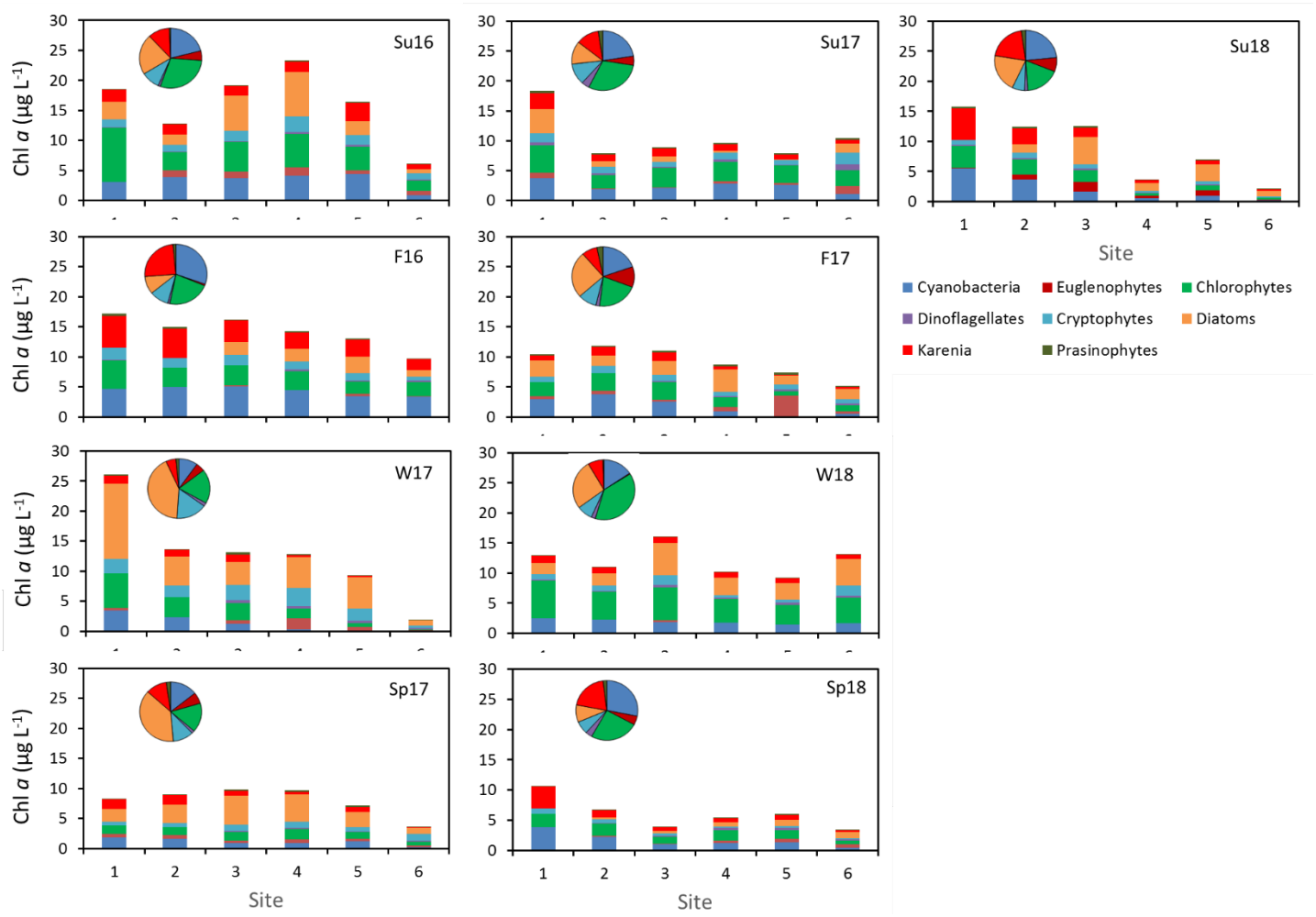

Figure 14. Phytoplankton class abundance relative to total chl *a* based on CHEMTAX model versus site for all quarterly sampling dates from summer 2016 through summer 2018 in Slat Bayou Estuary. Pie plots reflect proportions of the class sum for all sites

Table 7. Percent surface irradiance reaching the bottom sediment for microphytobenthos production.

	% Surface Irradiance								
site	Su16	F16	W17	Sp17	Su17	F17	W18	Sp18	Su18
1	8.5	28.0	5.1	3.9	5.5	15.3	5.6	3.5	3.0
2	0.8	8.2	0.3	0.0	2.5	5.4	0.2	4.2	3.8
3	0.1	4.9	0.0	1.1	3.5	4.4	0.0	9.2	0.2
4	0.0	1.6	0.0	1.5	0.5	3.6	0.0	1.5	1.2
5	0.2	2.7	1.9	3.5	3.1	9.4	1.9	2.1	6.0
6	1.4	4.8	8.6	2.0	1.7	6.0	0.0	6.8	4.3

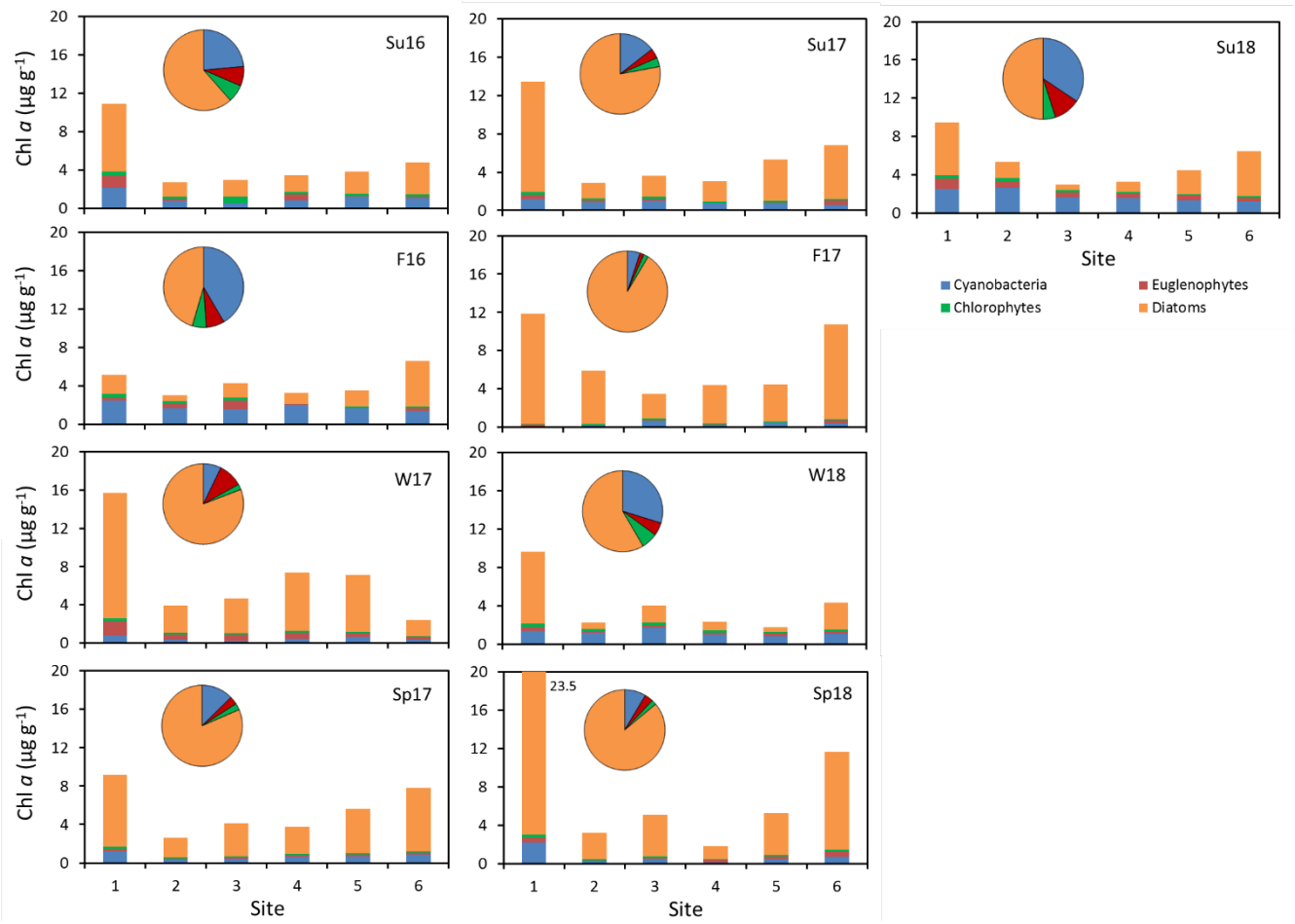

Figure 15. Microphytobenthos class abundance relative to total chl *a* based on CHEMTAX model versus site for all quarterly sampling dates from summer 2016 through summer 2018 in Slat Bayou Estuary. Pie plots reflect proportions of the class sum for all sites

a higher percentage of surface photosynthetically active radiation (PAR) reaching the bottom for microphytobenthos production. This is due to the shallow depth at site 1, 0.5 m, and the lower light attenuation coefficient at the deeper site 6. However, there was not a significant correlation between total chlorophyll *a* in microphytobenthos and the percent PAR reaching the bottom when all surveys are analyzed. No other physicochemical parameters measured in the water column correlated significantly with total chlorophyll *a* or abundance of specific classes of microphytobenthos for the overall data set.

The SSU rDNA sequence analysis identified cyanobacteria and eukaryotic algae at greater taxonomic specificity than the CHEMTAX analysis of photopigment profiles. It is important to note that the two methods do not yield the same relative abundances of algal classes for either phytoplankton or microphytobenthose (Fig. 16), in part due to the differences in DNA extraction efficiency and gene copy number relative to chlorophyll *a* content for cyanobacteria and eukaryotic algea. The relative abundance of cyanobacteria in the phytoplankton is 3.3 times greater by SSU rDNA than CHEMTAX analyses. For phytoplankton communities overall sites and survey dates, the relative abundance of chlorophytes, cryptophytes, euglenoids, dinoflagellates, and prasinophytes were about 2.5, 14, 5, 2.7, and 17 times less in the SSU rDNA sequence analysis than CHEMTAX model results for photopigments. *Karenia* SSU rDNA sequences were extremely rare, and less abundant than other algal taxa known to contain gyroxanthin-diester or gyroxanthin-diester-like pigment, including the toxic Pelagophyte, *Aureococcus anophagefferens,* and the toxic Prymnesiophyte, *Phaeocystis globosa* and *Chrysochromulina* sp. Both classes were detected by SSU rDNA, but due to their low relative abundance (≤0.01%) so they were excluded in CHEMTAX modeling. The most dominant cyanobacterium in the phytoplankton was *Synechococcus* (45 % of all phytoplankton SSU rDNA sequences), *Cyanobacterium* (6 %), *Cyanobium* (5 %) and *Atelocyanobacterium* sp. (5 %); however the last genera includes species known to be a heterotrophic N_2-fixing endosymbiont of Prymnesiophyte, *Chrysochromulina* sp. The dominant diatom genera in the phytoplankton communities were *Skeletonema* sp., (7 %) *Thalassiosira* sp. (5%), and dominant Chlorophyte was *Ostreococcus* sp.(4 %). There were an additional ten more minor algal classes detected by SSU rDNA sequences, which were not included in CHEMTAX modelling.

Likewise, cyanobacteria in the microphytobenthos were 2.3 times greater in relative abundance based on SSU rDNA than CHEMTAX modelling of photopigments. Diatoms, chlorophytes, and euglenoids were 1.4, 3, and 8 times less in SSU rDNA relative abundance than that in CHEMTAX modeling. Cyanobacteria genera dominant in the microphytobenthos include, *Synechococcus* sp. (24 % of all microphytobenthos SSU rDNA sequences), *Cyanobacterium* sp. (12 %), *Cyanobium* sp. (4 %), Dominant diatom genera include *Thalassiosira* (16 %), *Skeletonema* (14 %), *Asterionellopsis* sp. (6 %), *Bacillaria* sp. (5 %). The diatom community richness of genera was greater in the microphytobenthos (32) than phytoplankton (n = 12). There was an additional twelve minor algal classes detected by SSU rDNA sequences, which were not included in CHEMTAX modelling. Although CHEMTAX model analysis was restricted to fewer classes for the microphytobenthos than phytoplankton, the genera level richness was great based on SSU rDNA sequences. Based on all SSU rDNA OTUs, the community structure between sites on each sampling date was more often driven by salinity for the phytoplankton than the microphytobenthos (Fig. 17).

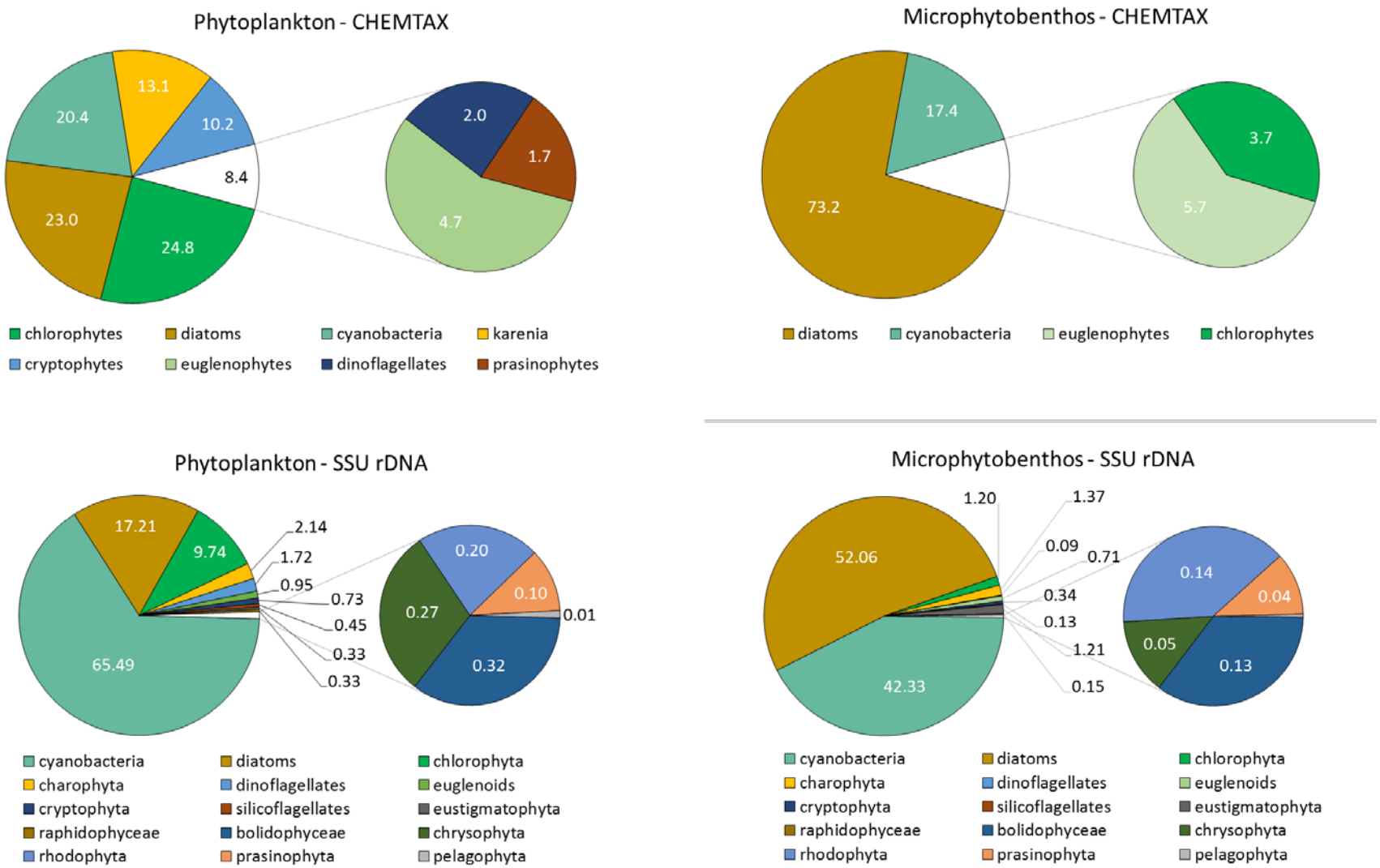

Figure 16. Relative proportions of algal classes for all sites and seasons sampled from summer 2016 through summer 2018 based on CHEMTAX modeling of photopigments(top) and SSU rDNA sequences (bottom) for phytoplankton (left) and microphytobenthos (right) communities.

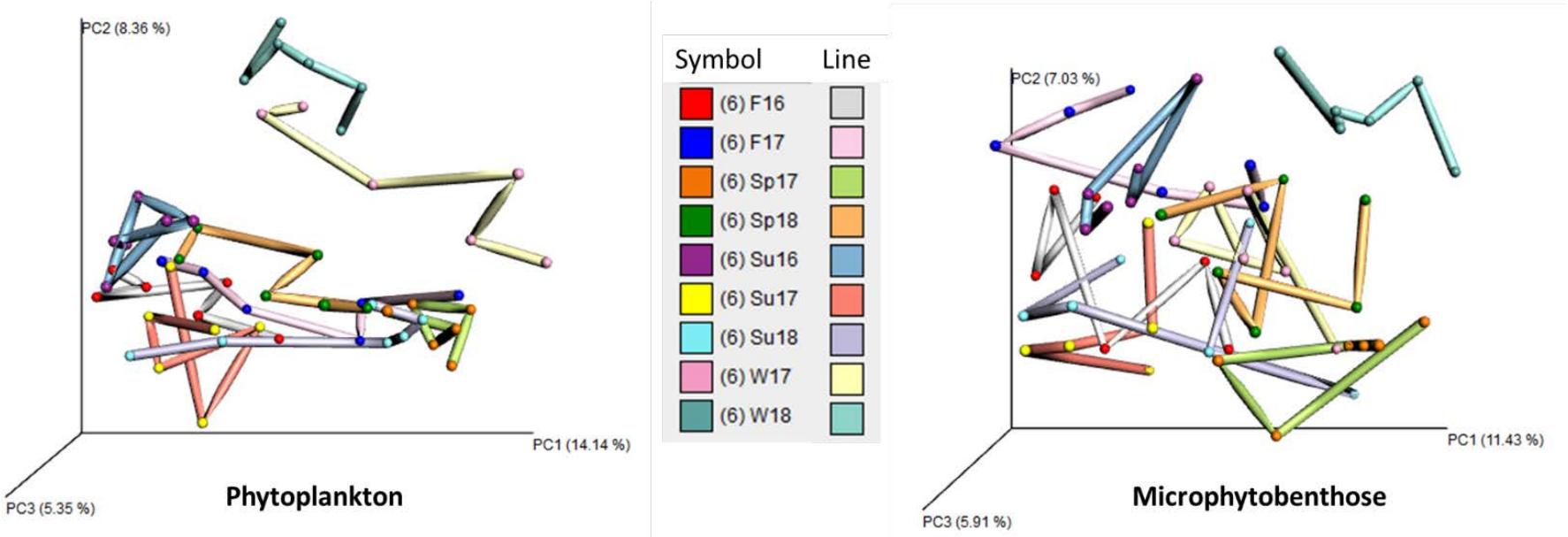

Figure 17 *(above)*. Principle coordinates analysis of Bray-Curtis dissimilarities for algal OTUs in phytoplankton (A) and microphytobenthos (B) for all sampling dates and sites. Sites per date connected based on increasing salinity gradient.

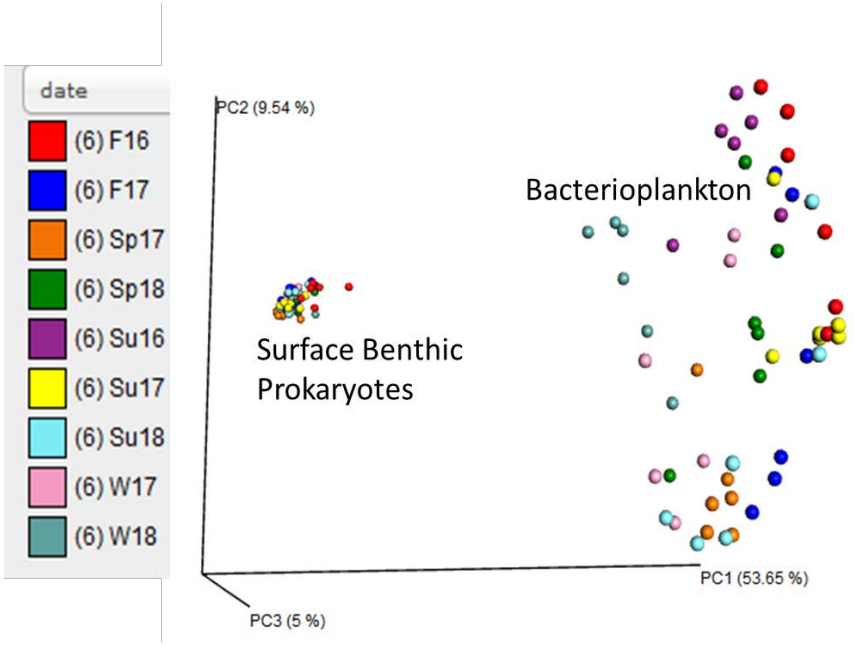

Figure 18 *(left)*. Principle coordinates analysis of Bray-Curtis dissimilarities for prokaryote OTUs in bacterioplankton (larger spheres) and surface benthic (smaller spheres) communities for all quarterly samplings and sites from summer 2016 through summer 2018 in Salt Bayou Estuary.

The importance of salinity in driving phytoplankton more so than microphytobenthis community structure was supported by Mantel test results between community distance and salinity matrices (r = 0.53 versus r = 0.14 for phytoplankton and MPB, respectively).

Quarterly Sampling of Salt Bayou Estuary Prokaryote Secondary Producer Communities:

Bacterioplankton and the surface benthic prokaryotes (non-cyanobacterial prokaryotes in the microphytobenthose samples) communities, like primary producers, were distinctly different (Fig. 18). This conclusion is based on a principle coordinates analysis (PCoA) of all SSU rDNA OTUs in both plankton and surface sediment samples, which explained 69 % of variance in the Bray-Curtis dissimilarity dataset, and ANOSIM test with $P < 0.01$. There were great differences among sites on many quarterly sampling dates for bacterioplankton (Fig. 18, see fall and winter surveys) than all sites and survey dates for surface benthic prokaryotes (ANOSIM), $P < 0.01$. When these results were analyzed separately, the first three PCoA for bacterioplankton and surface benthic prokaryotes explained 60 % and 36 % of variance, respectively (Fig. 19). Salinity was a more important driver of community differences among sites on most survey date for bacterioplankton than surface benthic prokaryotes. Exceptions to the latter were in summer 2016 and 2017, when there was the least variability in salinity among survey dates.

Based on the overall data sets for each community, the diversity of dominant prokaryote orders (>1 % relative abundance), excluding cyanobacteria, was in the surface benthos (Fig. 20). Based on survey data relative abundance (all sites), Pelagibacterales was 8-30 % of the bacterioplankton, with the lowest abundance when average salinity was lowest (Su16, F16, and W18), which is not unexpected for this common marine bacterium.

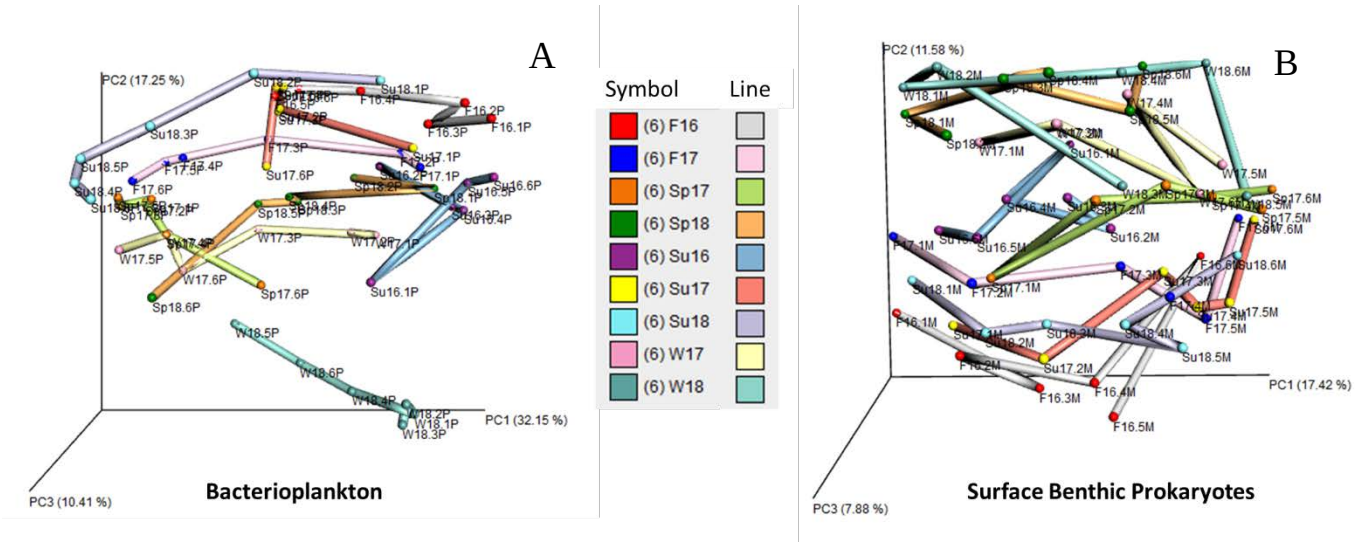

Figure 19. Principle coordinates analysis of Bray-Curtis dissimilarities for prokaryote OTUs in bacterioplankton (A) and surface benthic (B) communities for all quarterly samplings and sites from summer 2016 through summer 2018 in Salt Bayou Estuary. Sites are connected by lines of increasing salinity for each date.

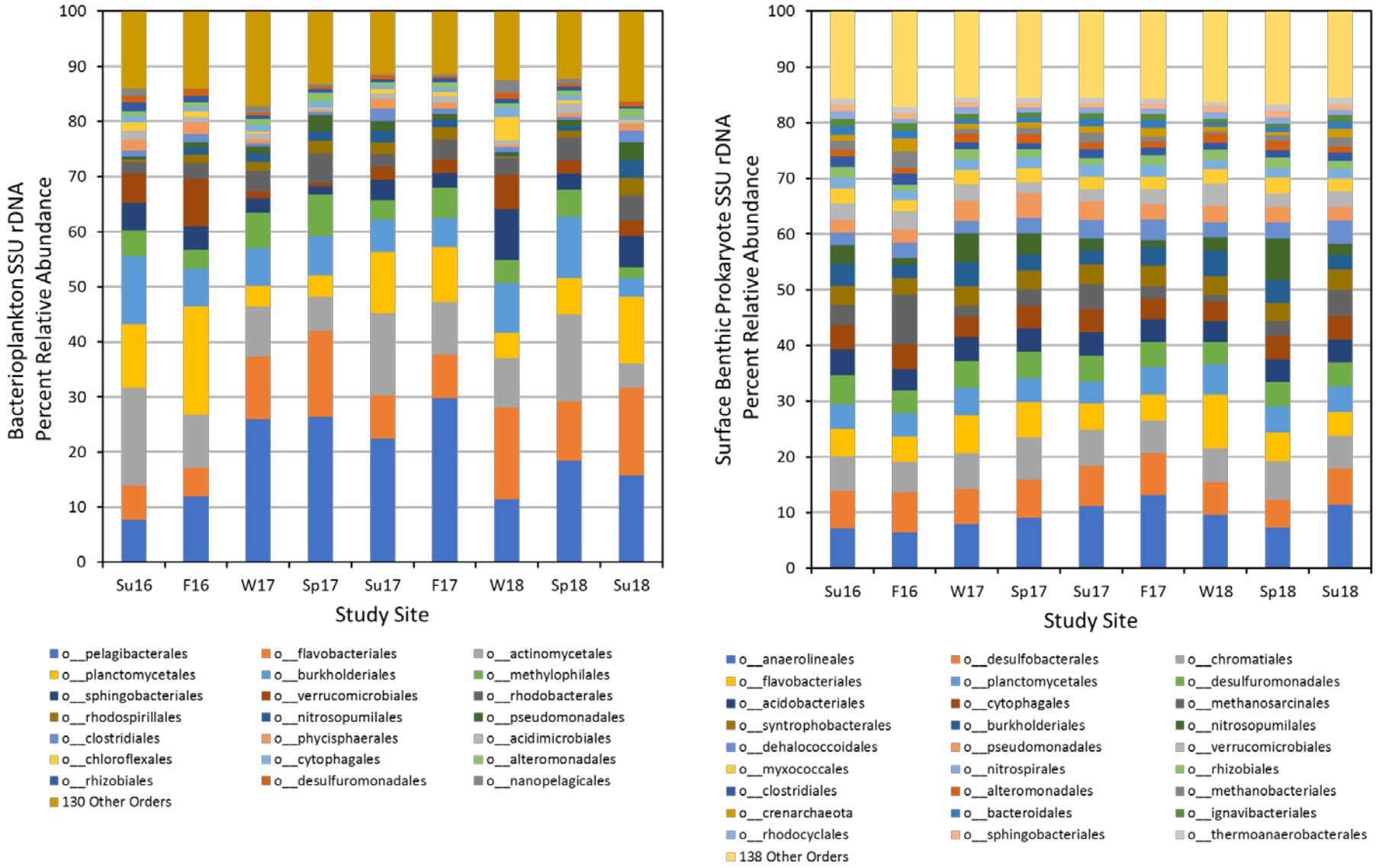

Figure 20. Percent relative abundance of SSU rDNA sequences for predominant orders of prokaryotes in the bacterioplankton (left) and surface sediment (right) for all site combined at each quarterly sampling from summer 2016 through summer 2018.

Table 8. Pearson correlation matrix for the abundance of dominant bacterioplankton orders and physicochemical parameters

	site	pelagibacterales	flavobacteriales	actinomycetales	planctomycetales	burkholderiales	methylophilales	sphingobacteriales	rhodobacterales	verrucomicrobiales	rhodospirillales	nitrosopumilales	pseudomonadales	clostridiales	phycisphaerales	acidimicrobiales	cytophagales	alteromonadales	chloroflexales	rhizobiales	desulfuromonadales	nanopelagicales
site	1.00																					
pelagibacterales	0.00	1.00																				
flavobacteriales	0.08	0.33	1.00																			
actinomycetales	-0.43	-0.06	-0.15	1.00																		
planctomycetales	-0.46	-0.34	-0.56	0.37	1.00																	
burkholderiales	-0.46	-0.15	0.09	0.87	0.29	1.00																
methylophilales	-0.22	0.58	0.44	0.40	-0.17	0.52	1.00															
sphingobacteriales	-0.54	-0.46	0.00	0.41	0.46	0.57	-0.03	1.00														
rhodobacterales	-0.03	0.36	0.63	-0.17	-0.25	0.07	0.43	-0.17	1.00													
verrucomicrobiales	-0.48	-0.53	-0.24	0.37	0.78	0.47	-0.09	0.74	-0.24	1.00												
rhodospirillales	0.09	0.59	0.20	-0.44	-0.20	-0.50	0.16	-0.53	0.43	-0.50	1.00											
nitrosopumilales	0.29	0.32	0.08	-0.48	-0.28	-0.54	-0.08	-0.43	0.25	-0.49	0.67	1.00										
pseudomonadales	-0.03	0.57	0.34	-0.42	-0.33	-0.41	0.24	-0.44	0.38	-0.50	0.79	0.56	1.00									
clostridiales	-0.35	-0.18	-0.30	0.29	0.48	0.06	-0.26	0.27	-0.42	0.40	-0.01	-0.17	-0.04	1.00								
phycisphaerales	-0.34	-0.28	-0.58	0.61	0.85	0.44	-0.04	0.44	-0.34	0.65	-0.24	-0.27	-0.36	0.52	1.00							
acidimicrobiales	-0.31	-0.01	-0.15	0.78	0.32	0.68	0.33	0.35	-0.17	0.33	-0.42	-0.45	-0.45	0.05	0.53	1.00						
cytophagales	-0.35	-0.06	0.29	0.39	0.12	0.69	0.50	0.62	0.27	0.39	-0.39	-0.31	-0.27	-0.17	0.12	0.38	1.00					
alteromonadales	0.05	0.28	0.62	-0.09	-0.25	0.19	0.55	-0.12	0.78	-0.16	0.47	0.29	0.41	-0.32	-0.25	-0.14	0.30	1.00				
chloroflexales	-0.38	-0.41	0.16	0.19	0.16	0.31	-0.06	0.66	-0.21	0.58	-0.47	-0.40	-0.39	0.27	0.13	0.08	0.32	-0.17	1.00			
rhizobiales	-0.34	-0.30	-0.06	0.66	0.48	0.78	0.27	0.50	0.16	0.56	-0.39	-0.35	-0.43	0.19	0.56	0.51	0.58	0.26	0.25	1.00		
desulfuromonadales	-0.41	-0.45	-0.06	0.43	0.58	0.53	0.04	0.66	-0.16	0.83	-0.38	-0.32	-0.28	0.36	0.63	0.31	0.40	0.01	0.58	0.59	1.00	
nanopelagicales	-0.28	-0.09	0.36	0.51	-0.10	0.68	0.28	0.53	0.15	0.15	-0.46	-0.34	-0.37	-0.05	0.01	0.40	0.62	0.14	0.42	0.56	0.21	1.00
bacteria	-0.61	0.22	0.23	0.73	0.40	0.81	0.65	0.56	0.24	0.49	-0.15	-0.30	-0.09	0.20	0.49	0.59	0.68	0.32	0.29	0.67	0.56	0.54
Salinity	0.46	0.24	0.14	-0.75	-0.44	-0.78	-0.25	-0.62	0.23	-0.59	0.66	0.64	0.56	-0.21	-0.50	-0.60	-0.58	0.27	-0.49	-0.60	-0.57	-0.55
Temp_C	0.07	-0.35	-0.24	0.25	0.16	0.07	-0.34	-0.07	-0.26	-0.03	0.04	0.05	0.12	0.40	0.31	0.03	-0.38	-0.17	-0.16	0.07	0.18	-0.18
TSS	-0.05	0.20	0.08	-0.09	-0.15	-0.03	0.19	-0.03	0.03	-0.07	0.10	0.36	0.29	-0.17	-0.08	-0.12	0.15	0.26	-0.19	-0.03	0.11	-0.04
PP_chla	-0.51	-0.16	-0.10	0.58	0.56	0.62	0.22	0.67	-0.01	0.65	-0.29	-0.21	-0.27	0.33	0.66	0.46	0.53	0.09	0.29	0.65	0.68	0.40
nh4	0.43	-0.36	-0.05	-0.15	-0.08	-0.04	-0.12	-0.18	-0.08	-0.07	-0.18	-0.09	-0.20	-0.09	-0.09	-0.14	-0.02	0.08	-0.08	0.11	-0.09	-0.04
no2	0.39	-0.11	0.02	-0.09	-0.16	-0.15	-0.13	-0.19	-0.01	-0.18	0.02	0.47	-0.08	-0.03	-0.11	-0.09	-0.06	0.01	-0.09	-0.04	-0.16	-0.07
no3	0.39	0.14	0.10	-0.33	-0.28	-0.25	0.08	-0.28	0.20	-0.30	0.19	0.13	0.04	-0.36	-0.36	-0.21	-0.11	0.12	-0.16	-0.20	-0.40	-0.11
din	0.52	-0.20	0.02	-0.25	-0.20	-0.16	-0.07	-0.27	0.03	-0.21	-0.03	0.07	-0.12	-0.21	-0.23	-0.19	-0.07	0.11	-0.13	-0.02	-0.25	-0.08
srp	-0.31	-0.29	-0.36	0.62	0.73	0.52	0.13	0.32	-0.23	0.64	-0.25	-0.30	-0.34	0.41	0.75	0.53	0.19	-0.01	0.05	0.59	0.55	0.09
din_srp	0.56	-0.04	0.18	-0.40	-0.39	-0.26	-0.02	-0.33	0.16	-0.35	0.08	0.13	0.00	-0.35	-0.44	-0.30	-0.11	0.18	-0.11	-0.18	-0.39	-0.08
sio2	-0.29	-0.04	-0.51	0.39	0.69	0.19	0.07	0.01	-0.17	0.42	0.02	-0.08	-0.07	0.47	0.69	0.30	-0.04	-0.15	-0.12	0.35	0.40	-0.25
doc	-0.57	-0.37	-0.32	0.78	0.70	0.76	0.18	0.61	-0.23	0.76	-0.48	-0.57	-0.50	0.46	0.73	0.58	0.44	-0.13	0.37	0.75	0.68	0.37

p < 0.05
p < 0.01
p < 0.001

Flavobacteriales, Actinomycetales, Planctomycetales, Burkholderiales, Methylophilales, Sphingobacteriales, and Verrucomicrobiales, all exceeded 8% of the bacterioplankton relative abundance in at least on survey period. Fewer orders had this degree of relative abundance in the surface benthos, which included Anaerolineales, Desulfobacterales, Chromatiales, and Flavobacteriales (Fig. 20). About 140 other aerobic and anaerobic Bacteria orders were in the surface benthic prokaryote community, as were the methanogenic Archaea, Methanobacteriales and Methanosarcinales, which had a strong positive correlation ($R^2 = 0.94$). No dominant orders of the surface benthic prokaryote community correlated with physicochemical parameters measured in the water column, including salinity, suggesting they may be more resilient to changes in water column conditions.

The proportion of dominant prokaryotes to total bacterioplankton abundance by site for each quarterly survey (Fig. 21) illustrates some of the correlations among taxa (Table 8). Sphingobacteriales had a moderate positive correlation with Verrucomicrobiales ($R^2 = 0.54$), and weaker positive correlations (R^2 values of 0.3 - 0.5) with Burkholderiales, Cytophagales, Chloroflexales, Desulfuromonadales. Burkholderiales also had a strong positive correlation with Actinomycetales, Rhizobiales, and weaker positive correlations with Acidomicrobiales, Cytophagales, and Nanopelagicales. Most of these orders (Actinomycetales, Burkholderiales, Sphingobacteriales, Verrucomycetales, Acidomicrobiales, Cytophagales, Rhizobiales, Desulfurmonadales, and Nanopelagicales) negatively correlated to some degree with salinity and positively correlated with DOC and SRP (Table 8). The latter result suggest that members of these orders may become more abundant in the bacterioplankton if the salinity regime decreases due to increased freshwater supply from north of the ICWW, via inverted siphons, which may bring additional terrestrial DOC into the estuary. In contrast, Rhodospirillales, Nitrosopumilales, and Pseudomonadales positively correlated with salinity. There was no correlation with water temperature for any dominant orders (Table 8) and Mantel test comparison of Bray-Curtis dissimilarities of bacterioplankton and temperature difference matrices were very weakly correlated ($R^2 = 0.01$), together inferring other factors than seasonal water temperature changes drive community structure. However, comparison of Bray-Curtis dissimilarities of bacterioplankton to either salinity or DOC gave moderate positive correlations, based on Mantel test results with R^2 values of 0.43 and 0.30, respectively. Controlling for salinity, the partial Mantel test R^2 for bacterioplankton communities and DOC reduced to 0.09. This result further suggests that salinity is a major driver of bacterioplankton community structure, and should be sensitive to increased freshwater inflows.

Salt Bayou Estuary Conclusion:

Over two years of continuous monitoring at the KJ-sonde site indicate that the target salinity regime of < 10 psu for 80% of time has not been met by the installation of the KLFP Baffle alone. In the past 16 month of continuous monitoring results at both the KJ and KLFP sonde sites were highly correlated, suggesting that future monitoring only needs to be performed at one of these sites. Saved resources can be diverted to begin monitoring in the upper portion of the estuary near the new inverted siphon outflow of freshwater from north of the ICWW.

Phytoplankton biomass, as chlorophyll *a*, did not follow distinct seasonality. In fact lower values were in spring months. Frequency of precipitation and wind patterns appear to have major influences on this ecosystem by causing salinity variation and turbidity events throughout the year. Based on low (< 11) DIN:SRP ratios, the ecosystem appears N-limited, yet phytoplankton biomass correlates with SRP, as did some major classed. Cyanobacteria, Diatoms and Chlorophytes dominate Phytoplankton communities; whereas Diatoms dominate the microphytobenthos. There is a potential for Karenia red tide blooms, given the ample gyroxanthin content in the phytoplankton; alternatively this pigment could be present in other taxa, such as the Pelagophyte, *Aureococcus anophagefferens*, and the toxic Prymnesiophyte, *Phaeocystis globosa* and *Chrysochromulina* sp., all detected by SSU rDNA analysis. Salinity was important in partly controling phytoplankton community structure, but not so much for the microphytobenthos community. Freshwater runoff contributes to DOC, an important driver of bacterioplankton biomass, as well as their community structure, in addition to salinity.

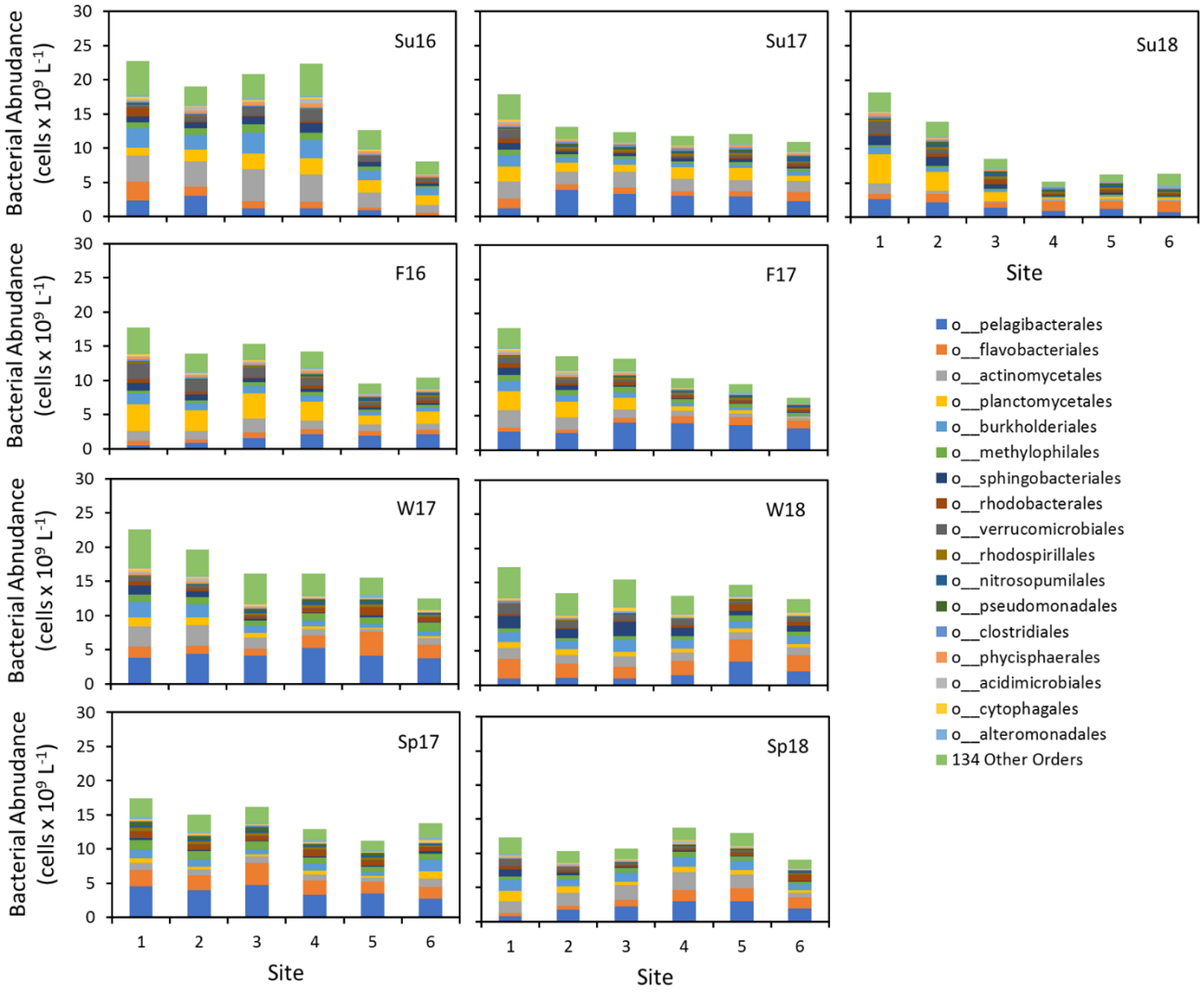

Figure 21. Bacterioplankton abundance of dominant prokaryote orders versus site for all Salt Bayou Estuary survey dates

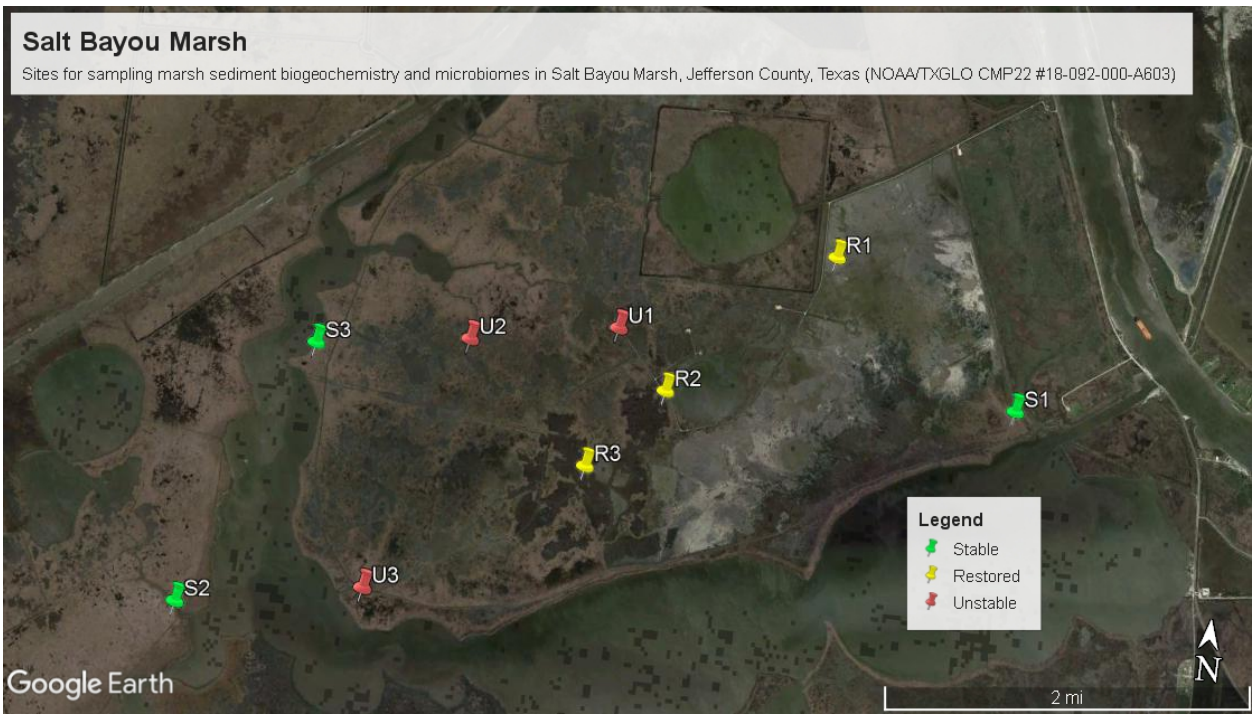

Figure 22. Map of Salt Bayou Watershed marsh sampling sites distinguished by habitat type, stable (S), unstable (U) and restored (R).

Task 3 - Monitor Marsh Sediment Biogeochemistry:

Seasonal Survey of Porewater and Sediment Geochemistry:

Four quarterly sampling campaigns of nine marsh sites (Fig. 22) have been completed and sediment and porewater geochemical parameters analyzed for winter, spring, and summer sampling. Variation among sites of similar habitat type (restored, stable and unstable) and within specific sites was large for porewater sulfide and sediment redox. However, phytotoxic levels of porewater sulfide (>1.0 mM) were typical at unstable marsh sites in both winter and spring (Fig. 23A). Porewater ammonium concentrations (Fig. 23B) at unstable sites were over 12 times greater than at restored sites in winter, but this difference decreased in spring as soil temperatures warmed (Fig. 24A) at the onset of the marsh grass growing season. Lower pH (Fig. 23D) in spring than winter suggests greater decomposition (microbial respiration) as the sediment warmed. Salinity (Fig. 23C) was lowest at these unstable sites compared the restored sites. One hypothesis for the cause of marsh vegetation dieback has been that higher salinity, and hence sulfate supply, drives greater sulfate reducer activity, which creates the potential for sulfide accumulation in porewaters. Instead, porewaters at restored sites had elevated chloride and salinity and

lowest values of both sulfide and sulfate relative to unstable sites (Fig. 23F), especially in winter. At stable sites, salinity was also elevated relative to unstable sites, and there was a more seasonal trend sulfide and sulfate. At these sites sulfide accumulated in winter and was nearly absent in summer and fall, when sulfate was in greater concentration. Overall sites and survey dates salinity correlated negatively with sulfide and positively with sulfate, although the relationship was weak (Table 9; R^2 values of 0.16 and 0.19, respectively). Additional factors are needed to explain sulfide accumulation in porewaters than salinity and sulfate content alone.

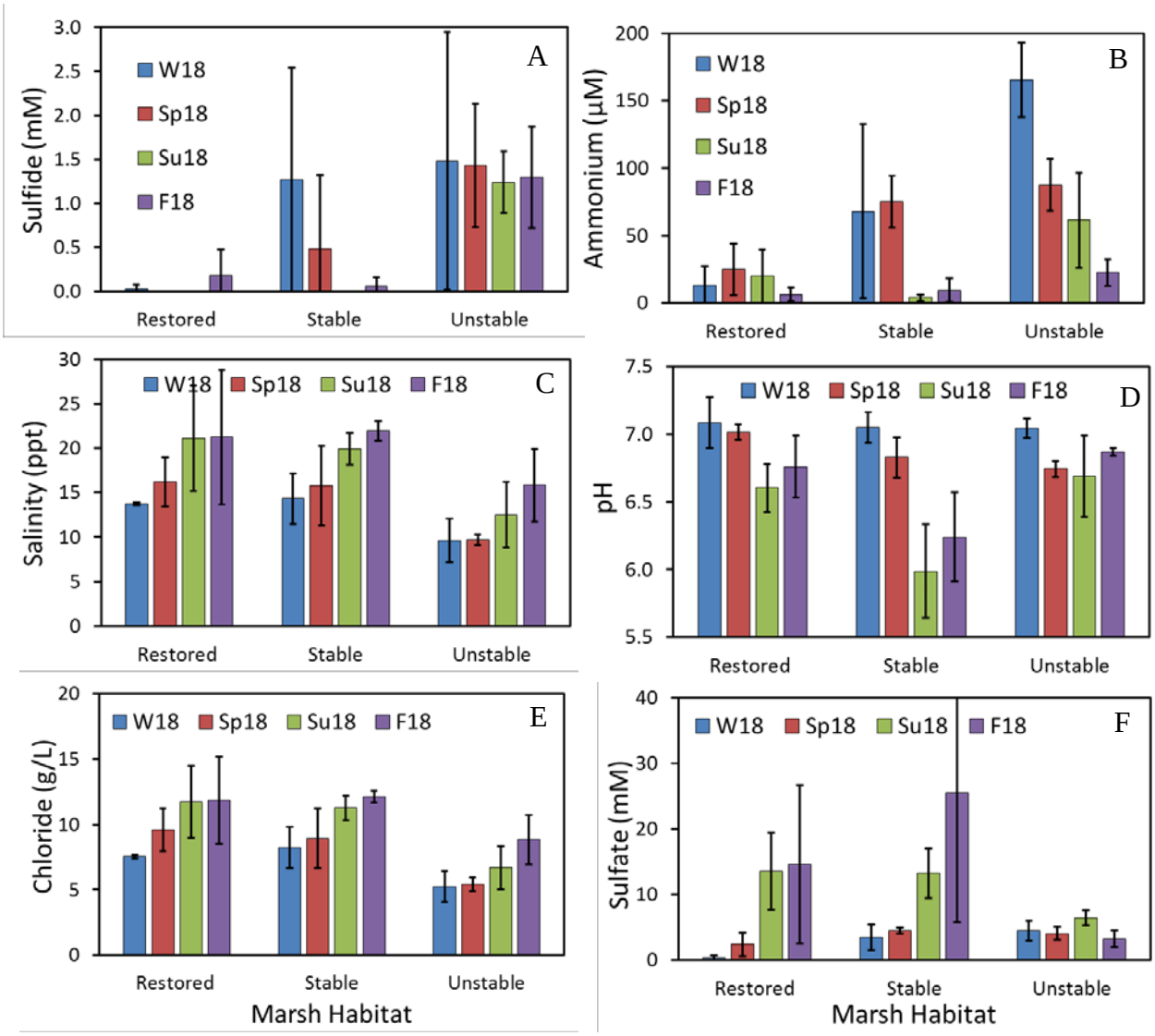

Figure 23. The mean (±SD; n=3 sites) of site means for sediment porewater analytes (A, sulfide; B, ammonium; C, salinity; D, pH; E, chloride, F, sulfate) by habitat type (restored, stable, unstable). Porewater was collected from a 15 cm sediment depth.

Subsidence and lack of sufficient accretion of marsh sediment facilitates inundation, water dominated sediments, and anaerobic conditions, especially when organic content is high. These conditions promote growth of sulfate reducing prokaryotes when there is a supply of sulfate and methanogens when sulfate is lacking. Marsh grass roots can also supply oxygen to the sediments; hence to mitigate anoxia at the rhizosphere. Redox potential at the 15 cm sediment depth of porewater sampling was most positive at stable sites during spring and summer, during the vegetation growing season (Fig. 24). Restored sites generally had lower redox potential than stable sites, except for winter when there was more senesced aboveground biomass. During spring sampling, the water table had dropped below the 15 cm sampling depth for porewater at stable and restored sites, but not at unstable sites, which is evidence of their higher elevation. Warmer temperatures weakly

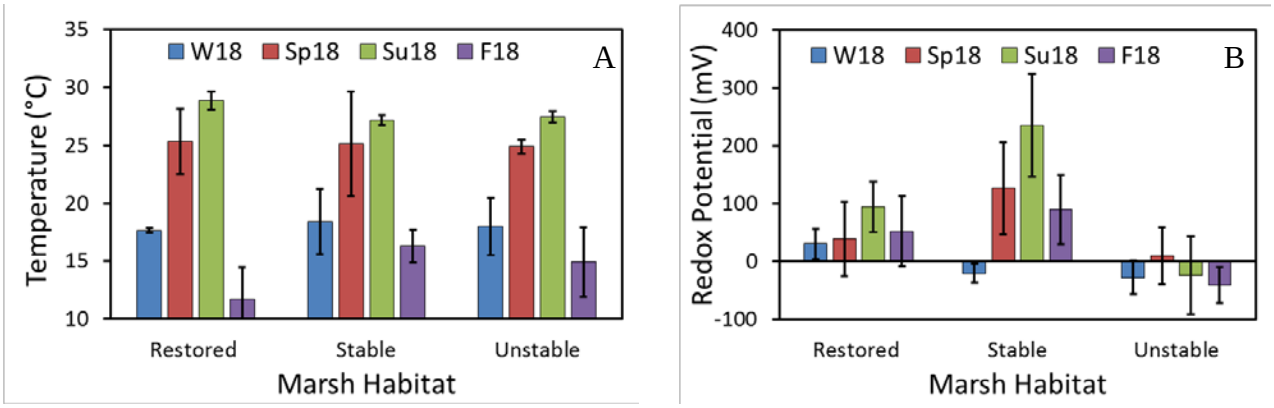

Figure 24. The mean (±SD; n=3) for sediment temperature (A) and redox potential (B) by habitat type (restored, stable, unstable). Measurements made at a 15 cm sediment depth.

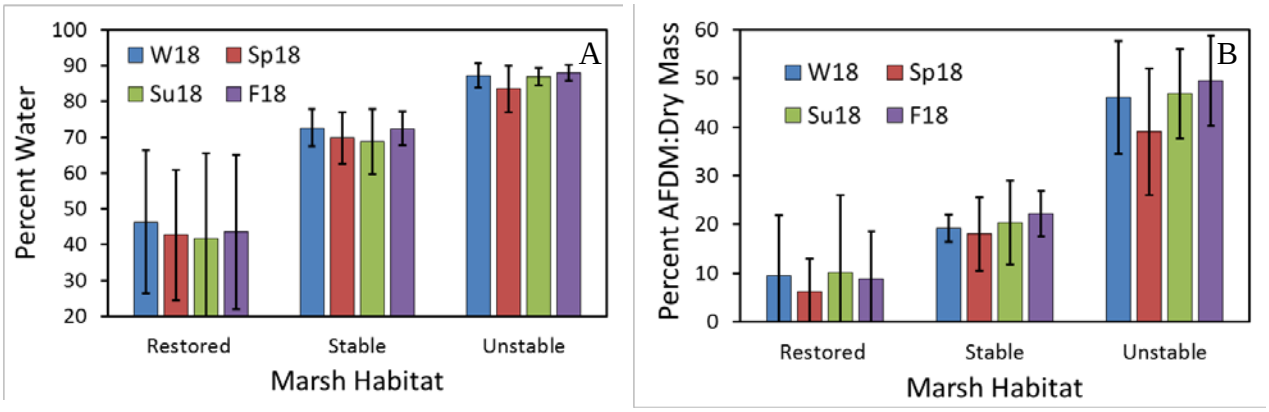

Figure 25. The mean (±SD; n=3) at each habitat type (restored, stable, unstable) for sediment percent water content (A) and percent ash free dry mass (AFDM) of dry sediment (B). Measurements made for homogenized sediment between 12.5 and 17.5 cm depths.

correlated (R^2 = 0.09) with more positive redox potential (Table 9). The most negative redox potential was at stable and unstable sites in winter, and unstable sites generally had negative redox values in other seasons. Redox negative correlated with water and organic content, but the relationship was weak (R^2 < 0.2; Table 9)

Unstable sites were selected because of their obvious state of inundation, so it was expected that these would have the highest water content (ca. 85 % of wet mass) and ash free dry mass (AFDM; a proxy for organic content; 45 % of dry mass) and restored sites the lowest water content and remaining dry mass with just about 10% organic content (Fig. 25). There was a strong correlation between water content and AFDM content (R^2 = 0.77), which also correlated with porewater ammonium and sulfide concentrations and negatively correlated with salinity (Table 9).

Table 9: Pearson correlation matrix for all marsh sediment and porewater parameters for all samples per site for all seasons from Feb 2018 through Dec 2018

	Chloride	Sulfate	Sulfide	Salinity	pH	NH_4+	NO_3-	ORP	Temp	Sed_H_2O
Chloride	1.00									
Sulfate	0.42	1.00								
Sulfide	-0.40	-0.23	1.00							
Salinity	0.99	0.44	-0.41	1.00						
pH	-0.32	-0.50	0.28	-0.34	1.00					
NH_4+	-0.54	-0.21	0.63	-0.54	0.23	1.00				
NO_3-	0.04	0.07	-0.12	0.03	0.01	-0.07	1.00			
ORP	0.38	0.33	-0.31	0.37	-0.46	-0.24	0.06	1.00		
Temp	-0.02	-0.07	-0.01	-0.03	-0.21	0.06	0.03	0.29	1.00	
Sed_H_2O	-0.53	-0.17	0.46	-0.51	-0.08	0.41	-0.23	-0.30	-0.04	1.00
SED_AFDM	-0.52	-0.18	0.40	-0.51	0.01	0.38	-0.31	-0.39	-0.04	0.88

Percent variance explained = < 20 %; 20-40 %; > 70%.
Non-signifcant relationships are grey.

Marsh Porewater and Sediment Geochemistry Overall Principle Components Analysis:

Principle component analysis reveals clear trends with site habitat type (restored, stable, and unstable) and season (Fig. 26). Using all transect point samples for all sites and quarterly survey dates, the first two PCs explained 58 % of variance in the dataset for

porewater and sediment geochemical parameters. Unstable sites were most similar throughout the year, suggested by the tighter clustering (Fig, 26). Generally, unstable sites were characterized by anaerobic conditions favoring decomposition of dead vegetative biomass by sulfate reducing bacteria, and more so in winter and spring. Specifically, the supply of organic matter and sulfate in anaerobic conditions leads to phytotoxic levels of sulfide and ammonium in porewaters. Stable sites were more similar to unstable sites than restored sites, except for the R1 site which clustered within the stable sites. These

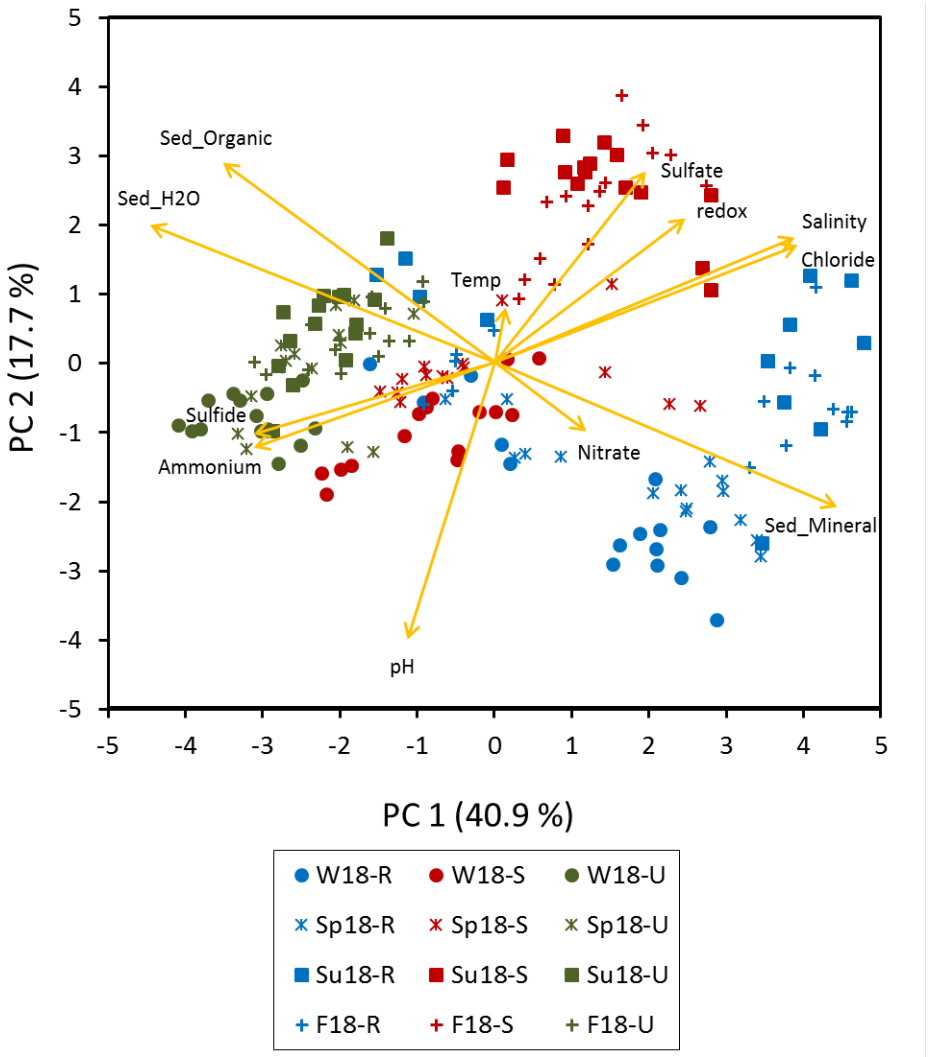

Figure 26. Principle component analyses of marsh sediment geochemical parameters analyzed to for four seasons sampled, with loading vectors for each parameter. Symbol color reflects restored (R), stable (S), and unstable (U) sites sampled in winter (circle), spring (hex), summer (box), and fall (cross) 2018.

differences were mostly driven by sediment content of water, organics and mineral fractions. Restored sites R2 and R3 , were distinct from all other sites, driven by highest mineral content. Stable and restored sites also had seasonal differences mostly driven by conditions of anaerobic decomposition in the winter and spring, versus summer and fall when redox, salinity, and sulfate values were greatest. Sites of higher sediment elevation due to natural accretion processes (i.e. stable sites) or by using dredge material to elevate the sties (i.e. restored sites), there is a progressive shift away from conditions of anaerobic decomposition and plant stress.

Task 4: Define the Sulfate-Reducing Bacterial Community Structure in Marsh Sediments

Total Prokaryote Analysis of Marsh Sediment Communities:

Marsh sediment DNA extracts were analyzed for both relative abundance and identification of both SSU rDNA and the dissimilatory sulfite reductase B-subunit gene (*dsr*B) operational taxonomic units (OTUs). An OTU was defined as a sequence similarity cluster of ≥ 95% similarity. Picking OTUs and identification were performed in OIIME. Beta-diversity was assessed separately for SSU rDNA and dsrB by Bray-Curtis dissimilarities of all respective OTUs and then principle coordinates analysis was performed. Triplots of the first three PCs for each target gene cluster by site and quarterly survey date (Fig. 27). Clustering by marsh habitat state (restored, stable, or instable) was significant (ANOSIM test; $P < 0.01$). However, as with the porewater and sediment geochemical parameters, the communities at site R1 falls between

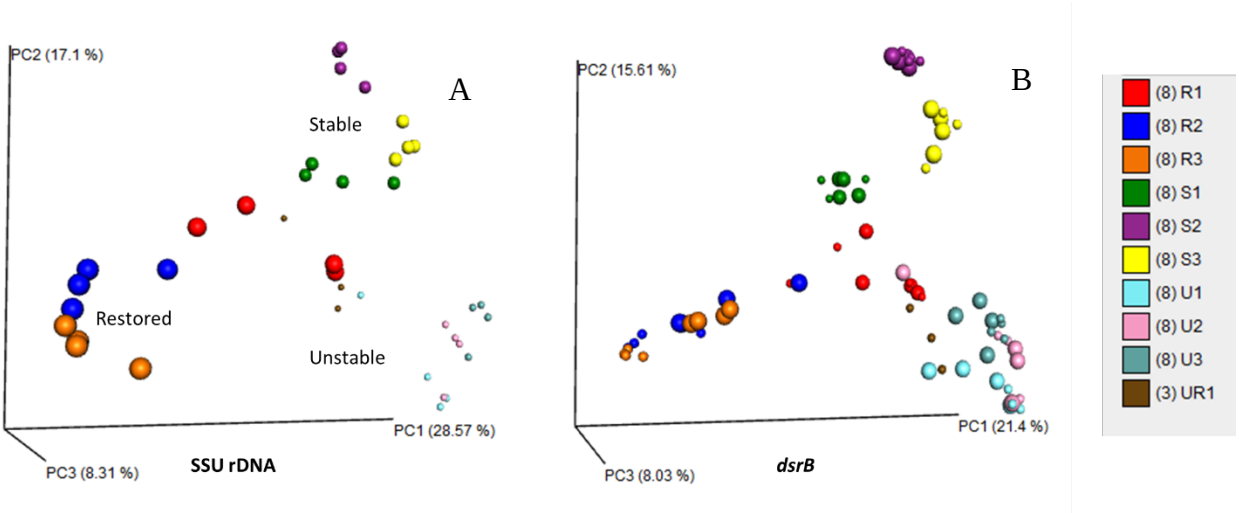

Figure 27. Principle coordinates analysis of Bray-Curtis dissimilarities for marsh sediment microbial communities (SSU rDNA; left; unstable small, stable mid-size, and restored large spheres) and specifically sulfate reducing communities (*dsr*B; right; DNA small and RNA large spheres) at all study sites and seasons based on OTUs.

the other restored sites and unstable sites. Three archived DNA extracts from the R1 site locations from fall, spring, and summer 2010, prior to BUDM restoration, were also included in these analyses. At this time the site was inundated and had geochemistry more similar to unstable sites reported here, and for this reason is labeled site UR1. The communities for UR1 cluster near the R1 site, which may suggest some degree of ineffectiveness of restoration at this site relative to R2 and R3, a time delay in seeing the full effect of restoration as R1 is a more recent project than R2 and R3. Comparison of the Bray-Curtis dissimilarity matrices for SSU rDNA (total prokaryote community) and dsrB (sulfate reducing prokaryotes only) were not significantly different (Mantel test; $P < 0.01$).

The overall taxonomic diversity at each site for all seasons combined was of similar composition for the total prokaryote community based on 25 dominant orders (> 1 % of all sequences; Fig. 28A). There was an additional 183 prokaryote orders identified in the dataset, which was not been explored in detail. Among the top 25 orders, there were numerous facultative anaerobic orders as well as obligate anaerobes, including 4 Cloroflexi (Green-Sulfur Bacteria), 4 methanogenic Euryarchaeota, and 6 sulfate reducing orders of varied phyla. There were differences in the relative abundances for some of these orders between site types. The methanogens, Methanosarcinales, Methanobacteriales, and Methanococcales were of greatest abundance in the unstable marsh sites compared to either stable or restored sites (Students-t test, $P< 0.01$; Fig, 29). The Cloroflexis order Dehalococcoidales, an organohalide respiring anaerobe, which like Methanobacteriales, and Methanococcales are hydrogenotrophic. The latter suggests an ample supply of H_2 from the fermentative portion of the community. In contrast, restored sites, or both restored and stable sites, had significantly greater relative abundance of sulfate reducing orders, Desulfobacterales, Desulfuromonadales, and Clostridiales, which includes Desulfotomaculum. In addition, Anaerolineales, Chromatiales, and Nitrospirales were in high abundance at restored and stable sites. All of these trends occurred each season. The less abundance of sulfate reducers and greater abundance of methanogens at the unstable sites was unexpected, especially given the elevated sulfide levels at unstable sites.

Sulfate Reducing Bacterial Analysis of Marsh Sediment Communities:

Focus was placed on defining any differences in the community of sulfate reducing bacteria (SRB), which include Bacteria and Archaea, as their metabolism results in sulfide production, which can accumulate to levels phytotoxic to coastal mash vegetation. The specific gene unique to this biogeochemical function is the dissimilatory sulfite reductase subunit-B gene (*dsr*B). Both DNA and RNA extracted from marsh sediments were analyzed for *dsr*B. The *dsr*B DNA sequencing, like that for SSU rDNA, is informative of community composition, but is limited to inferring the level of activity, growth, of function. Analysis of *dsr*B RNA relative to the *dsr*B DNA can provide insights to the relative activity (based on gene expression to RNA) of specific taxa. Bray-Curtis dissimilarity analyses of the each *dsr*B dataset, DNA and RNA, gave similar results for all sites and quarterly survey dates based on principle components analysis (Fig. 27B), and there was no significant difference in Bray-Curtis dissimilarity matrices (Mantel test; $R^2 = 0.88$; $P < 0.01$).

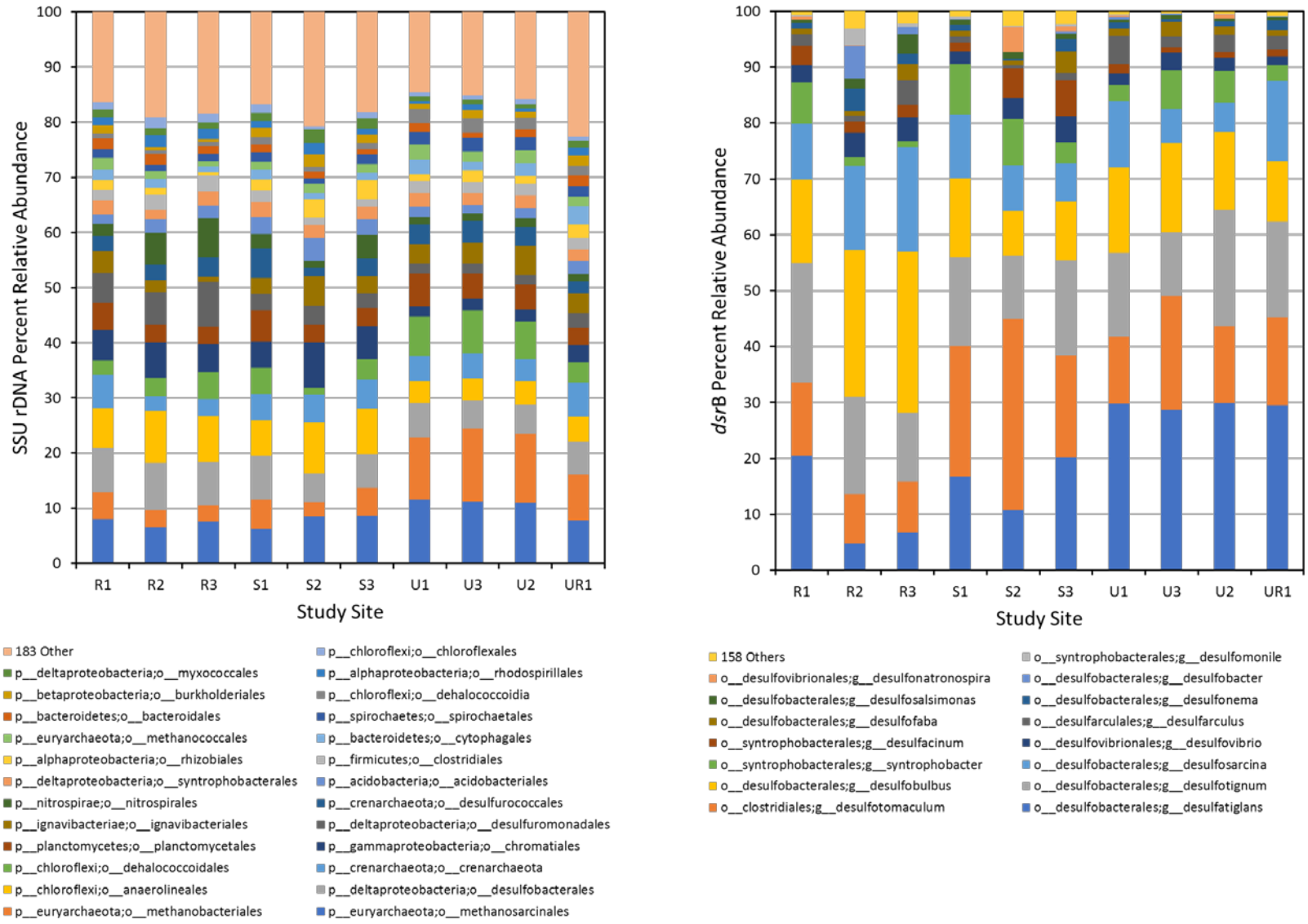

Figure 28. Percent relative abundance of SSU rDNA (left) and *dsr*B DNA (right) sequences for predominant orders and genera, respectively, at all marsh sediment sites for the combined seasonal samples.

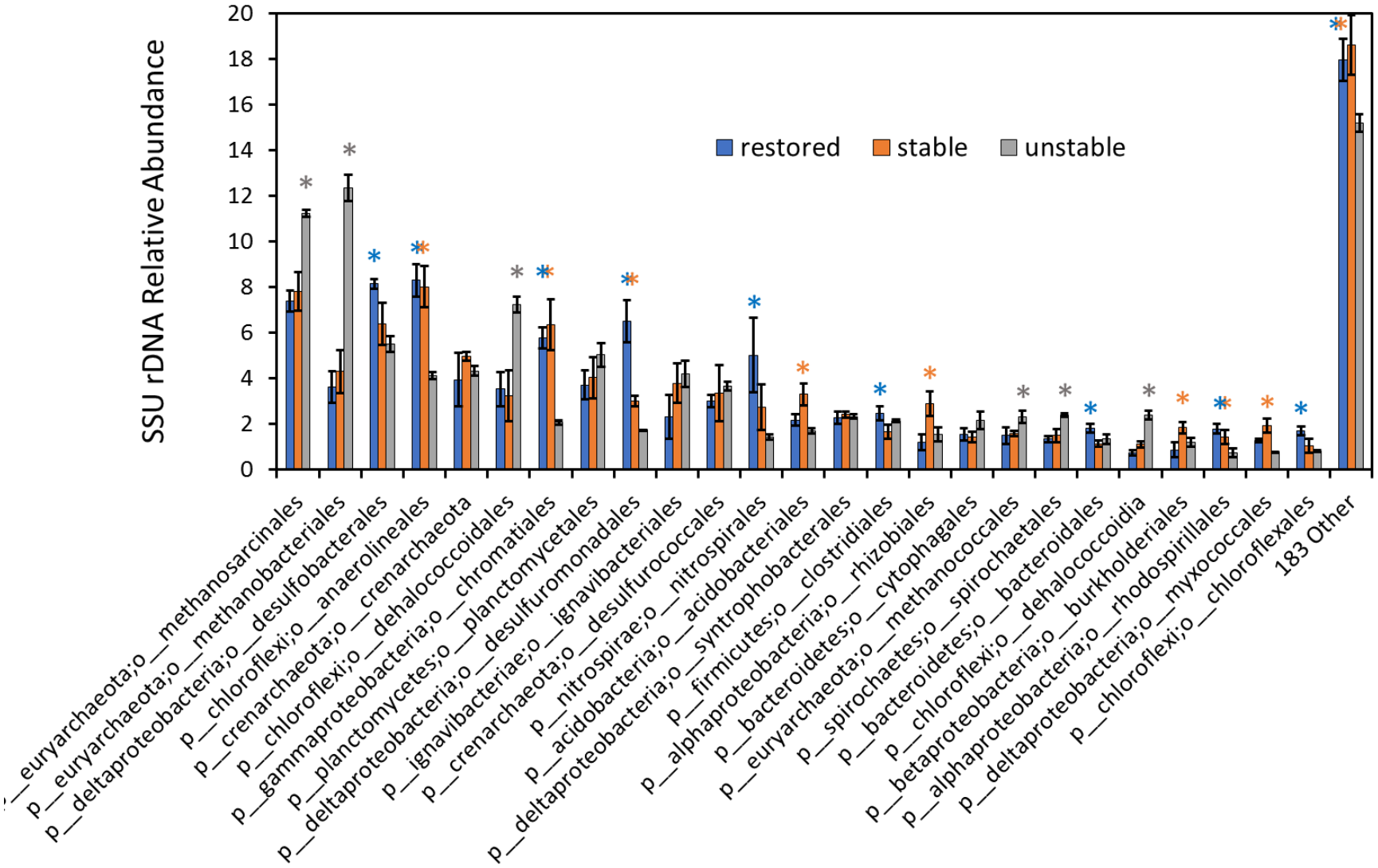

Figure 29. Mean (± SD) relative abundance of dominant prokaryote orders for restored, stable and unstable sites across all quarterly surveys of marsh sediment prokaryote communities. Error bars are ± 95% confidence intervals.

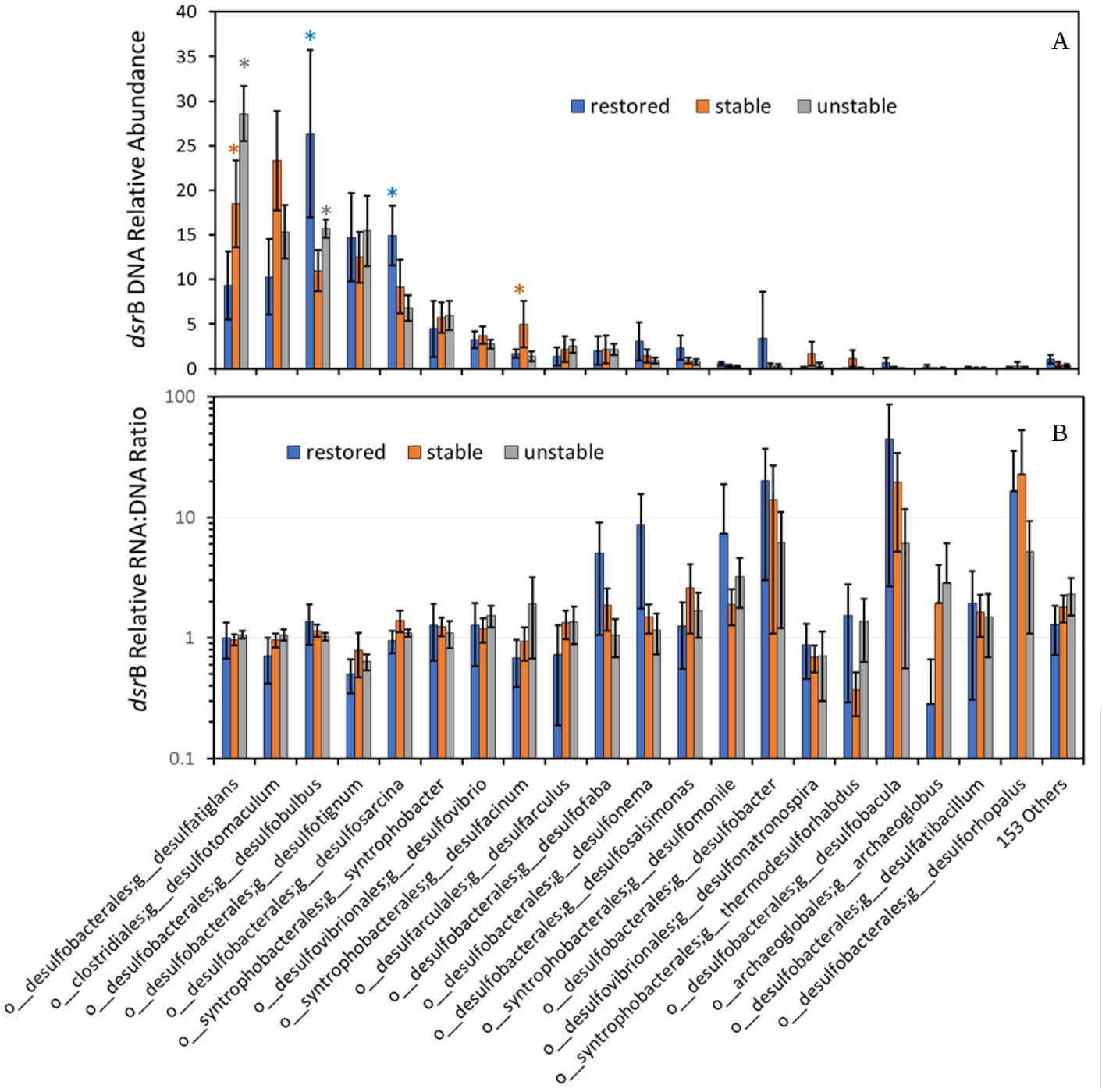

Figure 30. Mean percent relative abundance of dsrB DNA sequences (A) and the ratio of relative abundances of dsrB RNA to DNA sequences (B) for the 20 most predominant genera of sulfate reducing prokaryotes at restored, stable and unstable marsh sites for all seasons. Error bars are ± 95% confidence interval.

Fifteen dominant genera (< 1 % relative abundance) were identified for both dsrB RNA to DNA, but there were 158 other genera of lesser abundance (Fig. 28B). Based on dsrB DNA, there were five genera with > 10 % relative abundance. Four genera are in the Delta-Proteobacteria order Desulfobacterales, *Desulfatiglans*, *Desulfobulbus*, *Desulfotignum*, and *Desulfosarcina*, and the other, *Desulfotomaculum*, is in the Firmicute order Clostridiales (Fig. 30A). There was a significant decreasing gradient in relative abundance of *Desulfatiglans* from unstable, to stable, to restored sites (Students-t test; $P > 0.05$), consistent with the differences in proportions of water, organic matter and mineral content at these site types. Both *Desulfobulbus* and *Desulfosarcina* were in greatest relative abundance at the restored sites (Students-t test; $P > 0.05$). *Desulfotomaculum* was more abundant at stable than restored sites (Students-t test; $P > 0.05$). Coincident dominance of the SRB *Desulfatiglans* and Dehalococcoidales members at unstable site infers conditions for hydrogenotrophic organohalide reduction metabolism, which is presumed more energy efficient than sulfate reduction in *Desulfatiglans*. Unstable sites are relatively low in porewater sulfate concentration and greatest in organic matter content throughout the year. The H_2 supply resulting from the more vigorous fermentative community decomposition, supported by greatest ammonium accumulation, may be greater at unstable sites. This condition together with the potential for sulfate limitation there would favor an SRB with alternate metabolism than sulfate reduction.

Again, the beta-diversity among the sediment SRB communities based on *dsrB* RNA was similar to that of *dsrB* DNA overall sites and seasons, and for the dominant SRB genera few had relative abundance rations of *dsrB* RNA:DNA ratios far from unity (Fig. 30B). For the five most dominant genera, this ratio only *Desulfotignum* was below unity, and overall mean ratios were not different among site types. In fact, no dominant SRB genera had significantly different *dsr*B RNA:DNA ratios among sites, nor did the mean of all 153 minor genera considered together (Students-t test; $P > 0.05$). However, there were some dominant genera with ratios from 10 to nearly 100 times unity, namely *Desulfobacter*, *Desulfobacula*, and *Desulforhopalus*. This infers much greater expression of SRB metabolic genes, and may contribute more to total sulfate reduction than their *dsr*B DNA relative abundance would suggest, but again this was similar among site types, restored, stable, and unstable. It is clear that conditions at all marsh sites support sulfate reduction metabolism, at least during some seasons, based on geochemistry and presence of SRB taxa, yet these data alone do not fully explain the greater accumulation of sulfide to phytotoxic levels at the unstable sites.

Additional Analysis of Porewater Dissolved Iron and Iron Reducing Bacteria:

Other factors than SRB sulfide production alone determine porewater concentration of sulfide, and these include both biotic and abiotic fates of sulfide, which connects iron biogeochemical cycling with that of sulfur in coastal marshes (Fig. 31). Sulfide oxidation is one fate, and although we have not yet analyzed these data for the presence of sulfide oxidizing bacteria, the rates of this oxygen requiring process is presumed negligible given the low redox at the 15 cm depth. A possible exception may be in the marsh grass rhizosphere where intimate association with the root tissues and their oxygen release can support SOBs and infer a means of

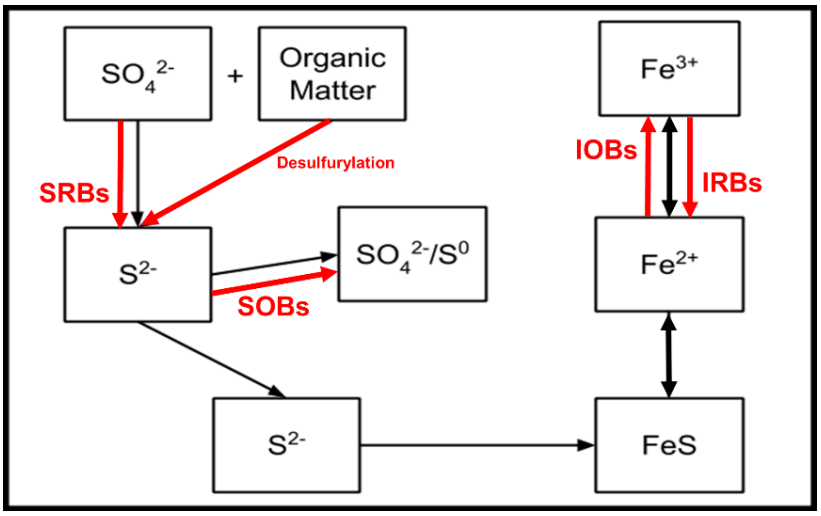

Figure 31. Model of the interactions in the iron and sulfur cycle in coastal marsh sediments and reaction of sulfur oxidizing bacteria (SOB), sulfate reducing bacteria (SRB), iron oxidizing bacteria (IOB), and iron reducing bacteria (IRB)

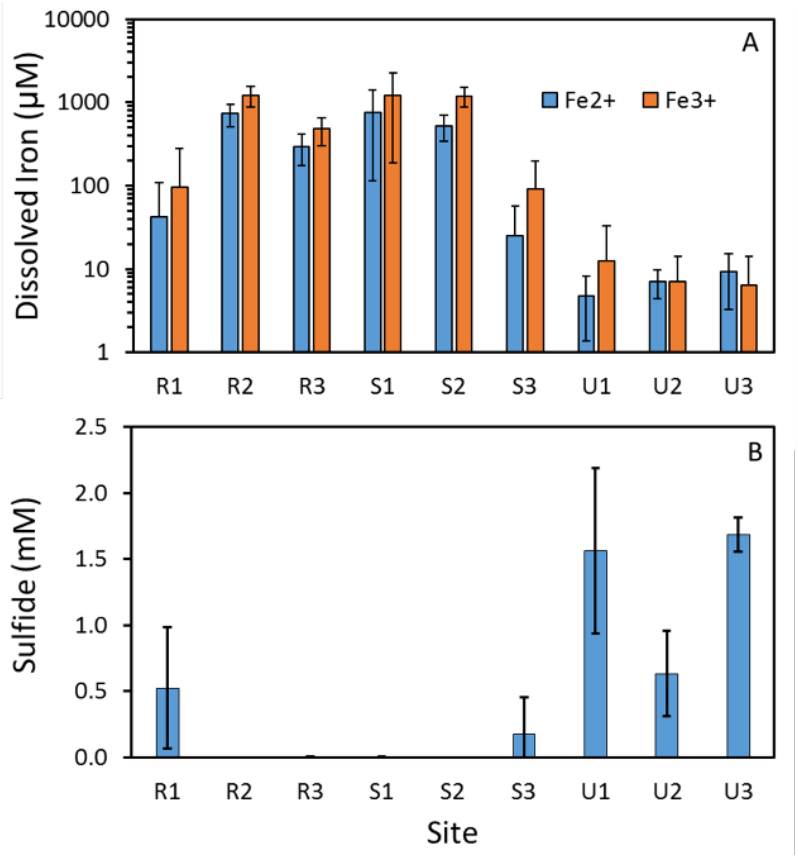

Figure 32. Porewater dissolved iron (A) and sulfide (B) at all nine sites in fall 2018.

sulfide detoxification for the plant root tissues. It is noteworthy, that elemental sulfur precipitation on surface sediment and on inundated vegetation is apparent in colder periods at the unstable sites, suggesting SOB activity there. .Another more plausible fate of sulfide in porewaters is reaction with dissolved iron species. The presence of iron oxyhydroxides (rust) precipitates on the sediment surface at restored sites during summer 2018 suggested seepage of porewaters with dissolved iron reacting with oxygen by abiotic and biotic processes, the later by iron oxidizing bacteria (IOB). Dissolved ferrous iron (Fe^{+2}) rapidly reacts abiotically with sulfide to produce ferrous sulfide, a black precipitate characteristic of anaerobic sediments. If the supply rate of ferrous iron can match sulfide production rate by SRBs then free dissolved sulfide concentration can remain at low concentrations, as seen at restored sites.

In fall 2018, some porewaters were preserved in the field by acidification and later analyzed by the ferrozine assay for dissolved total and ferrous iron concentrations, whose difference was inferred to be the ferric iron (Fe^{+3}). Concentrations of both dissolved iron species ranged 100-fold among the nine sites, with significantly higher concentration at restored and stable sites than unstable sites, with sites R1 and S3 being lower than their two respective counterpart sites (Fig. 32A). The R1 and S3 sites were the only restored and stable sites in Fall 2018 with measurable sulfide concentrations; however, these concentrations were still less than at unstable (Fig 32B). The source of dissolved iron is dissolution of iron minerals, and iron reducing bacteria (IRB) anaerobically respire with ferric iron to produce ferrous iron, which reacts with sulfide taking it out of solution in porewaters (Fig. 31).

As a first step to understanding the microbiology of iron biogeochemistry at Salt Bayou marsh sediment sites was to determine the IRB taxa with the potential for iron reduction metabolism and understand trends in their relative abundances among sites. There were six IRB genera, including *Geothermobacter, Geobacter, Geoalkalibacter, Acidithiobacillus, Shewanella, Desulfuromusa.* Overall sites and seasons the relative abundance of all IRBs to the total bacterial community in marsh sediments ranged from 2.8 to 5.4%, most of which was attributed to the two genera *Geobacter* (0.7 – 2.7 %; Fig. 33A) and *Acidithiobacillus* (0.2 – 1.8%; Fig. 33B). *Geobacter* abundance relative to all IRBs was about two-times greater at restored sites than stable and unstable sites in most seasons (Fig. 33C). In contrast, *Acidithiobacillus* at restored sites was about a fifth of its relative abundance to all IRBs than at both natural sites, stable and unstable, for all season (Fig. 33D). It is important to note that some *Acidithiobacillus* spp. have very diverse and plastic anaerobic metabolic potential, including sulfate reduction, and iron oxidation using nitrate. The dredge material sediment, with about 2 and 4 times greater mineral content than stable and unstable sites, respectively, appears to favor *Geobacter* spp. and suppress *Acidithiobacillus* spp. It may be that the additional iron load of dredge material is responsible for this difference.

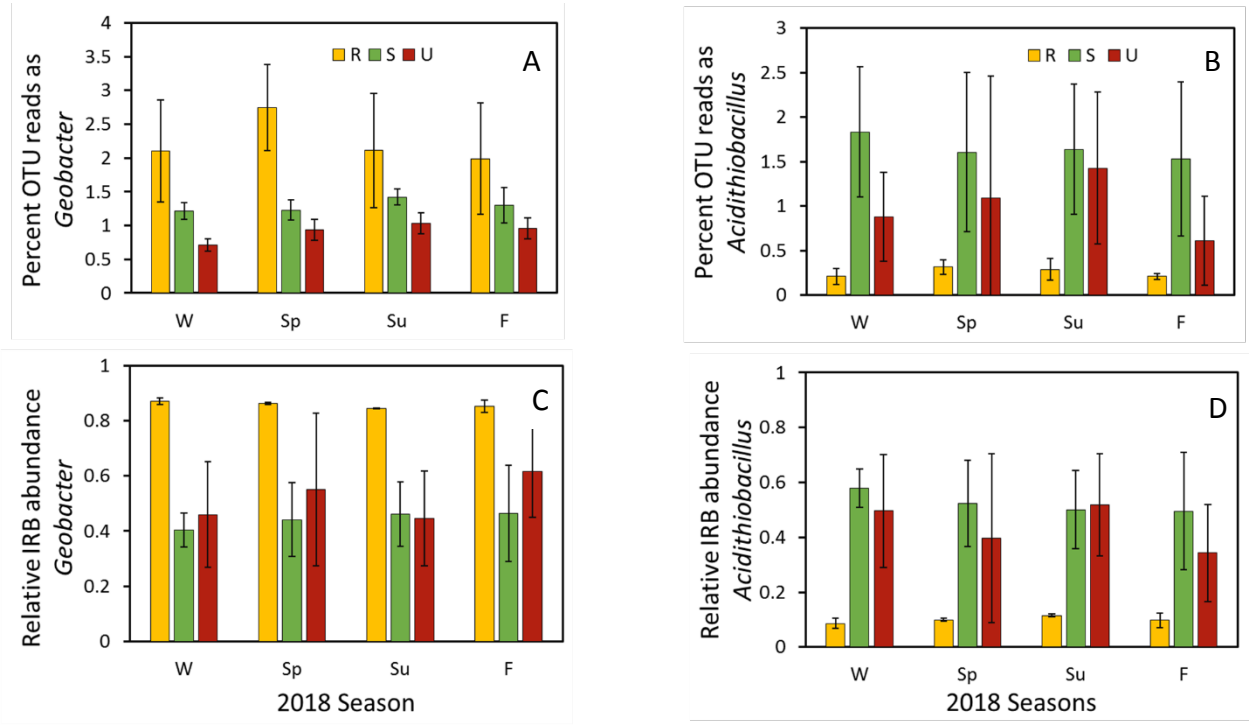

Figure 33. Two dominant genera of marsh sediment iron reducing bacteria, *Geobacter* spp. (A, B) and *Acidithiobacillus spp*. (C, D) unique to specific marsh habitat types, as percent of all marsh sediment community OUT reads (A, C) and as relative abundance of just iron reducing bacteria (B, D). Error bars are ± 95% CI.

Salt Bayou Watershed Marsh Conclusions:

The inundated sediments at unstable marsh sites, presumably due to subsidence and low sediment accretion rates, had sediment geochemistry and microbiology most distinct from the BUDM restored sites. These unstable sites had sediments that were mostly water, most negative redox, high organic content, and high porewater concentrations of sulfide and ammonium relative to stable and restored sites. There was little seasonal variation in these conditions at unstable, in contrast stable and restored sites. The R1 site was restored more recently (2011) than the other two restored sites (2005). R1 had some geochemical conditions more aligned with stable sites, and based on molecular analysis of this site in 2011 pre-restoration and post-restoration in 2018 there had not been as much change as compared to other restored sites. The S3 site had some geochemical conditions more similar to unstable sites and the other two stable sites, suggesting it is in decline. The phytotoxic sulfide level in porewaters at unstable sites was not correlated to salinity, which has been a target parameter for Salt Bayou Watershed restoration. Iron biogeochemistry needs consideration in understand levels of sulfide accumulation, as sites in fall 2018 with greatest dissolved iron in porewaters had no detectable sulfide.

Both the total microbial community and specifically SRB communities were analyzed using molecular methods, which revealed dominant taxa that were distinct in their relative abundance for specific site types. Unstable sites had microbial communities with greater proportions of hydrogenotrophic methanogenic orders of Archaea than SRB orders, in contrast to stable and restored sites. Methanogen dominance at unstable sites may have implications for the ability of marsh in this state of health to sequester and store carbon versus carbon loss, including that in the form of methane. The specific genus of SRB, *Desulfatiglans* and the Chloroflexis order Dehalococcoidales both dominated at unstable sites and both can use organohalide reduction metabolism based on H_2. The presence of hydrogenotrophic taxa dominating at unstable site suggests a vigorous fermentative community of cellulose decomposers supplying H_2. Other SRB genera were distinctly greater in abundance at restored sites. There were also IRB genera whose abundance was distinct among site types, specifically *Geobacter* at restored sites. Conclusively, microbial community analysis based on DNA is effective in distinguishing differences in marsh health at natural sites and restored sites, but RNA based analysis contributed little additional information.

Future monitoring of natural marsh health and restoration effectiveness, should continue using most methods and parameters, but there is some rationale for changing sampling frequency and number of sites. When seasonal differences were observed in geochemical and microbiology parameters they most distinguishable between winter, a period of vegetation senescence and net decomposition, and summer during peak vegetation growth. More sites of different states of health and periods post restoration are needed to increase the rigor of assessment for prioritizing areas in most need of restoration, as well as, restoration effectiveness. Sampling during two versus all four seasons would allow future monitoring at double the sites at similar cost. Additional costs savings would be to keep microbial community analysis based on DNA, as RNA analysis appears to be an unnecessary added cost. Sediment porewater dissolved iron needs to be added to the routine analyses. Collectively, vegetation health, marsh elevation change, and biogeochemistry, makes for the best assessment of marsh health and restoration effectiveness. To be able to correlate all parameters across the landscape, and model specific parameters assessable to the landscape, i.e. broader geospatial scales, may allow modeling and mapping other parameters. High resolution remote sensing of vegetation health and elevation, coupled with ground truthing and sediment biogeochemistry (geochemistry and microbiology) measurements is proposed for mapping a comprehensive marsh health index.

Task 5: Student Driven Outreach and Education:

Student Educational Impacts:


Lab analysis of plankton DNA extracts

Task 5 involved seventeen Lamar University undergraduate students in the BS Biology and BS Environmental Science majors, and one MS Biology graduate student, during the contract period. An additional six students in the LU STAIRSTEP fellowship program were instrumental in assisting the initial collection and lab analyses of Salt Bayou Estuary samples collected from summer 2016 to summer 2017. This pre-contract effort was done without external funding; hence could not afford photopigment analyses and microbial community sequencing costs. This contract had a budget and task adjustment along with a no cost extension to cover the costs of photopigment analysis and microbial community sequencing for the earlier sampling period and to incorporation all of these data in the analyses for this final research report. For these reasons, it is imported to acknowledge the contributions of and outcomes of these earlier student efforts in this final report as well.


S2-SITE Marsh sediment porewater sampling.

Research training of undergraduate students involved research methods in the field and laboratory, which was extensive. All students were provide readings and discussion of the overall problem and objectives of the research topic (estuary or marsh) of their responsibility. Typically students then worked one-on-one with the PI or graduate student to master a particular set of field tasks and laboratory analyses, as multifaceted field and lab works requires specialist that also know the big picture. In the field and lab students worked collaboratively, as a team, in accomplishing tasks. This approach has been an effective in working with undergraduate students. With data in hand, students were also responsible for entry, plotting, and analysis, as well as prepare abstracts for research poster presentations and poster design. Most of the undergraduate students were able to enroll in course credit (3 hours toward their degree) for their research involvement. The graduate student funded on the contract took on the responsibility of the marsh survey portion of the project. Winter 2018 was an intense training period, after which the student led the training and orchestration of the marsh field sampling team for the remaining three quarters, and was subsequently responsible for sediment nucleic acid extractions and sequence analyses. This graduate student is expected to graduate in fall 2019

A total of six different research posters were presented at peer reviewed conferences, including the Gulf Estuary Research Society (GERS) meetings. There are an additional two abstracts accepted for presentation at the Coastal and Estuarine Research Federation (CERF) Meeting in Mobile Alabama, November 2019. Two presentations, Adams et al., 2019 and Snowden et al., 2019, were awarded first and third place posters at the LU Undergraduate Research Expo in April 2019, respectively. All conference posters are included as pdf files in the deliverables zip file, and references listed below.

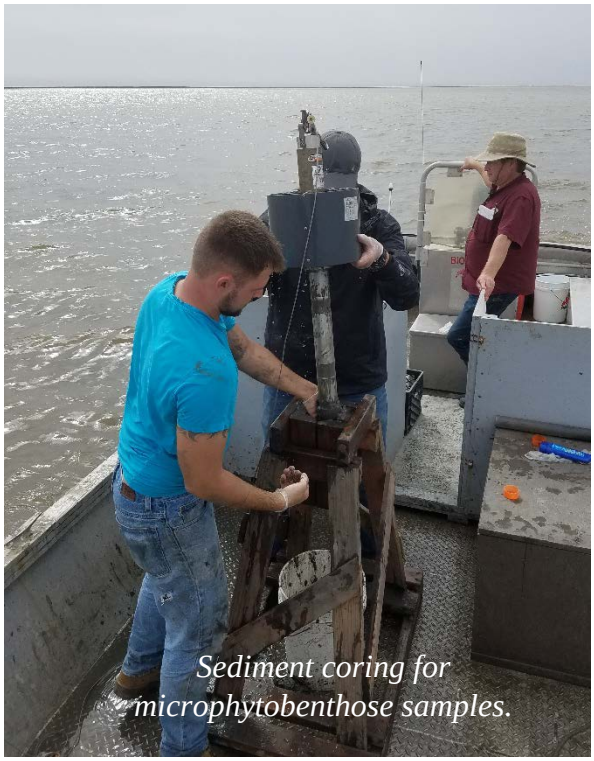

Sediment coring for microphytobenthose samples.

Research Presentations:

McCawley, Travis I., Claudia Marroquine, Linda Pham, Datron Brown, Tran B. T. Nguyen and Matthew P. Hoch. 2016. **The arrowhead redox-sipper: an all-in-one marsh sediment porewater and redox sampler.** Gulf Estuarine Research Society Meeting 2016, Nov 2016, Pensacola, FL.

Dugas, Keith, Datron.A.Brown, Katelin. Catching, Claudia Marroquin, Taylor Marshall, Hostin May, Tran B.T. Nguyen, Linda K. Pham, and Matthew P. Hoch. 2017. **Preliminary assessment of Salt Bayou Watershed Estuary prior to enhancement of freshwater inflows.** LU Undergraduate Research Expo 2017, Apr 2017, Beaumont, TX.

Dugas, Keith, Katelin Catching, Ricardo Saldaña, Emily J. Smith, and Matthew P. Hoch. 2018. **Continuous Monitoring of Salinity in Salt Bayou Watershed: Impact of Hurricane Harvey.** LU Undergraduate Research Expo 2018, Apr 2018, Beaumont, TX.

Smith, Emily J., Amanda Essoh, Jordan D. Snowden, and Matthew P. Hoch. 2018. **Geochemical evaluation of salt marsh elevated by Beneficial Use of Dredge Material in Southeast Texas.** Gulf Estuarine Research Society Meeting 2018, Galveston, TX.

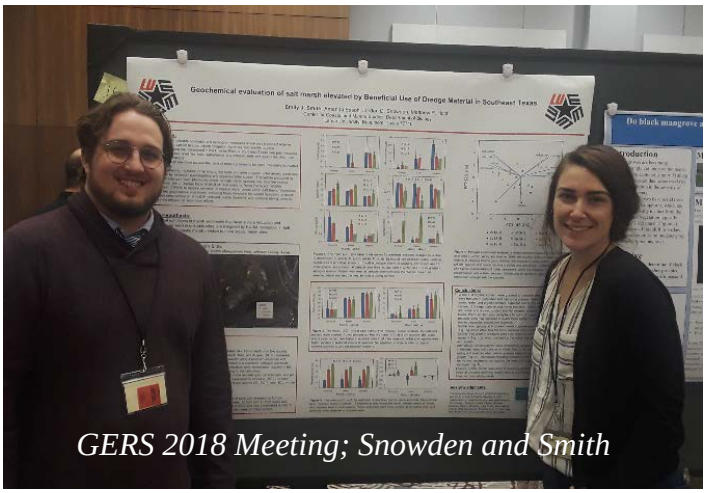

GERS 2018 Meeting; Snowden and Smith

Snowden, Jordan, Emily J. Smith, Carrie Martin, and Matthew P. Hoch. 2019. **Sediment Porewater Salinity Versus Sulfide: Which Affects Deterioration of Salt Marsh Health?** LU Undergraduate Research Expo 2019, Apr 2019, Beaumont, TX. *(3rd Place Award Poster)*

Adams, Shannon A, Emily J. Smith, Matthew P. Hoch. 2019. **Iron Biogeochemistry and Microbiology in Natural and Dredged Material Restored Salt Marsh Sites in Southeast Texas.** LU Undergraduate Research Expo 2019, Apr 2019, Beaumont, TX. *(1st Place Award Poster)*

LU UR Expo, 2019; Snowden and Adams

Matthew P. Hoch. 2019. **Bacterioplankton, phytoplankton, and microphytobenthose community dynamics in a shallow well-mixed estuary experiencing hydrologic modifications.** Coastal & Estuarine Research Federation Meeting 2019, Nov 2019, Mobile, AL. *(abstract accepted)*

Smith, Emily J., and Matthew P. Hoch. 2019. **Sulfate reducer communities in assessing Chenier Plain saltmarsh health: subsiding versus dredge material elevated sites.** Coastal & Estuarine Research Federation Meeting 2019, Nov 2019, Mobile, AL. *(abstract accepted)*

Student Educational Outreach Activities:

Another goal in Task 5 was to run educational workshops to high school students and Community College presentations of undergraduate research experiences, as had been done prior to the contract start with LU STAIRSTEP fellows who assisted in the initial Salt Bayou Estuary studies. However, high school teacher contacts were lost as a result of them moving due to the closure of Central High School, Beaumont Independent School District (BISD), in the aftermath of Hurricane Harvey in fall 2017. Attempts to establish new reliable contacts at other BISD high schools were unsuccessful. Classroom sessions at Lamar State Community College were also problematic do to scheduling conflicts when these were attempted in fall 2018 and spring 2019. But this did not stop the team of students. As a substitute, approved by the GLO contract manager, we sought out five community and LU campus events for setting up educational outreach activities booths related to watershed function, plankton ecology, and molecular microbial ecology approaches relevant to the project research. Student research posters of preliminary results were also made accessible to discuss at these events. We presented at the following events in 2018-2019: 1) Central High School Workshop, Apr 2017; 2) Neches River Festival, Apr 2018; 3) Kuntz Outdoors Festival, Oct 2018; 4) LU Earth Day Celebration, Apr 2019; and 6) Neches River Festival, Apr 2019.

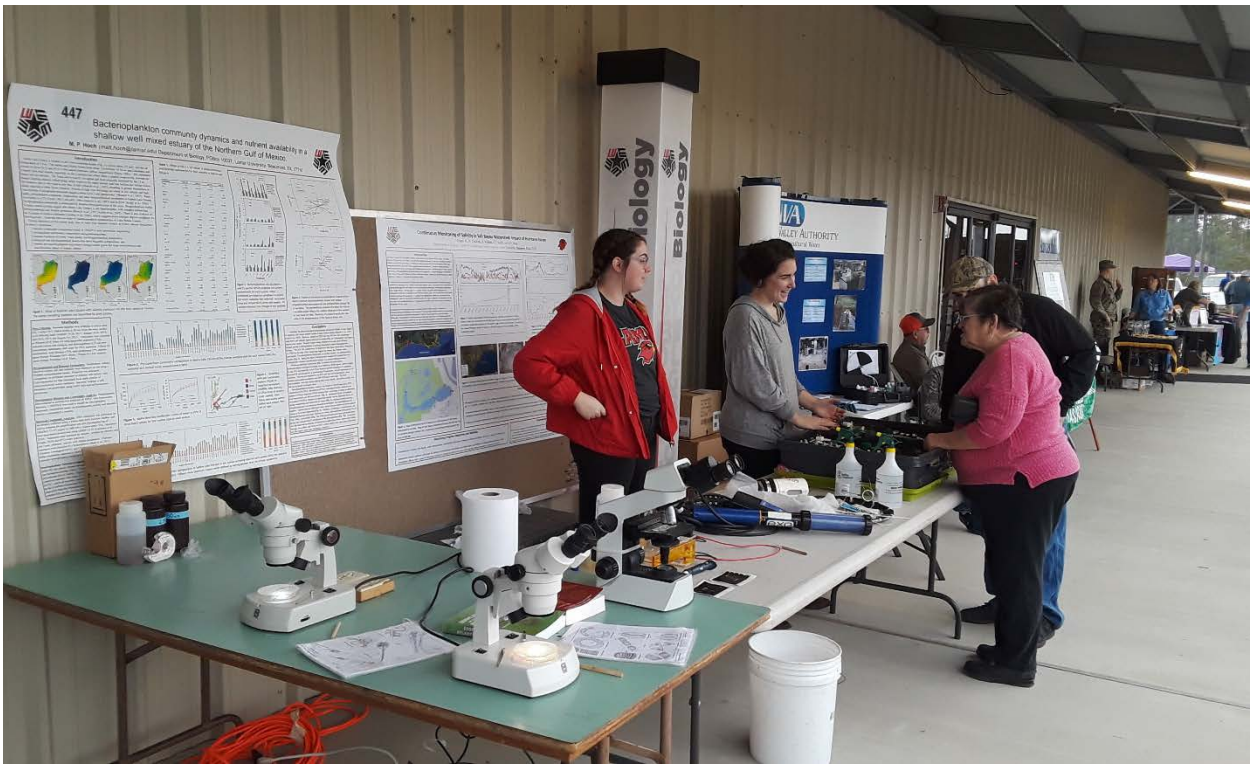
447
Biology


LAMAR


Biolo
One River
One C
LXX


Biology
Biology

Salt Bayou Watershed Restoration Workgroup Interactions:

Outreach to local Salt Bayou Watershed stakeholders was also performed twice, once at project initiation in January 2018 and at contract end in July 2019. This was in the form of presentations by the PI to the Salt Bayou Watershed Restoration Workgroup (SBWRW), chaired by Dr. Michael Reszutek (TPWD, J.D. Murphree W. M. A.) and including stakeholders from U.S.FWS, TPDW Fisheries Unit, Ducks Unlimited, Jefferson County Government, and Community. Presentation are include in the deliverables for this task.

The early January 2018 meeting of the SBWRW reviewed the on-going efforts in the estuary and the plan for marsh sampling. The estuary study design had already been approved by the Monitoring Subcommittee of the SBWRW, of which the PI is a member. Preliminary results of continuous monitoring at KJ-sonde site were discussed and the group came to an agreement on the placement of the older YSI 600SL sonde to KLFP. An overview of the parameters and approaches used for marsh sediment survey was presented. More discussion centered on the site selection and means of access to coastal marsh sites in the J.D. Murphree W. M. A.

The July 2019 meeting of the SBWRW, focused data presentation of all years of study in the estuary and marsh sediment biogeochemistry results from surveys in 2018. Effectively the highlights of results from this report were presented. The pdf file for the slides presented is included n the deliverable zip file.

Acknowledgments:

Contributions to field sample collection and laboratory analyses from student employees (Emily J. Smith, Keith Dugas, Ashley Tran, Ricardo Saldaña, Jordan Snowden, Bailey Schmoker, Angel Bell, and Amanda Essoh) and volunteers (Shannon Adams, Tran Nguyen, Katelin Catching, Ashley Tran, Ashley Borel, Hayden Henslee, Heather Low, Danny Abdullah, Jennifer Caltzonzin, and Tara Forst) are greatly appreciated. Special thanks to Emily J. Smith, Tran Nguyen, Katelin Catching Keith Dugas, Ricardo Saldaña, Shannon Adams for participating in developing and offering educational outreach activities. Thanks to the Lamar University, Center for Advances in Water and Air Quality (CAWAQ) for IC analysis assistance and purchase of the YSI 600SL sonde in summer 2016, and to the Department of Biology for transportation and boat use. Special thanks to staff of the Texas Parks and Wildlife, J. D. Murphree Wildlife Management Area, for logistical support in accessing sites in the marsh interior. Thanks to members of the Salt Bayou Watershed Restoration Workgroup for providing feedback on these findings and suggestions for the monitoring program into the future.

Appendix A: Depth profiles of salinity, water temperature, dissolved oxygen, and pH for eight quarterly samplings of Salt Bayou Estuary. Winter 2017 was not profiled.

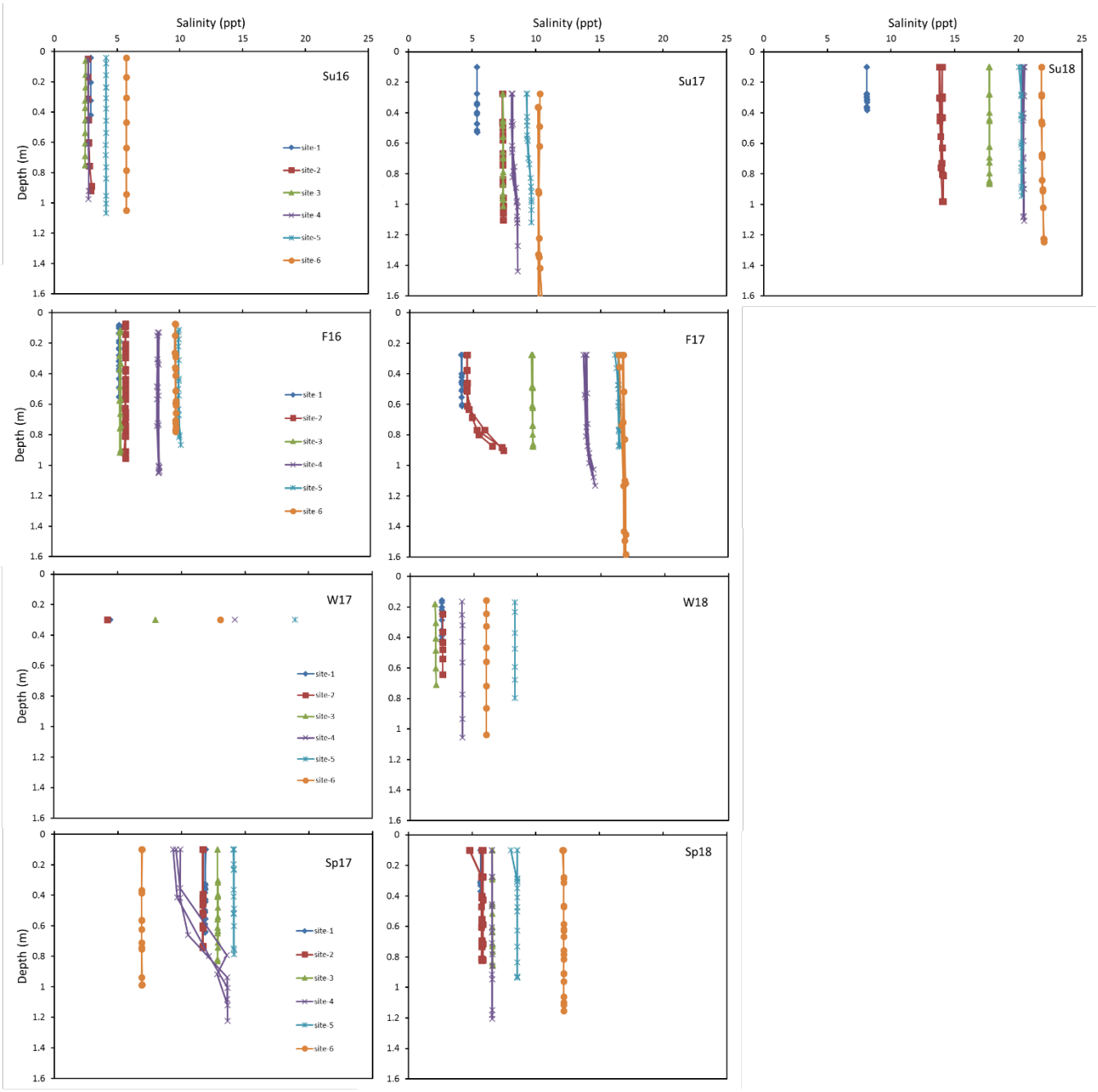

Figure A1. Salinity profiles for the quarterly surveys of Salt Bayou Estuary.

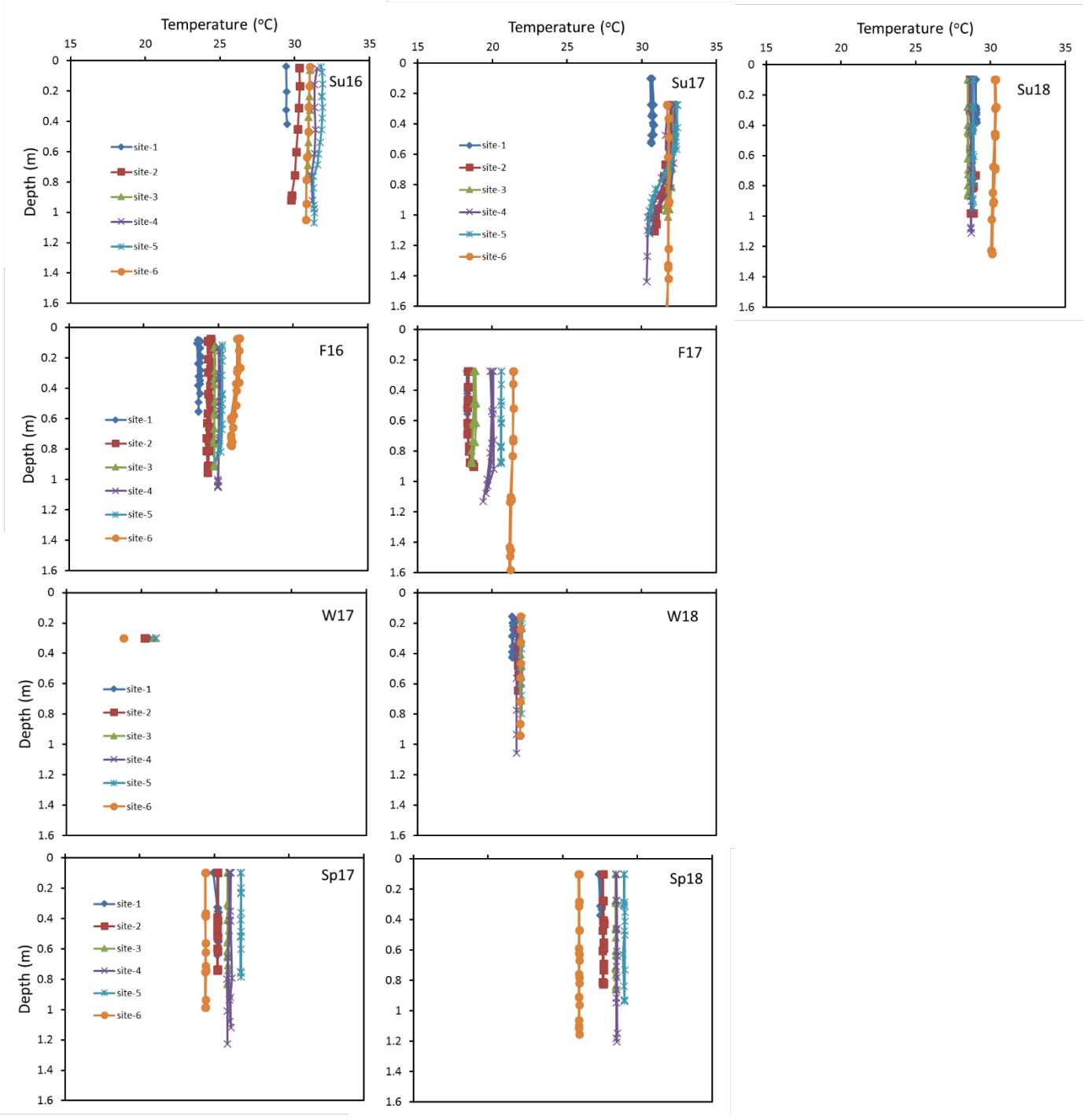

Figure A2. Water temperature profiles for the quarterly surveys of Salt Bayou Estuary.

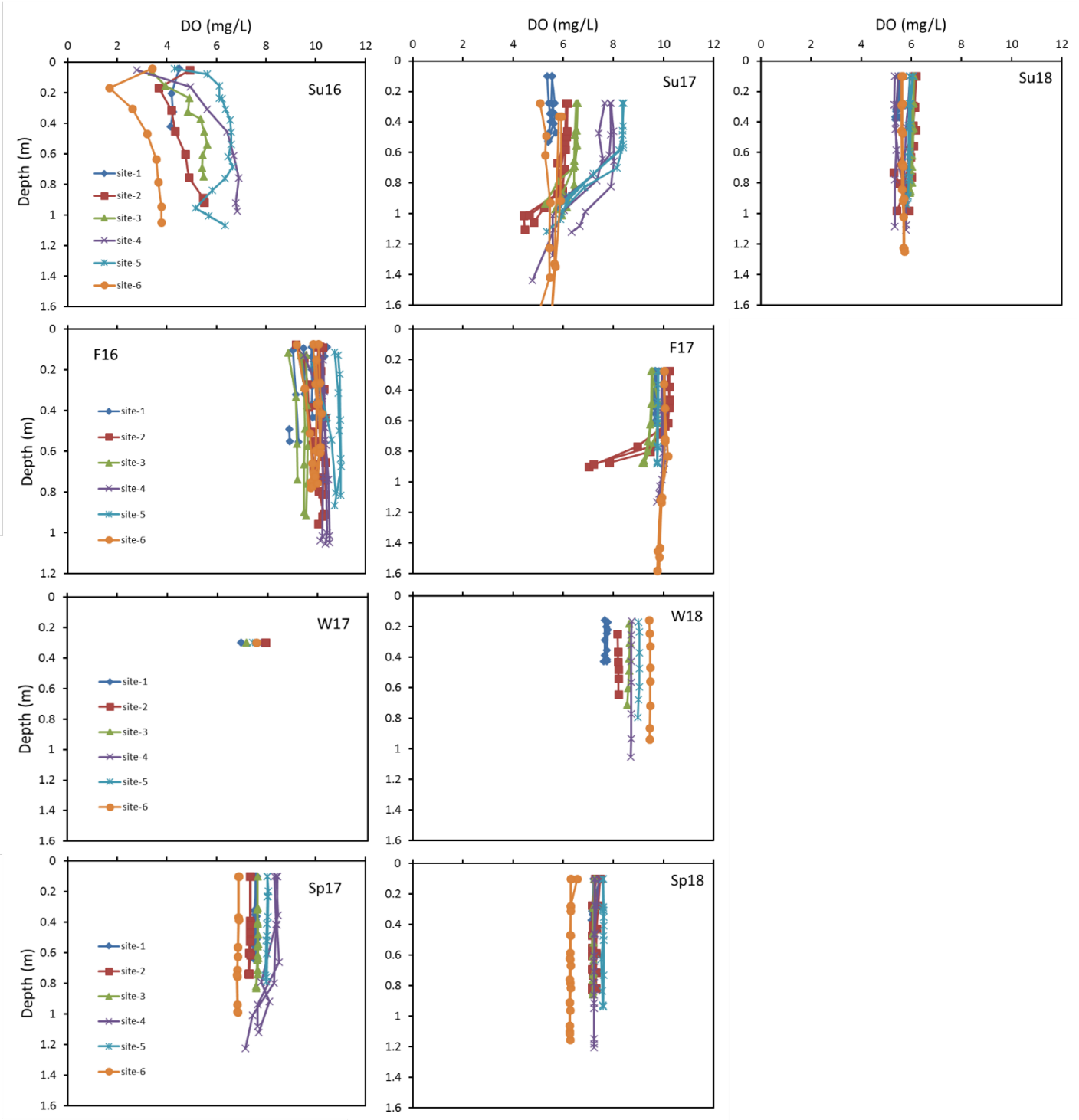

Figure A3. Dissolved oxygen (DO) profiles for the quarterly surveys of Salt Bayou Estuary.

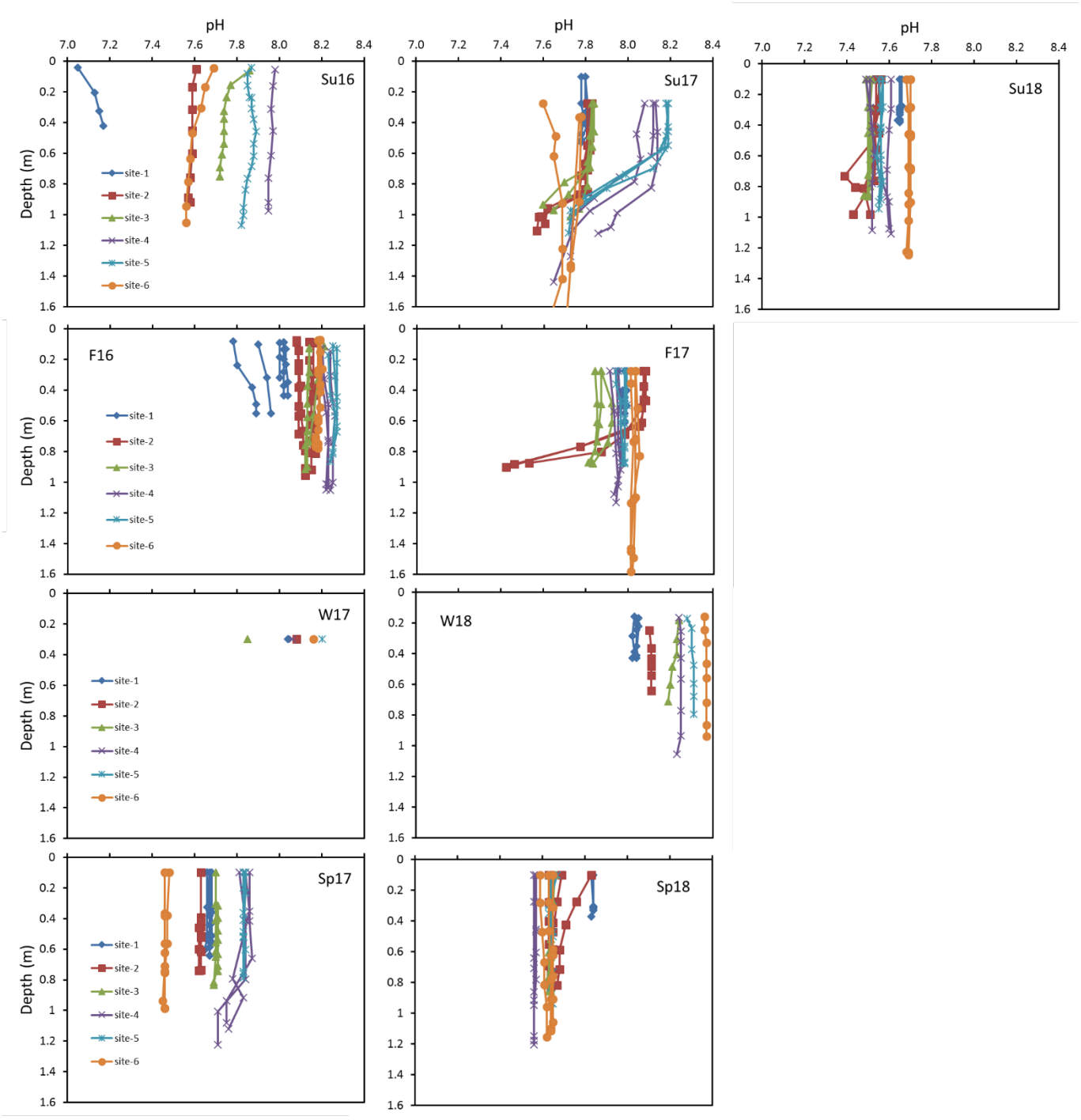

Figure A4. The pH profiles for the quarterly surveys of Salt Bayou Estuary.

Appendix B: Photopigments analyzed by HPLC for quarterly sampling of phytoplankton and microphytobenthos from summer 2016 through summer 2018.

Table B1. Phytoplankton photopigment concentrations (μg chl *a* L^{-1}) for all sampling sites and survey dates.

Name	Chl_c1c2	perid	ButFuc	fuco	h_fuco	neo	pras	viola	diadino	anther	allo	diato	lut	zea	gyro	Chl_b	Chl_a	a_car	b_car
Su16_KJS-1	0.49	0.04	0.03	1.94	0.04	0.30	0.05	0.67	0.72	0.28	0.42	0.33	1.25	2.95	0.51	1.61	18.51	0.29	2.93
Su16_KJS-2	0.19	0.05	0.01	1.04	0.00	0.21	0.03	0.30	0.46	0.22	0.31	0.15	0.25	3.29	0.42	0.92	12.86	0.13	2.43
Su16_KJS-3	0.42	0.02	0.03	2.70	0.00	0.26	0.01	0.45	0.71	0.20	0.49	0.22	0.50	2.88	0.38	1.12	19.14	0.25	2.60
Su16_KJS-4	0.77	0.21	0.09	3.65	0.00	0.36	0.03	0.48	1.01	0.26	0.77	0.33	0.61	3.51	0.43	1.44	23.29	0.51	2.95
Su16_KJS-5	0.49	0.22	0.09	2.02	0.00	0.31	0.07	0.34	0.68	0.28	0.49	0.22	0.44	4.28	0.78	1.02	16.44	0.24	2.79
Su16_KJS-6	0.25	0.16	0.03	0.49	0.00	0.14	0.02	0.15	0.17	0.07	0.31	0.07	0.21	0.83	0.18	0.59	6.09	0.30	0.62
F16_KJS-1	0.50	0.10	0.04	1.70	0.14	0.23	0.12	0.53	1.17	0.42	0.71	0.35	0.55	5.19	1.49	1.22	17.16	0.20	3.13
F16_KJS-2	0.36	0.02	0.08	1.30	0.13	0.18	0.10	0.33	0.97	0.38	0.57	0.30	0.34	5.31	1.34	0.88	14.98	0.08	2.90
F16_KJS-3	0.33	0.04	0.01	1.82	0.07	0.14	0.05	0.17	0.89	0.29	0.48	0.22	0.38	4.36	0.90	0.72	16.18	0.13	3.03
F16_KJS-4	0.48	0.21	0.10	1.95	0.13	0.17	0.08	0.19	0.82	0.28	0.43	0.22	0.40	4.40	0.71	0.70	14.22	0.17	2.58
F16_KJS-5	0.49	0.16	0.02	2.28	0.09	0.12	0.07	0.14	0.72	0.18	0.37	0.20	0.27	3.45	0.73	0.75	13.01	0.17	1.97
F16_KJS-6	0.28	0.16	0.01	1.01	0.05	0.11	0.05	0.13	0.48	0.17	0.20	0.14	0.31	3.11	0.46	0.58	9.71	0.08	1.76
W17_KJS-1	1.63	0.00	0.01	6.16	0.12	0.28	0.06	0.51	3.02	0.39	0.75	0.29	0.61	3.09	0.31	1.27	26.09	0.33	3.80
W17_KJS-2	0.63	0.00	0.02	2.77	0.08	0.23	0.06	0.35	1.48	0.26	0.61	0.20	0.35	2.32	0.28	0.73	13.72	0.20	2.03
W17_KJS-3	0.48	0.42	0.05	2.67	0.15	0.31	0.13	0.29	1.02	0.29	0.89	0.23	0.35	1.67	0.33	1.23	13.13	0.65	1.65
W17_KJS-4	0.69	0.31	0.01	2.78	0.04	0.24	0.03	0.21	0.71	0.11	0.99	0.14	0.18	0.59	0.08	1.28	12.89	0.74	0.85
W17_KJS-5	0.74	0.23	0.02	2.70	0.04	0.10	0.02	0.09	0.65	0.04	0.68	0.12	0.06	0.22	0.02	0.45	9.28	0.46	0.51
W17_KJS-6	0.17	0.09	0.00	0.43	0.01	0.03	0.01	0.02	0.11	0.01	0.14	0.02	0.02	0.06	0.01	0.11	1.87	0.09	0.09
Sp17_KJS-1	0.27	0.00	0.01	1.46	0.08	0.10	0.03	0.12	0.47	0.09	0.20	0.10	0.17	1.75	0.40	0.61	8.31	0.10	1.06
Sp17_KJS-2	0.26	0.00	0.00	1.87	0.08	0.11	0.04	0.11	0.52	0.09	0.24	0.11	0.15	1.50	0.40	0.63	9.05	0.10	1.08
Sp17_KJS-3	0.65	0.13	0.05	2.94	0.14	0.18	0.06	0.16	0.96	0.15	0.35	0.20	0.17	1.17	0.20	0.63	9.76	0.12	0.86
Sp17_KJS-4	0.60	0.17	0.03	2.50	0.08	0.15	0.09	0.15	0.89	0.18	0.33	0.25	0.22	1.10	0.10	0.87	9.73	0.15	0.76
Sp17_KJS-5	0.47	0.07	0.02	1.69	0.13	0.13	0.09	0.11	0.48	0.13	0.23	0.13	0.14	1.43	0.21	0.67	7.18	0.06	0.63
Sp17_KJS-6	0.23	0.17	0.01	0.50	0.01	0.05	0.02	0.05	0.17	0.05	0.35	0.03	0.07	0.24	0.03	0.28	3.62	0.19	0.13
Su17_KJS-1	0.64	0.34	0.05	2.68	0.15	0.28	0.09	0.65	1.27	0.30	0.48	0.32	0.40	3.56	0.65	1.57	18.33	0.28	0.94
Su17_KJS-2	0.29	0.21	0.02	0.84	0.05	0.12	0.07	0.17	0.45	0.14	0.36	0.14	0.30	1.96	0.29	0.63	7.89	0.14	0.78
Su17_KJS-3	0.31	0.20	0.03	0.96	0.06	0.18	0.08	0.26	0.49	0.15	0.27	0.14	0.46	2.17	0.36	0.84	8.94	0.14	0.88
Su17_KJS-4	0.28	0.28	0.03	0.58	0.07	0.22	0.08	0.23	0.51	0.19	0.40	0.17	0.47	2.92	0.30	1.05	9.67	0.19	1.04
Su17_KJS-5	0.19	0.12	0.02	0.44	0.06	0.20	0.07	0.19	0.36	0.17	0.26	0.13	0.45	2.81	0.22	0.85	7.88	0.02	1.31
Su17_KJS-6	0.65	0.71	0.04	1.01	0.06	0.23	0.05	0.33	0.68	0.15	0.63	0.14	0.30	1.23	0.17	1.31	10.41	0.06	0.21

Table B1: *(continued)*

Name	Chl_c1c2	perid	ButFuc	fuco	h_fuco	neo	pras	viola	diadino	anther	allo	diato	lut	zea	gyro	Chl_b	Chl_a	a_car	b_car
F17_KJS-1	0.36	0.00	0.05	1.47	0.11	0.14	0.04	0.20	1.15	0.25	0.30	0.18	0.24	2.80	0.21	0.74	10.39	0.09	1.16
F17_KJS-2	0.30	0.00	0.06	1.16	0.10	0.17	0.07	0.23	0.97	0.30	0.36	0.22	0.32	3.51	0.34	1.03	11.84	0.05	1.47
F17_KJS-3	0.40	0.14	0.02	1.60	0.10	0.20	0.11	0.25	0.86	0.24	0.32	0.20	0.34	2.54	0.37	0.95	10.99	0.04	1.12
F17_KJS-4	0.56	0.19	0.03	2.16	0.08	0.19	0.11	0.17	0.78	0.16	0.25	0.24	0.20	1.16	0.11	0.92	8.69	0.07	0.64
F17_KJS-5	0.44	0.29	0.03	1.14	0.09	0.31	0.06	0.11	0.80	0.14	0.29	0.35	0.11	0.37	0.03	2.45	7.41	0.10	0.34
F17_KJS-6	0.39	0.17	0.02	1.10	0.07	0.12	0.07	0.12	0.44	0.10	0.25	0.13	0.12	0.65	0.05	0.65	5.14	0.08	0.28
W18_KJS-1	0.41	0.13	0.03	1.41	0.10	0.30	0.06	0.58	0.96	0.34	0.33	0.16	0.81	2.63	0.31	1.17	12.94	0.13	1.27
W18_KJS-2	0.29	0.06	0.01	1.39	0.05	0.20	0.02	0.37	0.74	0.25	0.29	0.15	0.64	2.33	0.26	0.67	10.95	0.03	0.00
W18_KJS-3	0.54	0.33	0.05	2.87	0.02	0.32	0.03	0.42	1.14	0.30	0.49	0.20	0.66	1.80	0.26	1.05	16.09	0.09	0.00
W18_KJS-4	0.31	0.10	0.05	1.75	0.02	0.23	0.02	0.30	0.67	0.21	0.15	0.13	0.52	1.70	0.25	0.58	10.19	0.02	0.00
W18_KJS-5	0.48	0.27	0.06	1.67	0.06	0.18	0.08	0.27	0.63	0.17	0.15	0.12	0.45	1.45	0.21	0.61	9.27	0.10	0.00
W18_KJS-6	0.64	0.22	0.07	2.47	0.07	0.22	0.04	0.35	0.81	0.19	0.54	0.13	0.57	1.61	0.20	0.63	13.13	0.26	0.50
Sp18_KJS-1	0.26	0.00	0.00	1.24	0.06	0.09	0.02	0.17	0.64	0.24	0.30	0.19	0.27	4.04	1.02	0.55	10.70	0.00	0.72
Sp18_KJS-2	0.12	0.06	0.00	0.66	0.04	0.10	0.02	0.15	0.43	0.17	0.21	0.11	0.26	2.39	0.35	0.59	6.77	0.00	0.00
Sp18_KJS-3	0.10	0.15	0.00	0.45	0.02	0.06	0.02	0.08	0.27	0.10	0.13	0.06	0.17	1.06	0.16	0.36	3.93	0.00	0.00
Sp18_KJS-4	0.19	0.27	0.00	0.55	0.02	0.10	0.05	0.12	0.35	0.11	0.06	0.07	0.25	1.28	0.18	0.63	5.48	0.00	0.00
Sp18_KJS-5	0.30	0.28	0.01	0.75	0.06	0.11	0.08	0.16	0.36	0.09	0.08	0.06	0.18	1.39	0.20	0.74	6.08	0.07	0.00
Sp18_KJS-6	0.20	0.13	0.01	0.51	0.02	0.06	0.01	0.07	0.19	0.04	0.06	0.03	0.06	0.43	0.07	0.37	3.36	0.09	0.00
Su18_KJS-1	0.25	0.14	0.10	0.82	0.14	0.18	0.08	0.24	0.60	0.32	0.23	0.23	0.38	4.78	1.32	0.75	15.75	0.09	0.00
Su18_KJS-2	0.33	0.12	0.07	1.18	0.07	0.19	0.10	0.22	0.39	0.20	0.26	0.11	0.25	3.17	0.63	0.94	12.43	0.12	0.42
Su18_KJS-3	0.60	0.15	0.04	2.64	0.07	0.23	0.10	0.28	0.48	0.11	0.24	0.10	0.20	1.65	0.38	1.42	12.61	0.12	1.30
Su18_KJS-4	0.19	0.09	0.01	0.84	0.01	0.07	0.01	0.04	0.13	0.04	0.10	0.03	0.04	0.59	0.16	0.26	3.67	0.05	0.00
Su18_KJS-5	0.35	0.10	0.01	1.41	0.04	0.10	0.06	0.11	0.26	0.05	0.16	0.04	0.08	0.86	0.15	0.69	7.01	0.08	0.00
Su18_KJS-6	0.14	0.02	0.00	0.55	0.01	0.02	0.01	0.04	0.12	0.03	0.05	0.02	0.02	0.26	0.06	0.12	2.07	0.00	0.00

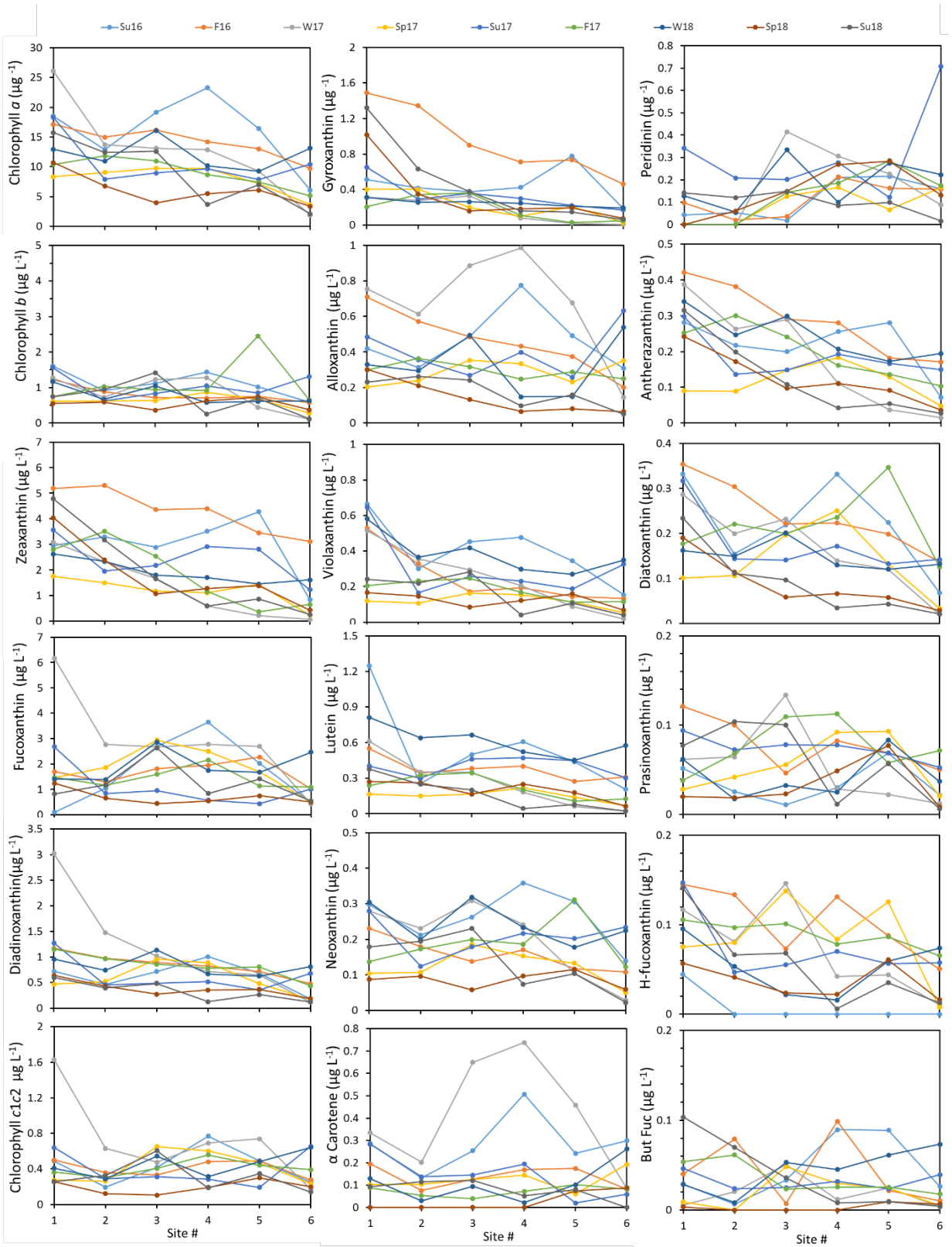

Figure B1. Phytoplankton photopigment concentration versus site for all survey dates.

Table B2. Microphytobenthos concentration (µg chl *a* g^{-1}) for all phytoplankton samples from all sites and survey dates.

Name	Chl_c1c2	fuco	diadino	diato	lut	zea	Chl_b	Chl_a	a_car	b_car
Su16-1	0.00	1.98	0.73	0.86	0.56	2.14	0.98	10.93	0.14	0.79
Su16-2	0.16	0.72	0.41	0.35	0.31	0.95	0.23	2.72	0.51	0.62
Su16-3	0.00	0.61	0.37	0.21	0.90	0.64	0.20	2.97	0.42	0.63
Su16-4	0.16	0.81	0.40	0.49	0.35	1.07	0.62	3.48	0.56	0.59
Su16-5	0.13	0.99	0.39	0.38	0.32	1.29	0.14	3.88	0.43	0.91
Su16-6	0.13	1.21	0.28	0.27	0.31	1.12	0.15	4.82	0.42	0.84
F16-1	0.00	0.89	0.64	0.87	0.61	2.66	0.36	5.12	0.07	0.64
F16-2	0.00	0.76	0.55	0.64	0.49	2.27	0.53	3.01	0.08	0.63
F16-3	0.13	0.60	0.45	0.54	0.43	1.82	0.79	4.29	0.44	0.90
F16-4	0.00	0.57	0.53	0.51	0.00	2.11	0.06	3.28	0.31	1.04
F16-5	0.00	0.77	0.34	0.68	0.31	1.69	0.05	3.51	0.30	0.85
F16-6	0.24	1.81	0.33	0.45	0.29	1.40	0.23	6.56	0.23	0.48
W17-1	0.33	3.56	1.03	0.66	0.36	0.71	1.07	15.72	0.28	0.00
W17-2	0.17	1.22	0.48	0.38	0.20	0.53	0.49	3.92	0.16	0.00
W17-3	0.22	1.24	0.46	0.26	0.16	0.34	0.52	4.67	0.24	0.00
W17-4	1.00	2.32	0.60	0.48	0.23	0.56	0.52	7.39	0.17	0.00
W17-5	0.33	2.25	0.45	0.29	0.13	0.68	0.30	7.15	0.28	0.51
W17-6	0.11	0.49	0.13	0.16	0.08	0.36	0.25	2.44	0.23	0.28
Sp17-1	0.33	2.60	0.65	0.69	0.32	1.13	0.25	9.21	0.56	0.84
Sp17-2	0.21	1.27	0.42	0.33	0.16	0.50	0.15	2.62	0.28	0.07
Sp17-3	0.26	1.67	0.46	0.38	0.19	0.54	0.16	4.16	0.36	0.08
Sp17-4	0.56	1.52	0.45	0.45	0.22	0.79	0.21	3.73	0.46	0.31
Sp17-5	0.27	1.74	0.38	0.37	0.13	0.67	0.17	5.62	0.40	0.48
Sp17-6	0.35	2.45	0.39	0.46	0.20	0.83	0.17	7.83	0.27	0.31
Su17-1	0.24	3.91	1.09	0.66	0.41	1.05	0.43	13.48	0.31	0.21
Su17-2	0.12	0.75	0.41	0.38	0.32	0.99	0.22	2.88	0.36	0.48
Su17-3	0.19	1.06	0.44	0.48	0.43	1.17	0.23	3.62	0.25	0.30
Su17-4	0.17	1.24	0.40	0.39	0.29	0.90	0.08	3.04	0.15	0.29
Su17-5	0.24	1.88	0.42	0.34	0.20	0.77	0.12	5.29	0.23	0.25
Su17-6	0.24	1.73	0.27	0.27	0.13	0.52	0.37	6.82	0.16	0.19
F17-1	0.25	6.44	1.27	0.43	0.16	0.33	0.23	11.89	0.18	0.00
F17-2	0.09	2.39	0.51	0.22	0.12	0.23	0.05	5.92	0.03	0.00
F17-3	0.00	1.01	0.27	0.29	0.22	0.68	0.11	3.50	0.18	0.25
F17-4	0.31	3.07	0.84	0.61	0.31	0.55	0.11	4.42	0.09	0.00
F17-5	0.25	2.65	0.54	0.39	0.19	0.72	0.07	4.46	0.09	0.26
F17-6	0.74	4.77	0.90	0.55	0.22	0.57	0.30	10.74	0.24	0.13
W18-1	0.27	3.20	0.93	1.01	0.45	1.51	0.41	9.68	0.30	0.24
W18-2	0.20	0.97	0.56	0.77	0.53	1.79	0.21	2.28	0.13	0.52
W18-3	0.30	1.50	0.63	0.99	0.69	2.33	0.30	4.00	0.22	0.62
W18-4	0.14	0.53	0.29	0.47	0.31	1.23	0.24	2.32	0.33	0.38
W18-5	0.11	0.66	0.31	0.48	0.30	1.29	0.34	1.79	0.18	0.47
W18-6	0.20	1.33	0.33	0.43	0.32	1.21	0.23	4.33	0.30	0.36
Sp18-1	0.00	6.29	1.38	1.09	0.38	1.74	0.42	23.51	0.32	0.63
Sp18-2	0.26	1.99	0.72	0.43	0.25	0.50	0.12	3.20	0.08	0.00
Sp18-3	0.32	2.13	0.65	0.39	0.25	0.58	0.16	5.10	0.12	0.00
Sp18-4	0.17	0.82	0.28	0.17	0.11	0.26	0.23	1.87	0.11	0.00
Sp18-5	0.27	2.34	0.45	0.33	0.18	0.67	0.29	5.28	0.15	0.12
Sp18-6	0.63	4.38	0.67	0.48	0.24	0.84	0.47	11.65	0.21	0.21
Su18-1	0.24	2.25	0.83	0.99	0.55	2.80	0.92	9.46	0.12	0.52
Su18-2	0.07	1.05	0.68	0.92	0.56	3.17	0.66	5.32	0.20	0.75
Su18-3	0.00	0.58	0.37	0.65	0.42	2.14	0.52	2.98	0.06	0.39
Su18-4	0.00	0.94	0.41	0.60	0.38	2.11	0.48	3.30	0.21	0.52
Su18-5	0.09	1.03	0.31	0.39	0.24	1.47	0.43	4.45	0.42	0.59
Su18-6	0.34	3.16	0.55	0.59	0.27	1.69	0.44	6.45	0.16	0.29

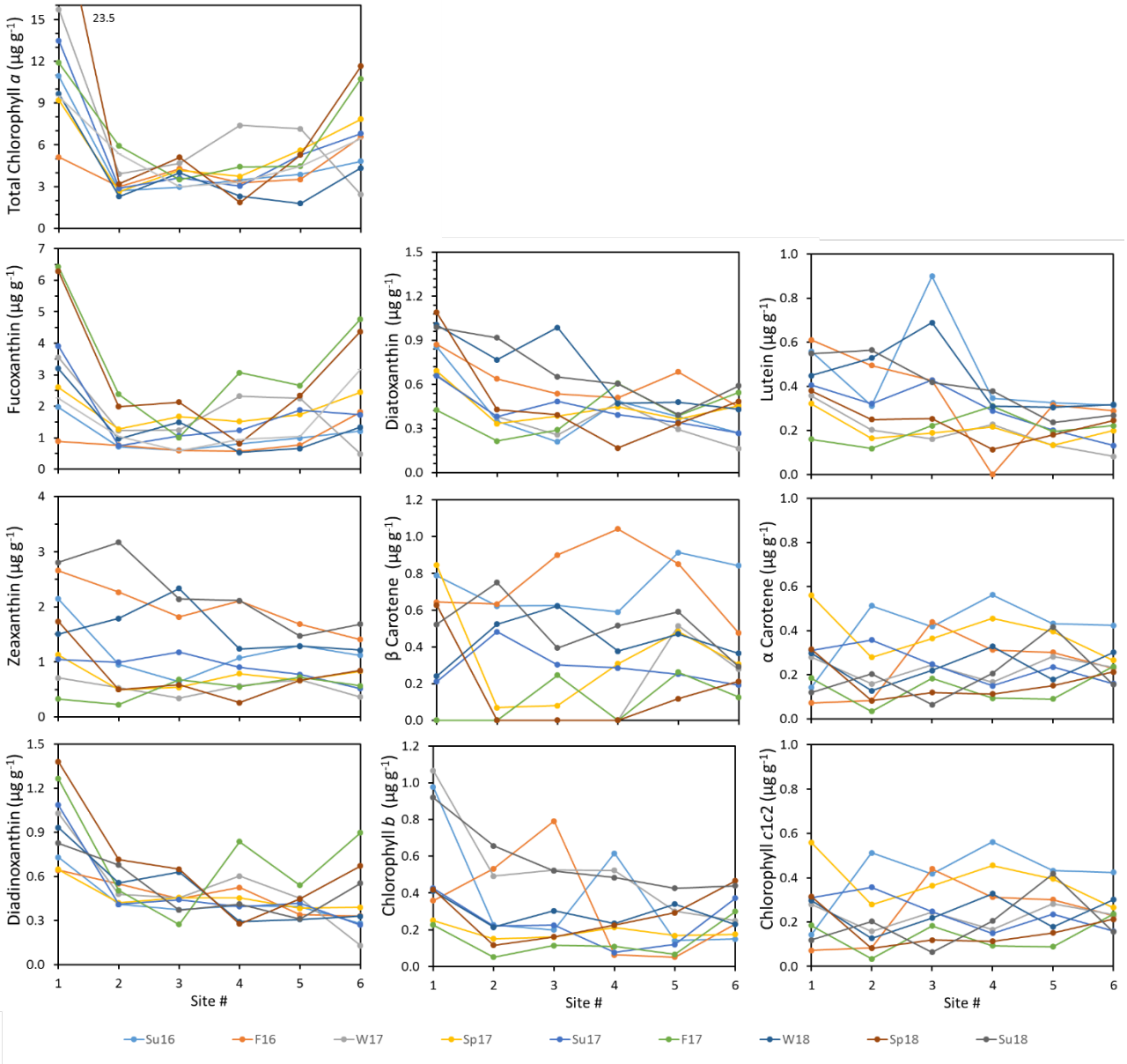

Figure B2. Microphytobenthos photopigment concentration versus site for all survey dates.

Appendix C: Relative abundance of dominant bacteria in the bacterioplankton and surface benthos, based on SSU rDNA.

Table C1. Relative abundance of twenty dominant bacterioplankton orders, representing 86 % of the overall average community.

Site	Pelagibacterales	Flavobacteriales	Actinomycetales	Planctomycetales	Burkholderiales	Methylophilales	Sphingobacteriales	Verrucomicrobiales	Rhodobacterales	Rhodospirillales	Nitrosopumilales	Pseudomonadales	Clostridiales	Phycisphaerales	Acidimicrobiales	Chloroflexales	Alteromonadales	Cytophagales	Rhizobiales	Desulfuromonadales	Nanopelagicales	130 other orders
Su16.1P	0.102	0.125	0.164	0.054	0.124	0.039	0.036	0.013	0.056	0.009	0.006	0.005	0.007	0.007	0.013	0.005	0.012	0.012	0.023	0.006	0.039	0.143
Su16.2P	0.159	0.071	0.195	0.090	0.112	0.053	0.044	0.038	0.008	0.010	0.002	0.004	0.009	0.017	0.031	0.008	0.007	0.008	0.007	0.007	0.009	0.111
Su16.3P	0.058	0.049	0.227	0.109	0.145	0.060	0.055	0.052	0.012	0.004	0.001	0.002	0.010	0.019	0.009	0.012	0.009	0.009	0.014	0.010	0.010	0.126
Su16.4P	0.052	0.046	0.177	0.107	0.121	0.044	0.062	0.072	0.014	0.004	0.002	0.002	0.010	0.024	0.029	0.014	0.009	0.011	0.020	0.014	0.010	0.155
Su16.5P	0.070	0.037	0.169	0.146	0.113	0.043	0.054	0.063	0.010	0.004	0.002	0.001	0.014	0.025	0.010	0.021	0.007	0.013	0.019	0.014	0.009	0.156
Su16.6P	0.021	0.052	0.133	0.181	0.128	0.040	0.046	0.076	0.025	0.005	0.003	0.001	0.013	0.027	0.006	0.028	0.008	0.016	0.018	0.020	0.004	0.150
F16.1P	0.027	0.039	0.081	0.217	0.093	0.022	0.067	0.129	0.032	0.009	0.006	0.002	0.017	0.019	0.007	0.026	0.009	0.012	0.017	0.013	0.001	0.157
F16.2P	0.061	0.033	0.095	0.216	0.077	0.028	0.060	0.118	0.025	0.010	0.007	0.003	0.022	0.020	0.010	0.015	0.008	0.011	0.017	0.015	0.001	0.148
F16.3P	0.101	0.057	0.129	0.238	0.067	0.039	0.035	0.091	0.013	0.007	0.004	0.005	0.013	0.017	0.015	0.007	0.005	0.009	0.008	0.009	0.002	0.126
F16.4P	0.150	0.051	0.087	0.193	0.064	0.040	0.033	0.073	0.032	0.020	0.010	0.011	0.014	0.028	0.008	0.004	0.009	0.007	0.009	0.013	0.001	0.143
F16.5P	0.205	0.070	0.099	0.140	0.045	0.040	0.027	0.042	0.037	0.025	0.042	0.017	0.011	0.020	0.012	0.002	0.010	0.006	0.006	0.010	0.002	0.129
F16.6P	0.200	0.064	0.088	0.172	0.055	0.042	0.026	0.053	0.032	0.026	0.015	0.018	0.011	0.023	0.005	0.003	0.011	0.005	0.007	0.011	0.001	0.136
W17.1P	0.170	0.071	0.131	0.059	0.101	0.046	0.060	0.027	0.025	0.004	0.001	0.004	0.007	0.010	0.015	0.007	0.005	0.015	0.007	0.004	0.020	0.211
W17.2P	0.225	0.058	0.153	0.061	0.096	0.057	0.040	0.022	0.019	0.005	0.003	0.005	0.008	0.014	0.024	0.005	0.005	0.010	0.007	0.003	0.024	0.157
W17.3P	0.256	0.067	0.097	0.043	0.067	0.048	0.017	0.014	0.020	0.011	0.025	0.017	0.006	0.009	0.008	0.002	0.008	0.016	0.007	0.010	0.011	0.242
W17.4P	0.327	0.112	0.059	0.023	0.050	0.066	0.008	0.008	0.041	0.021	0.028	0.023	0.004	0.005	0.005	0.001	0.012	0.011	0.006	0.007	0.003	0.179
W17.5P	0.266	0.223	0.028	0.013	0.037	0.062	0.015	0.005	0.075	0.029	0.021	0.019	0.006	0.002	0.002	0.001	0.024	0.010	0.004	0.004	0.001	0.154
W17.6P	0.300	0.163	0.075	0.017	0.057	0.104	0.014	0.004	0.050	0.024	0.016	0.010	0.003	0.001	0.010	0.002	0.013	0.013	0.006	0.002	0.009	0.106
Sp17.1P	0.264	0.136	0.062	0.037	0.072	0.082	0.015	0.007	0.053	0.026	0.016	0.037	0.005	0.002	0.002	0.002	0.014	0.013	0.004	0.006	0.000	0.144
Sp17.2P	0.265	0.146	0.054	0.029	0.067	0.084	0.012	0.007	0.048	0.026	0.022	0.032	0.006	0.002	0.002	0.001	0.014	0.012	0.004	0.007	0.001	0.160
Sp17.3P	0.291	0.202	0.057	0.020	0.043	0.073	0.008	0.006	0.042	0.022	0.015	0.037	0.013	0.001	0.001	0.001	0.013	0.006	0.004	0.006	0.000	0.137
Sp17.4P	0.256	0.161	0.069	0.041	0.081	0.070	0.013	0.008	0.072	0.021	0.015	0.022	0.004	0.002	0.007	0.001	0.017	0.012	0.009	0.004	0.005	0.108
Sp17.5P	0.310	0.160	0.047	0.024	0.051	0.074	0.011	0.007	0.072	0.028	0.022	0.037	0.005	0.002	0.001	0.001	0.018	0.005	0.004	0.004	0.000	0.117
Sp17.6P	0.199	0.126	0.087	0.078	0.125	0.062	0.027	0.009	0.039	0.016	0.013	0.008	0.003	0.003	0.010	0.003	0.016	0.021	0.015	0.003	0.020	0.119
Su17.1P	0.067	0.077	0.141	0.124	0.095	0.041	0.055	0.069	0.034	0.014	0.004	0.006	0.010	0.019	0.018	0.017	0.008	0.015	0.009	0.014	0.001	0.161
Su17.2P	0.299	0.066	0.138	0.100	0.058	0.034	0.031	0.015	0.014	0.025	0.010	0.022	0.027	0.013	0.009	0.008	0.005	0.002	0.005	0.007	0.001	0.114
Su17.3P	0.269	0.077	0.181	0.090	0.065	0.035	0.026	0.011	0.015	0.023	0.009	0.020	0.033	0.011	0.009	0.006	0.003	0.002	0.004	0.006	0.002	0.102
Su17.4P	0.258	0.059	0.148	0.147	0.048	0.028	0.037	0.018	0.015	0.023	0.015	0.019	0.029	0.024	0.007	0.008	0.004	0.003	0.005	0.006	0.001	0.099
Su17.5P	0.240	0.069	0.135	0.143	0.044	0.028	0.042	0.021	0.025	0.024	0.019	0.020	0.024	0.027	0.006	0.007	0.005	0.006	0.005	0.006	0.001	0.106
Su17.6P	0.204	0.122	0.152	0.070	0.050	0.044	0.028	0.012	0.035	0.021	0.062	0.011	0.016	0.014	0.013	0.004	0.008	0.009	0.008	0.007	0.004	0.107

Table C1. *(continued)*

Site	Pelagibacterales	Flavobacteriales	Actinomycetales	Planctomycetales	Burkholderiales	Methylophilales	Sphingobacteriales	Verrucomicrobiales	Rhodobacterales	Rhodospirillales	Nitrosopumilales	Pseudomonadales	Clostridiales	Phycisphaerales	Acidimicrobiales	Chloroflexales	Alteromonadales	Cytophagales	Rhizobiales	Desulfuromonadales	Nanopelagicales	130 other orders
F17.1P	0.153	0.031	0.145	0.156	0.084	0.048	0.056	0.051	0.037	0.008	0.003	0.002	0.008	0.017	0.014	0.018	0.005	0.017	0.014	0.006	0.005	0.122
F17.2P	0.180	0.036	0.137	0.164	0.070	0.052	0.051	0.037	0.029	0.011	0.004	0.004	0.007	0.019	0.032	0.012	0.006	0.014	0.013	0.005	0.004	0.113
F17.3P	0.303	0.051	0.092	0.125	0.056	0.064	0.018	0.028	0.034	0.021	0.008	0.011	0.012	0.013	0.010	0.004	0.009	0.007	0.007	0.004	0.002	0.121
F17.4P	0.379	0.096	0.077	0.063	0.039	0.061	0.011	0.014	0.034	0.028	0.019	0.013	0.011	0.007	0.008	0.001	0.010	0.004	0.004	0.003	0.001	0.116
F17.5P	0.376	0.123	0.056	0.053	0.035	0.057	0.011	0.013	0.038	0.031	0.023	0.013	0.011	0.007	0.005	0.001	0.013	0.004	0.004	0.003	0.001	0.123
F17.6P	0.413	0.150	0.056	0.024	0.030	0.046	0.012	0.005	0.043	0.032	0.037	0.014	0.007	0.002	0.006	0.001	0.016	0.003	0.004	0.003	0.001	0.094
W18.1P	0.054	0.168	0.092	0.052	0.081	0.031	0.106	0.089	0.018	0.004	0.001	0.003	0.015	0.005	0.004	0.098	0.006	0.011	0.007	0.015	0.026	0.115
W18.2P	0.080	0.154	0.092	0.065	0.089	0.034	0.093	0.081	0.015	0.004	0.002	0.002	0.011	0.005	0.009	0.075	0.006	0.013	0.007	0.013	0.027	0.121
W18.3P	0.063	0.113	0.097	0.039	0.112	0.041	0.134	0.058	0.014	0.005	0.003	0.003	0.008	0.003	0.011	0.026	0.008	0.029	0.010	0.008	0.032	0.183
W18.4P	0.112	0.159	0.095	0.041	0.097	0.045	0.094	0.062	0.027	0.005	0.004	0.005	0.007	0.004	0.012	0.019	0.008	0.019	0.008	0.010	0.021	0.146
W18.5P	0.232	0.223	0.072	0.037	0.073	0.053	0.046	0.034	0.066	0.007	0.002	0.007	0.003	0.002	0.006	0.005	0.010	0.014	0.005	0.007	0.008	0.087
W18.6P	0.160	0.192	0.086	0.039	0.092	0.049	0.069	0.049	0.045	0.005	0.003	0.006	0.004	0.004	0.016	0.013	0.010	0.020	0.009	0.012	0.015	0.105
Sp18.1P	0.064	0.043	0.136	0.122	0.129	0.044	0.082	0.074	0.037	0.008	0.002	0.006	0.007	0.009	0.007	0.015	0.009	0.014	0.012	0.009	0.005	0.165
Sp18.2P	0.170	0.056	0.178	0.096	0.102	0.051	0.042	0.039	0.022	0.009	0.005	0.010	0.010	0.013	0.020	0.009	0.005	0.006	0.006	0.007	0.011	0.136
Sp18.3P	0.205	0.097	0.200	0.043	0.131	0.058	0.017	0.011	0.029	0.010	0.005	0.011	0.003	0.008	0.021	0.003	0.006	0.007	0.005	0.006	0.008	0.115
Sp18.4P	0.220	0.114	0.194	0.057	0.107	0.053	0.013	0.011	0.021	0.011	0.005	0.012	0.005	0.007	0.032	0.002	0.004	0.005	0.004	0.005	0.010	0.108
Sp18.5P	0.230	0.144	0.160	0.051	0.102	0.048	0.012	0.009	0.036	0.014	0.006	0.011	0.003	0.005	0.019	0.004	0.008	0.007	0.004	0.010	0.006	0.113
Sp18.6P	0.210	0.182	0.077	0.041	0.092	0.041	0.015	0.007	0.101	0.023	0.021	0.020	0.003	0.003	0.008	0.002	0.018	0.013	0.009	0.004	0.011	0.103
Su18.1P	0.143	0.042	0.087	0.233	0.055	0.016	0.073	0.099	0.016	0.011	0.004	0.011	0.011	0.021	0.013	0.009	0.003	0.007	0.008	0.010	0.001	0.126
Su18.2P	0.158	0.083	0.040	0.197	0.039	0.018	0.100	0.041	0.032	0.026	0.030	0.027	0.010	0.022	0.002	0.002	0.010	0.006	0.005	0.012	0.001	0.140
Su18.3P	0.162	0.089	0.030	0.153	0.032	0.020	0.086	0.012	0.073	0.039	0.056	0.033	0.007	0.015	0.002	0.001	0.017	0.006	0.004	0.010	0.000	0.153
Su18.4P	0.178	0.283	0.042	0.040	0.023	0.025	0.024	0.005	0.053	0.039	0.032	0.049	0.042	0.003	0.002	0.001	0.016	0.004	0.004	0.006	0.000	0.130
Su18.5P	0.189	0.191	0.039	0.067	0.028	0.024	0.043	0.008	0.060	0.049	0.044	0.043	0.026	0.004	0.003	0.001	0.021	0.003	0.003	0.007	0.000	0.149
Su18.6P	0.122	0.247	0.026	0.049	0.023	0.012	0.023	0.007	0.041	0.025	0.036	0.032	0.028	0.006	0.004	0.001	0.021	0.007	0.006	0.007	0.000	0.277

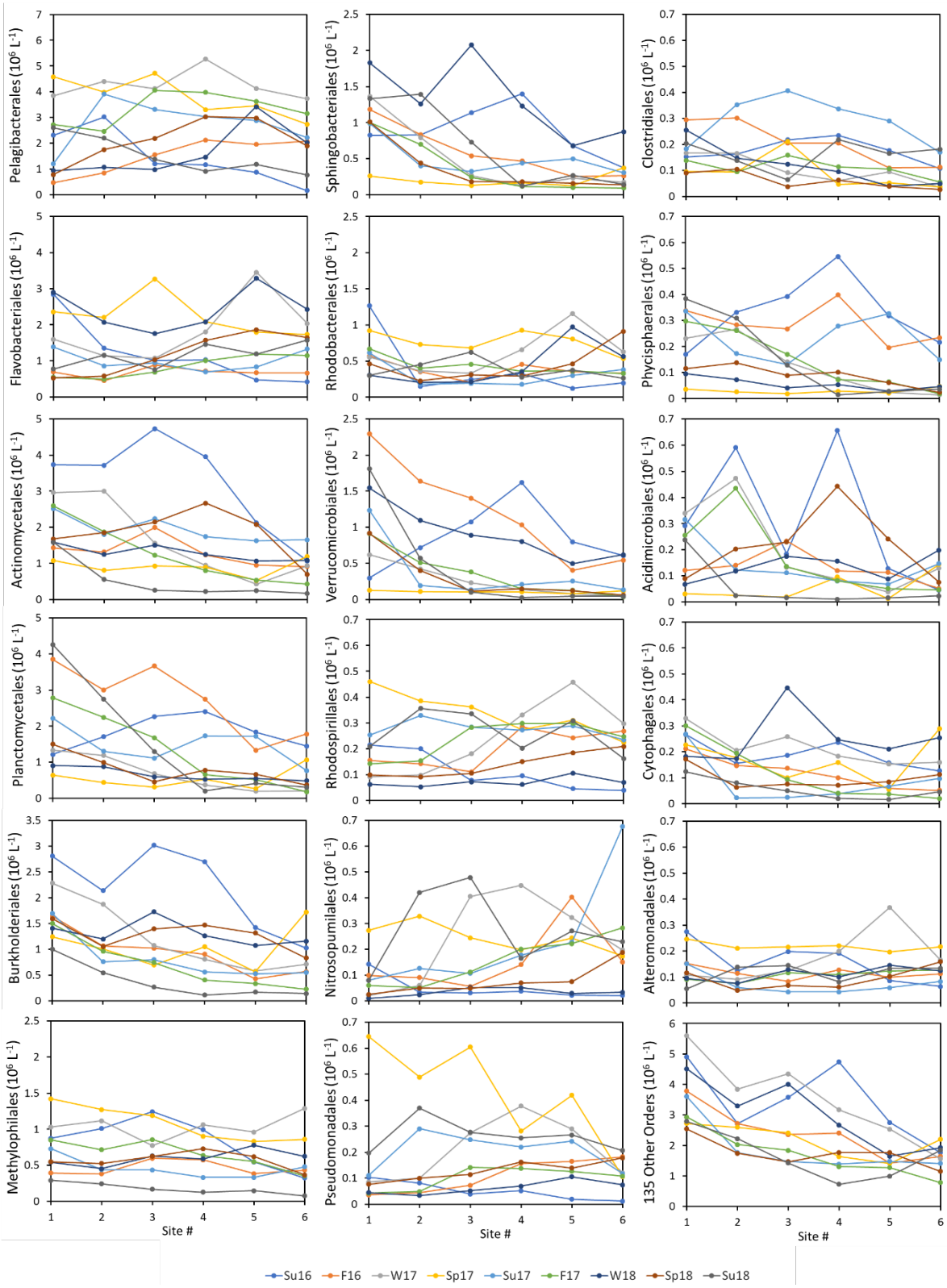

Figure C1. Bacterioplankton abundance of major orders versus site for all quarterly sampling dates of plankton from summer 2016 through summer 2018.

Table C2. Relative abundance of twenty dominant benthic prokaryote community orders, representing 78 % of the overall average community.

site	Anaerolineales	Desulfobacterales	Chromatiales	Flavobacteriales	Planctomycetales	Desulfuromonadales	Acidobacteriales	Cytophagales	Methanosarcinales	Syntrophobacterales	Burkholderiales	Nitrosopumilales	pseudomonadales	Dehalococcoidales	Verrucomicrobiales	Myxococcales	Nitrospirales	Rhizobiales	Clostridiales	Alteromonadales	Methanobacteriales	144 other orders
Su16.1M	0.067441	0.068638	0.053758	0.088099	0.052221	0.048852	0.037474	0.060112	0.010876	0.022342	0.038301	0.020481	0.024987	0.017008	0.038021	0.02218	0.0185	0.020082	0.024766	0.012811	0.004714	0.248338
Su16.2M	0.102382	0.078389	0.061315	0.058474	0.045415	0.050937	0.045716	0.045558	0.026611	0.035148	0.034307	0.03226	0.023183	0.030499	0.026849	0.022612	0.017169	0.014869	0.017423	0.011378	0.009838	0.209667
Su16.3M	0.069103	0.066651	0.067155	0.045561	0.04511	0.056997	0.051382	0.041379	0.034771	0.033932	0.041689	0.03157	0.029195	0.019257	0.029479	0.029854	0.020677	0.01816	0.01736	0.013591	0.015992	0.221134
Su16.4M	0.066758	0.067309	0.060383	0.036372	0.045829	0.052642	0.045503	0.045553	0.038514	0.029759	0.040656	0.040631	0.021518	0.021443	0.029208	0.026202	0.025413	0.017961	0.018361	0.011836	0.020654	0.237497
Su16.5M	0.066793	0.057454	0.061937	0.030389	0.042211	0.05224	0.049288	0.032293	0.061427	0.040845	0.039107	0.048281	0.019726	0.027203	0.025078	0.031506	0.01716	0.017864	0.017891	0.011477	0.021574	0.228257
Su16.6M	0.061573	0.06539	0.067605	0.03862	0.038567	0.050123	0.047174	0.041716	0.041636	0.04185	0.044185	0.021766	0.019737	0.023687	0.029092	0.02645	0.022473	0.01895	0.020258	0.014119	0.014226	0.250804
F16.1M	0.047597	0.074144	0.04914	0.032743	0.037591	0.040533	0.041363	0.0375	0.095999	0.034298	0.0347	0.009177	0.015944	0.022878	0.034739	0.020312	0.016903	0.012288	0.019975	0.010072	0.027519	0.284587
F16.2M	0.065607	0.052854	0.049003	0.039108	0.044721	0.040214	0.0371	0.040378	0.106159	0.030811	0.027964	0.016286	0.015989	0.030391	0.037654	0.021521	0.016471	0.012374	0.017843	0.008072	0.031262	0.258218
F16.3M	0.072259	0.068725	0.051771	0.048029	0.042452	0.041602	0.034325	0.047581	0.099338	0.026616	0.019713	0.011288	0.020682	0.029002	0.033386	0.018102	0.019981	0.009886	0.018326	0.008514	0.032939	0.245482
F16.4M	0.066792	0.067703	0.059617	0.04333	0.039967	0.045024	0.044215	0.042175	0.094797	0.032831	0.020394	0.014259	0.025798	0.028134	0.026799	0.022063	0.02015	0.010563	0.015851	0.010114	0.029828	0.239598
F16.5M	0.075242	0.092055	0.054835	0.042726	0.031567	0.038062	0.034066	0.039546	0.099953	0.033799	0.013057	0.01271	0.021798	0.038022	0.019218	0.017748	0.020287	0.007324	0.016625	0.009021	0.039733	0.242606
F16.6M	0.051293	0.090468	0.069277	0.076416	0.0545	0.046378	0.031939	0.064056	0.026493	0.017323	0.017033	0.01012	0.045734	0.013279	0.046733	0.019515	0.013939	0.009911	0.033728	0.01439	0.01186	0.235614
W17.1M	0.059028	0.066918	0.059476	0.067674	0.044854	0.049532	0.046197	0.034308	0.013294	0.040453	0.067273	0.015023	0.02895	0.020535	0.041735	0.025337	0.022203	0.01998	0.01385	0.016197	0.004509	0.242674
W17.2M	0.075397	0.058613	0.064251	0.063112	0.045809	0.051461	0.047597	0.032169	0.019451	0.041541	0.046689	0.055412	0.032039	0.023849	0.030064	0.028117	0.019538	0.019898	0.012501	0.014679	0.006589	0.211224
W17.3M	0.077009	0.051956	0.064132	0.060298	0.047051	0.048889	0.044817	0.035735	0.025	0.035933	0.044301	0.07451	0.031134	0.021866	0.02812	0.026705	0.018601	0.020016	0.011515	0.014318	0.008739	0.209357
W17.4M	0.086519	0.049298	0.063477	0.074034	0.052145	0.045501	0.04242	0.039689	0.018136	0.032111	0.042931	0.068164	0.040595	0.022327	0.02973	0.025028	0.016048	0.019377	0.010572	0.01691	0.00606	0.198928
W17.5M	0.102861	0.061835	0.068436	0.085363	0.045342	0.045558	0.038405	0.038898	0.022503	0.032179	0.025853	0.049263	0.044691	0.028218	0.025577	0.024297	0.012592	0.015587	0.009636	0.020986	0.009833	0.192086
W17.6M	0.082421	0.090193	0.06479	0.059392	0.063447	0.040973	0.040431	0.036538	0.021063	0.028048	0.025607	0.046168	0.045123	0.019734	0.021918	0.023247	0.022663	0.017984	0.011827	0.013902	0.010308	0.214225
Sp17.1M	0.078302	0.07145	0.066319	0.045614	0.034453	0.037251	0.034154	0.036742	0.065002	0.039196	0.032718	0.020032	0.021677	0.034334	0.022769	0.021049	0.020196	0.014137	0.013434	0.013763	0.022994	0.254413
Sp17.2M	0.093638	0.049637	0.071526	0.055872	0.044509	0.047215	0.042745	0.036899	0.039516	0.036376	0.032354	0.054661	0.03053	0.031801	0.020199	0.025641	0.019661	0.015803	0.010645	0.013396	0.012574	0.214802
Sp17.3M	0.081361	0.06041	0.085831	0.066223	0.045686	0.058839	0.050371	0.038231	0.014267	0.038403	0.035032	0.032862	0.044729	0.030477	0.018737	0.031619	0.022179	0.01541	0.009383	0.016424	0.004599	0.198926
Sp17.4M	0.099164	0.061657	0.069019	0.066141	0.040909	0.046792	0.04447	0.047777	0.032434	0.031115	0.025582	0.051291	0.047284	0.023595	0.019095	0.026313	0.018205	0.014882	0.009285	0.015597	0.011145	0.198248
Sp17.5M	0.106676	0.080448	0.083179	0.07497	0.039041	0.049616	0.044611	0.041426	0.013032	0.03227	0.024298	0.025991	0.058207	0.029504	0.018292	0.027302	0.014579	0.014015	0.008882	0.020567	0.005442	0.187652
Sp17.6M	0.08315	0.097702	0.08453	0.07315	0.058132	0.041827	0.033823	0.041901	0.01125	0.022051	0.017387	0.036715	0.063804	0.020167	0.024495	0.023227	0.017928	0.015223	0.01013	0.021231	0.004851	0.197325
Su17.1M	0.081749	0.064157	0.057433	0.034712	0.031206	0.034454	0.032754	0.034272	0.097321	0.036032	0.028944	0.014085	0.018411	0.03157	0.027563	0.016726	0.022691	0.013053	0.016863	0.013296	0.029476	0.263231
Su17.2M	0.088615	0.066609	0.06283	0.035807	0.032417	0.048181	0.044065	0.032013	0.072191	0.047307	0.025651	0.023311	0.022006	0.040245	0.019087	0.02327	0.022302	0.010357	0.01489	0.008985	0.026337	0.233523
Su17.3M	0.105342	0.076432	0.069189	0.046467	0.042846	0.055314	0.049202	0.044007	0.024815	0.034732	0.031706	0.014104	0.036902	0.029598	0.024479	0.025289	0.024922	0.014027	0.021652	0.01143	0.012408	0.205137
Su17.4M	0.131658	0.074433	0.063431	0.042976	0.04249	0.047543	0.045935	0.041155	0.03642	0.037846	0.023567	0.020699	0.036723	0.033688	0.018392	0.025236	0.022095	0.013718	0.013506	0.012671	0.013142	0.202677
Su17.5M	0.138337	0.079484	0.065232	0.053163	0.04247	0.045558	0.043091	0.039901	0.029678	0.037568	0.020647	0.021336	0.037383	0.037937	0.01781	0.023065	0.016686	0.012875	0.012338	0.01175	0.013228	0.200463
Su17.6M	0.124106	0.072794	0.07224	0.06584	0.052419	0.043634	0.040302	0.054105	0.011182	0.021191	0.020256	0.0329	0.047993	0.022706	0.024616	0.022429	0.015818	0.013684	0.02048	0.013684	0.004662	0.202958

Table C2. *(continued)*

site	Anaerolineales	Desulfobacterales	Chromatiales	Flavobacteriales	Planctomycetales	Desulfuromonadales	Acidobacteriales	Cytophagales	Methanosarcinales	Syntrophobacterales	Burkholderiales	Nitrosopumilales	pseudomonadales	Dehalococcoidales	Verrucomicrobiales	Myxococcales	Nitrospirales	Rhizobiales	Clostridiales	Alteromonadales	Methanobacteriales	144 other orders
F17.1M	0.081422	0.060928	0.05511	0.041603	0.040769	0.039922	0.037437	0.029777	0.037422	0.040419	0.053019	0.007367	0.012937	0.032525	0.037846	0.020728	0.024003	0.019968	0.016811	0.01111	0.014954	0.283925
F17.2M	0.118461	0.055666	0.055297	0.026969	0.045568	0.050888	0.046136	0.026771	0.038295	0.046268	0.038875	0.026335	0.015524	0.039298	0.028381	0.024196	0.023919	0.018784	0.017279	0.007907	0.013834	0.235351
F17.3M	0.132869	0.092886	0.052564	0.041355	0.055925	0.048209	0.046783	0.032344	0.004983	0.043291	0.038138	0.003741	0.024366	0.039524	0.033155	0.021541	0.0274	0.01712	0.012268	0.009757	0.00361	0.218169
F17.4M	0.167661	0.067557	0.060571	0.045946	0.051379	0.04408	0.044448	0.038688	0.02153	0.037353	0.026854	0.012065	0.026677	0.043508	0.02236	0.02364	0.0198	0.015674	0.011629	0.009737	0.008688	0.200153
F17.5M	0.169117	0.081066	0.06117	0.056681	0.0427	0.04126	0.035897	0.043266	0.02481	0.036514	0.019279	0.009376	0.029363	0.045157	0.018212	0.021955	0.016103	0.013325	0.011781	0.014045	0.011151	0.197772
F17.6M	0.116246	0.092063	0.065593	0.067551	0.063224	0.038575	0.037261	0.045628	0.006313	0.022814	0.021746	0.019377	0.047394	0.025881	0.025813	0.02291	0.016761	0.016747	0.012941	0.013283	0.003437	0.218443
W18.1M	0.058005	0.050689	0.063575	0.0529	0.054921	0.040449	0.042936	0.026792	0.009236	0.036217	0.086818	0.011694	0.018021	0.023504	0.051183	0.028391	0.017483	0.025453	0.015723	0.013119	0.003069	0.269821
W18.2M	0.07687	0.044042	0.061839	0.05934	0.057011	0.041712	0.038779	0.043172	0.01847	0.0392	0.053235	0.048842	0.017684	0.026442	0.042232	0.02946	0.017249	0.018947	0.014161	0.012126	0.006821	0.232365
W18.3M	0.121338	0.094314	0.049071	0.061921	0.064089	0.047979	0.045011	0.024535	0.002052	0.047339	0.039786	0.005006	0.024608	0.035828	0.02602	0.028304	0.024506	0.0179	0.012035	0.01349	0.00163	0.213237
W18.4M	0.09163	0.047041	0.062859	0.097215	0.059618	0.037464	0.033338	0.044429	0.016662	0.030981	0.038214	0.050952	0.032387	0.021766	0.034316	0.024351	0.016207	0.019623	0.010448	0.01756	0.006215	0.206727
W18.5M	0.152638	0.075757	0.066743	0.095229	0.049139	0.040767	0.03626	0.031592	0.009743	0.038258	0.021485	0.011508	0.037222	0.036333	0.027946	0.025714	0.012864	0.015344	0.009495	0.020464	0.003821	0.181678
W18.6M	0.077528	0.040597	0.06158	0.210872	0.045181	0.030193	0.025362	0.04521	0.004962	0.019484	0.029582	0.018174	0.052674	0.014158	0.053286	0.019265	0.009211	0.017476	0.007697	0.023136	0.002576	0.191796
Sp18.1M	0.077256	0.049088	0.060539	0.059941	0.038263	0.037257	0.039255	0.047279	0.03094	0.03062	0.054733	0.016878	0.017447	0.037549	0.036703	0.022873	0.013056	0.022596	0.016061	0.017651	0.007848	0.266167
Sp18.2M	0.075346	0.044854	0.065642	0.035462	0.048356	0.043563	0.042243	0.037643	0.039231	0.037406	0.038563	0.083061	0.016767	0.033444	0.02334	0.028978	0.017494	0.019497	0.014244	0.012464	0.017731	0.224672
Sp18.3M	0.070464	0.044687	0.073869	0.038407	0.054386	0.048357	0.047618	0.035504	0.023167	0.034499	0.045371	0.076744	0.02226	0.029461	0.022985	0.032643	0.018589	0.021269	0.014444	0.015603	0.008555	0.221118
Sp18.4M	0.070882	0.044124	0.066062	0.043546	0.046581	0.042771	0.041852	0.039277	0.034771	0.029911	0.039054	0.119512	0.026312	0.024998	0.019192	0.029399	0.016276	0.019428	0.012716	0.014279	0.011534	0.207524
Sp18.5M	0.083195	0.057996	0.068699	0.058149	0.044256	0.042143	0.038883	0.040282	0.025255	0.032769	0.036434	0.093101	0.02969	0.028865	0.017979	0.028683	0.015881	0.016608	0.012103	0.014048	0.008269	0.206713
Sp18.6M	0.061608	0.059278	0.081491	0.07974	0.044366	0.043327	0.036709	0.054931	0.007998	0.02199	0.035463	0.058284	0.053061	0.017272	0.026382	0.033089	0.015877	0.015669	0.010669	0.02521	0.003027	0.214559
Su18.1M	0.08367	0.063036	0.05166	0.034891	0.038242	0.037595	0.037183	0.037007	0.062756	0.036743	0.039182	0.009597	0.014153	0.03955	0.048838	0.021458	0.019738	0.016916	0.016755	0.009818	0.018048	0.263165
Su18.2M	0.109648	0.058771	0.054794	0.037371	0.038371	0.048742	0.0469	0.038408	0.043886	0.043862	0.028269	0.014458	0.015641	0.04701	0.031075	0.022388	0.017655	0.01824	0.017215	0.008138	0.019411	0.239745
Su18.3M	0.109589	0.075998	0.049982	0.040998	0.057044	0.049546	0.044689	0.041395	0.032424	0.039704	0.030822	0.011137	0.01907	0.045304	0.034129	0.020877	0.019826	0.015494	0.016558	0.008369	0.012983	0.224061
Su18.4M	0.125225	0.064923	0.062184	0.041795	0.042528	0.043958	0.041159	0.040156	0.049129	0.036746	0.02138	0.026478	0.024363	0.043164	0.021013	0.021991	0.018899	0.012994	0.014082	0.010977	0.016344	0.220512
Su18.5M	0.127754	0.065413	0.060654	0.044899	0.043421	0.038819	0.035171	0.04299	0.065871	0.037969	0.016592	0.032844	0.023365	0.043003	0.016566	0.020187	0.016174	0.010643	0.012722	0.010852	0.023155	0.210936
Su18.6M	0.121398	0.067043	0.073064	0.061625	0.051268	0.040167	0.037809	0.052643	0.033079	0.024602	0.017726	0.024532	0.050117	0.032588	0.024238	0.022062	0.015241	0.012729	0.010554	0.014259	0.014806	0.198448

Appendix D: Salt Bayou Marsh porewater and sediment geochemistry.

Table D1. Salt Bayou Marsh porewater and sediment geochemistry for quarterly surveys.

sample	chloride g/L	sulfate mM	sulfide mM	salinity psu	pH	NH_4 µM	NO_3 µM	redox mV	Temperature °C	% Sed H_2O	% Sed AFDM of Wet	% Sed Mineral	% Sed AFDM of Dry
3/18 R1-1	9.08	0.12	0.29	16.0	7.15	36.60	7.79	-20.3	17.0	69.20	4.85	25.95	15.75
3/18 R1-2	6.71	0.08	0.00	12.0	6.96	0.99	5.80	-32.0	17.3	75.86	5.95	18.20	28.02
3/18 R1-3	6.50	0.07	0.11	12.5	6.98	24.47	6.62	21.0	17.5	82.51	7.05	10.45	40.29
3/18 R1-4	8.40	0.10	0.00	15.0	6.97	1.65	0.46	24.0	17.8	71.01	5.70	23.29	25.51
3/18 R1-5	7.34	0.09	0.02	14.0	6.96	84.11	5.33	11.3	18.0	59.52	4.35	36.14	10.73
3/18 R2-1	6.56	0.06	0.00	12.0	6.99	0.55	2.74	11.0	17.5	22.75	0.82	76.42	1.07
3/18 R2-2	6.10	0.07	0.00	11.0	7.06	1.32	33.09	111.3	17.8	31.47	1.37	67.17	2.13
3/18 R2-3	7.85	0.10	0.00	14.5	7.02	6.61	10.71	55.7	18.0	40.18	1.91	57.91	3.19
3/18 R2-4	7.02	0.08	0.00	13.5	6.90	1.10	14.99	9.3	18.0	43.21	2.22	54.56	3.95
3/18 R2-5	9.11	0.12	0.00	17.0	6.81	6.83	10.23	28.3	18.0	46.25	2.53	51.22	4.72
3/18 R3-1	7.03	1.02	0.00	13.0	7.19	5.95	3.05	17.7	17.5	28.65	1.69	69.66	2.36
3/18 R3-2	10.15	0.09	0.00	18.0	7.37	2.09	2.26	105.0	17.5	30.47	1.90	67.62	2.75
3/18 R3-3	8.12	1.61	0.00	14.0	7.36	4.41	2.36	50.7	17.5	32.29	2.12	65.58	3.14
3/18 R3-4	6.05	1.97	0.00	11.0	7.40	15.43	0.47	65.7	17.5	34.11	2.12	63.77	3.22
3/18 R3-5	7.05	0.01	0.00	12.5	7.19	2.54	0.34	-1.3	17.5	35.92	2.12	61.96	3.30
3/18 S1-1	11.62	0.10	0.02	19.0	7.03	0.44	4.37	47.0	19.0	70.30	5.88	23.81	19.81
3/18 S1-2	9.13	0.12	0.00	16.0	7.31	0.88	7.45	36.0	19.3	72.18	5.80	22.02	20.92
3/18 S1-3	10.49	0.08	0.00	18.0	7.12	0.66	1.57	62.0	19.5	74.05	5.72	20.23	22.03
3/18 S1-4	10.52	3.19	0.59	17.0	7.04	29.65	6.61	-126.0	19.0	69.73	5.88	24.39	19.75
3/18 S1-5	10.18	0.39	0.00	17.0	7.28	1.32	3.34	-33.7	18.5	65.40	6.04	28.56	17.46
3/18 S2-1	7.35	7.02	2.48	13.0	7.17	93.70	1.49	89.3	19.0	71.78	4.93	23.30	17.45
3/18 S2-2	7.87	5.83	3.55	13.0	7.12	112.43	2.40	-45.0	19.0	72.96	5.13	21.91	19.04
3/18 S2-3	5.30	3.23	2.68	11.0	7.13	86.31	3.31	-14.7	19.0	74.15	5.33	20.52	20.63
3/18 S2-4	6.86	4.93	2.45	11.0	7.00	167.11	8.52	-133.3	18.5	77.45	4.81	17.74	21.43
3/18 S2-5	6.01	4.82	2.01	11.0	6.92	216.27	6.14	-23.3	18.0	80.75	4.28	14.97	22.22
3/18 S3-1	7.46	4.28	1.12	14.0	7.00	125.44	6.32	21.5	17.5	64.85	4.68	30.47	13.32
3/18 S3-2	7.54	4.46	1.21	13.0	7.02	22.38	6.73	-48.7	17.3	71.25	4.42	24.33	15.98
3/18 S3-3	7.82	4.59	1.22	14.5	6.83	92.15	0.48	-34.7	17.0	77.64	4.17	18.19	18.63
3/18 S3-4	7.75	4.76	0.96	14.5	6.86	49.38	1.38	-78.0	17.5	76.10	4.83	19.07	20.11
3/18 S3-5	7.42	4.51	0.73	13.0	6.93	23.15	3.01	-26.7	18.0	74.57	5.49	19.94	21.59
3/18 U1-1	4.03	2.88	0.74	7.0	7.12	227.07	0.64	-36.0	17.5	89.44	6.26	4.30	59.30
3/18 U1-2	3.73	3.31	0.16	7.0	7.04	108.58	0.31	-42.0	17.8	89.42	6.13	4.45	57.97
3/18 U1-3	4.06	3.56	0.93	7.5	6.95	172.18	0.18	-24.7	18.0	89.39	6.01	4.60	56.63
3/18 U1-4	4.66	2.38	1.34	8.5	7.04	198.19	0.73	-91.3	17.5	89.44	5.86	4.70	55.48
3/18 U1-5	5.16	3.13	1.21	9.0	7.00	212.74	1.11	-105.0	17.0	89.48	5.71	4.81	54.32
3/18 U2-1	3.64	3.85	0.13	7.0	7.37	129.19	0.19	40.0	18.0	88.74	5.40	5.86	47.98
3/18 U2-2	4.72	4.82	0.70	9.0	7.28	160.05	2.09	10.7	18.0	88.84	5.33	5.83	47.77
3/18 U2-3	4.21	3.94	0.39	7.5	7.12	79.81	0.09	139.6	18.0	88.93	5.27	5.80	47.57
3/18 U2-4	4.44	4.61	0.19	8.5	6.82	131.39	0.05	-92.7	18.0	87.62	5.68	6.70	46.03
3/18 U2-5	5.59	2.48	0.68	11.0	7.02	167.99	0.15	-113.3	18.0	86.31	6.09	7.60	44.50
3/18 U3-1	7.07	5.99	3.62	12.0	7.02	195.77	3.11	108.5	18.5	89.11	5.38	5.51	49.38
3/18 U3-2	5.96	5.83	2.51	11.0	7.06	131.39	0.29	-54.7	18.8	85.83	5.17	9.00	38.91
3/18 U3-3	6.75	8.79	3.10	12.0	6.98	189.38	5.92	-8.0	19.0	82.55	4.96	12.49	28.44
3/18 U3-4	7.18	5.49	3.28	13.0	6.91	193.12	3.36	-143.0	18.5	81.41	5.06	13.53	27.29
3/18 U3-5	7.60	7.03	3.27	14.0	6.92	182.10	2.10	-5.7	18.0	80.28	5.16	14.57	26.14

Table D1. *(continued; spring 2018)*

sample	chloride g/L	sulfate mM	sulfide mM	salinity psu	pH	NH_4 µM	NO_3 µM	redox mV	Temperature °C	% Sed H_2O	% Sed AFDM of Wet	% Sed Mineral	% Sed AFDM of Dry
5/18 R1-1	7.37	3.18	0.00	13.0	7.01	2.43	4.18	-67.9	25.0	76.40	5.27	18.33	22.32
5/18 R1-2	8.03	8.85	0.00	14.0	7.00	4.52	2.74	-37.3	25.0	68.55	4.50	26.95	15.91
5/18 R1-3	6.20	4.05	0.00	11.0	7.01	5.95	2.73	-19.5	25.0	60.70	3.73	35.56	9.50
5/18 R1-4	8.16	0.06	0.00	15.0	6.92	19.62	10.16	-24.1	25.5	59.27	3.87	36.86	9.49
5/18 R1-5	6.68	5.45	0.01	12.0	6.98	37.81	4.69	-10.7	26.0	57.84	4.00	38.16	9.48
5/18 R2-1	12.63	0.18	0.00	22.0	7.69	1.43	0.80	22.7	24.0	24.95	1.02	74.03	1.36
5/18 R2-2	8.59	2.33	0.00	14.0	6.69	70.88	6.74	79.0	25.0	29.85	1.29	68.86	1.88
5/18 R2-3	12.58	1.16	1.57	21.0	6.73	70.77	6.08	142.9	26.0	34.75	1.56	63.68	2.40
5/18 R2-4	11.26	3.75	1.33	18.0	6.90	109.57	1.93	155.9	25.0	31.55	1.33	67.13	1.96
5/18 R2-5	9.84	6.58	0.00	16.0	6.90	14.00	1.59	69.7	24.0	28.34	1.09	70.57	1.53
5/18 R3-1	11.62	0.07	0.00	18.5	7.06	1.98	8.51	-22.7	27.0	24.97	0.91	74.12	1.21
5/18 R3-2	11.26	0.14	0.00	18.0	7.12	6.06	7.53	55.7	26.5	29.47	1.29	69.24	1.87
5/18 R3-3	10.85	0.08	0.00	18.0	7.10	7.28	3.12	145.3	26.0	33.97	1.67	64.36	2.53
5/18 R3-4	9.72	0.06	0.00	17.0	7.08	5.40	9.76	27.0	25.5	38.01	2.13	59.86	3.50
5/18 R3-5	9.14	0.07	0.00	15.5	7.05	15.10	8.17	64.1	25.0	42.05	2.59	55.36	4.47
5/18 S1-1	11.04	0.02	0.11	18.5	7.00	0.88	0.11	137.8	26.0	55.00	4.93	40.08	10.95
5/18 S1-2	12.20	4.54	0.00	21.0	6.98	0.66	9.65	78.0	26.5	60.29	2.80	36.91	6.44
5/18 S1-3	12.21	4.00	0.29	21.5	6.95	1.65	7.81	183.1	27.0	65.58	0.67	33.75	1.93
5/18 S1-4	13.30	9.00	0.54	23.0	6.91	54.01	1.56	255.1	26.0	64.13	5.65	30.22	15.22
5/18 S1-5	12.06	6.02	0.70	21.0	7.09	0.55	13.67	32.3	25.0	62.68	10.63	26.68	28.50
5/18 S2-1	8.51	6.69	1.37	14.5	6.72	199.96	10.94	201.8	26.0	71.13	5.51	23.36	19.10
5/18 S2-2	7.46	0.18	1.14	13.5	6.82	234.79	0.00	167.4	26.0	73.13	5.49	21.38	20.53
5/18 S2-3	6.70	4.70	1.46	12.0	6.81	200.62	7.46	277.2	26.0	75.14	5.46	19.40	21.96
5/18 S2-4	6.22	3.70	1.78	12.0	6.85	134.70	6.06	193.2	25.5	74.85	5.41	19.74	21.53
5/18 S2-5	6.50	4.06	1.77	11.5	6.87	16.53	0.48	160.4	25.0	74.56	5.37	20.07	21.10
5/18 S3-1	7.14	3.69	1.97	13.0	6.71	102.62	2.41	26.9	24.0	74.09	4.88	21.03	18.83
5/18 S3-2	7.51	4.39	1.65	13.5	6.73	15.10	1.60	30.8	24.5	74.21	4.85	20.94	18.81
5/18 S3-3	7.54	4.08	1.79	14.0	6.72	84.22	0.71	89.6	25.0	74.33	4.82	20.85	18.78
5/18 S3-4	7.76	5.12	1.35	14.0	6.66	35.60	7.20	82.8	23.5	74.97	4.97	20.06	19.86
5/18 S3-5	7.84	7.91	0.52	14.5	6.63	43.76	6.26	-19.1	22.0	75.61	5.11	19.28	20.94
5/18 U1-1	4.06	2.55	1.05	8.5	6.72	100.64	0.34	-67.1	25.0	69.89	4.55	25.56	15.10
5/18 U1-2	4.43	0.52	1.94	9.0	6.76	66.69	5.44	-63.7	25.5	73.61	5.39	21.00	21.31
5/18 U1-3	5.27	5.56	0.19	10.0	6.61	17.53	0.28	138.7	26.0	77.33	6.24	16.43	27.52
5/18 U1-4	4.97	3.58	1.01	9.5	6.66	121.47	0.24	8.4	25.5	81.14	6.12	12.74	33.72
5/18 U1-5	5.23	5.22	0.47	9.5	6.69	36.38	0.31	12.3	25.0	84.95	6.01	9.04	39.92
5/18 U2-1	4.42	5.05	0.19	8.0	6.43	52.47	0.81	96.9	22.0	85.12	6.24	8.64	41.92
5/18 U2-2	5.21	5.53	0.60	9.5	6.49	10.47	0.21	74.0	24.0	85.31	6.06	8.63	41.23
5/18 U2-3	4.95	1.76	2.41	9.0	6.93	157.41	0.32	83.3	26.0	85.50	5.88	8.62	40.53
5/18 U2-4	6.04	0.68	3.22	10.0	7.12	199.30	0.38	66.9	25.5	83.41	5.90	10.69	36.10
5/18 U2-5	6.31	5.26	4.73	11.0	7.06	141.76	4.25	-18.2	25.0	81.32	5.92	12.77	31.67
5/18 U3-1	5.76	5.36	1.02	10.0	6.63	67.79	8.06	-74.3	25.0	89.25	5.83	4.92	54.24
5/18 U3-2	6.25	5.88	1.37	10.5	6.75	108.58	1.42	-83.6	24.5	88.67	5.49	5.84	48.76
5/18 U3-3	6.03	4.77	1.21	10.5	6.72	57.10	3.22	84.3	24.0	88.10	5.15	6.75	43.28
5/18 U3-4	6.21	5.53	1.33	11.0	6.76	94.14	1.84	-64.8	25.0	89.05	5.45	5.50	50.39
5/18 U3-5	5.97	6.52	0.70	10.0	6.85	78.81	1.46	-50.0	26.0	90.00	5.75	4.25	57.49

Table D1. *(continued; summer 2018)*

sample	chloride g/L	sulfate mM	sulfide mM	salinity psu	pH	NH_4 µM	NO_3 µM	redox mV	Temperature °C	% Sed H_2O	% Sed AFDM of Wet	% Sed Mineral	% Sed AFDM of Dry
8/18 R1-1	9.69	5.70	0.007	17.0	6.85	13.18	0.53	-18.6	27.0				
8/18 R1-2	8.43	6.92	0.002	15.0	6.69	32.12	0.66	-33.6	27.5	83.74	7.41	8.85	45.58
8/18 R1-3	9.74	4.72	0.003	17.0	6.82	55.30	0.62	98.6	28.0	83.74	7.41	8.85	45.58
8/18 R1-4	7.74	10.92	0.002	14.5	6.88	86.36	0.49	130.2	28.5	79.23	6.50	14.27	33.85
8/18 R1-5	8.99	6.44	0.002	15.5	6.78	26.06	0.68	60.9	29.0	74.72	5.59	19.69	22.12
8/18 R2-1	11.02	1.52	0.002	20.0	7.31	2.78	2.46	23.1	27.0	21.80	0.76	77.43	0.98
8/18 R2-2	10.05	32.76	0.002	19.0	6.76	3.02	3.24	66.3	28.5	27.30	1.18	71.52	1.68
8/18 R2-3	10.91	38.92	0.002	20.0	5.96	3.50	3.50	145.7	30.0	32.79	1.61	65.60	2.39
8/18 R2-4	10.71	13.47	0.002	20.0	6.40	5.55	1.95	192.7	30.5	33.81	1.72	64.46	2.61
8/18 R2-5	11.48	19.49	0.002	21.0	6.30	17.27	3.60	237.4	31.0	34.84	1.84	63.32	2.83
8/18 R3-1	15.24	4.36	0.003	27.0	6.94	20.60	0.19	65.5	30.0	25.39	1.39	73.22	1.86
8/18 R3-2	lost porwater sample							122.3	30.0	25.41	1.41	73.18	1.89
8/18 R3-3	16.02	13.05	0.003	27.5	6.42	4.70	0.66	117.3	30.0	25.43	1.44	73.13	1.93
8/18 R3-4	15.20	20.72	0.003	28.0	6.02	12.42	0.65	105.7	29.0	29.96	1.89	68.15	2.75
8/18 R3-5	lost porewater sample							99.6	28.0	34.50	2.34	63.16	3.57
8/18 S1-1	12.34	18.76	0.004	21.5	6.31	6.21	0.45	331.3	27.0	69.71	7.32	22.98	24.15
8/18 S1-2	11.93	15.73	0.000	20.0	6.32	6.21	0.42	344.7	27.0	62.28	6.05	31.67	17.38
8/18 S1-3	12.49	24.25	0.000	22.0	6.16	3.64	1.01	287.7	27.0	54.85	4.79	40.37	10.60
8-18 S1-4	12.94	18.76	0.000	22.5	6.57	13.48	2.04	228.0	27.0	55.44	4.08	40.48	9.13
8-18 S1-5	12.68	15.76	0.001	24.0	6.57	5.61	2.28	182.0	27.0	56.04	3.37	40.60	7.66
8/18 S2-1	10.80	14.21	0.000	20.5	5.85	3.64	5.60	311.7	27.5	71.05	6.09	22.85	21.05
8/18 S2-2	10.63	13.05	0.001	20.0	5.88	2.42	1.50	255.0	27.3	73.41	5.80	20.79	21.87
8-18 S2-3	10.64	10.41	0.001	19.5	5.92	2.12	1.16	291.7	27.0	75.77	5.50	18.73	22.70
8/18 S2-4	10.08	9.02	0.002	17.5	5.75	1.67	5.89	314.0	26.5	75.10	5.60	19.30	22.49
8/18 S2-5	9.44	8.16	0.002	17.0	5.79	3.33	0.83	310.4	26.0	74.43	5.70	19.87	22.29
8/18 S3-1	10.58	10.28	0.002	18.5	5.76	2.27	1.84	303.4	28.0	75.93	6.56	17.51	27.24
8/18 S3-2	10.40	7.99	0.001	17.5	5.96	4.24	1.69	108.7	28.0	77.53	6.91	15.56	31.03
8/18 S3-3	11.35	10.57	0.001	19.5	5.77	1.67	3.97	34.0	28.0	79.12	7.27	13.61	34.81
8/18 S3-4	11.38	11.75	0.002	20.0	5.86	2.27	2.63	130.1	27.5	70.50	6.16	23.34	24.03
8/18 S3-5	11.04	10.76	0.001	19.0	5.35	2.27	1.31	93.5	27.0	61.88	5.05	33.07	13.26
8/18 U1-1	5.86	5.52	1.542	11.0	6.95	14.61	0.39	41.2	27.0	87.28	7.33	5.39	57.64
8/18 U1-2	5.05	0.36	1.436	10.0	7.10	5.43	0.42	-4.8	27.5	87.69	6.51	5.80	52.71
8/18 U1-3	5.40	0.88	1.946	10.0	7.23	14.01	0.52	55.8	28.0	88.09	5.69	6.22	47.78
8/18 U1-4	6.59	8.64	0.763	13.0	6.77	43.71	0.62	112.8	28.5	86.57	5.66	7.78	42.70
8/18 U1-5	6.60	8.81	1.604	11.0	7.09	32.48	0.47	37.7	29.0	85.04	5.63	9.33	37.61
8/18 U2-1	5.26	6.77	0.757	10.0	6.55	96.20	1.75	-105.7	28.0	85.56	6.40	8.05	44.28
8/18 U2-2	5.18	9.97	0.072	10.0	6.24	57.12	2.06	-125.0	27.8	86.17	6.28	7.54	45.48
8/18 U2-3	4.68	8.64	0.263	9.0	6.37	107.57	8.00	-21.0	27.5	86.79	6.17	7.04	46.69
8/18 U2-4	5.50	8.19	0.140	10.0	6.36	60.90	6.60	-98.0	26.8	84.47	5.80	9.73	38.57
8/18 U2-5	5.29	4.35	2.943	10.0	6.83	129.99	2.34	-80.0	26.0	82.15	5.43	12.41	30.45
8/18 U3-1	9.35	6.29	1.626	17.0	6.60	60.75	4.75	-67.0	27.5	87.49	6.56	5.95	52.45
8-18 U3-2	9.35	7.06	1.713	17.5	6.66	90.90	2.38	-104.7	27.3	88.87	6.18	4.95	55.99
8/18 U3-3	8.23	6.55	0.004	15.0	6.44	20.45	2.61	78.7	27.0	90.25	5.80	3.94	59.54
8/18 U3-4	8.99	7.13	2.130	17.0	6.49	74.08	2.49	-38.3	27.0	89.78	5.31	4.91	52.29
8/18 U3-5	9.17	7.66	1.648	17.0	6.65	112.11	2.37	-36.0	27.0	89.30	4.82	5.88	45.03

Table D1. *(continued; fall 2018)*

sample	chloride g/L	sulfate mM	sulfide mM	salinity psu	pH	NH_4 µM	NO_3 µM	redox mV	Temperature °C	% Sed H_2O	% Sed AFDM of Wet	% Sed Mineral	% Sed AFDM of Dry
11/18 R1-1	8.44	8.62	0.069	15.0	6.67	17.99	2.50	91.4	10.0	71.81	6.03	22.15	21.41
11/18 R1-2	8.33	4.24	0.882	15.0	6.71	11.35	2.26	47.9	10.0	72.68	6.19	21.14	22.68
11/18 R1-3	9.19	5.31	0.702	16.0	6.99	10.26	0.00	28.7	10.0	73.54	6.34	20.12	23.96
11/18 R1-4	8.17	3.48	0.974	15.0	6.94	1.45	0.00	-124.3	10.0	71.98	6.15	21.88	22.04
11/18 R1-5	7.32	3.75	0.000	13.0	6.88	4.47	0.00	-30.4	10.0	70.42	5.95	23.63	20.12
11/18 R2-1	8.56	18.74	0.001	16.0	6.60	2.17	3.16	77.4	10.0	26.45	0.77	72.78	1.04
11/18 R2-2	8.94	27.65	0.001	16.0	6.38	10.50	1.02	146.2	10.0	26.38	1.23	72.39	1.68
11/18 R2-3	11.12	41.02	0.001	21.0	6.72	3.02	3.57	122.1	10.0	26.30	1.70	72.00	2.31
11/18 R2-4	12.48	31.50	0.002	21.0	6.56	19.92	3.54	106.4	10.5	31.83	1.93	66.23	2.88
11/18 R2-5	13.49	39.59	0.002	23.0	6.24	14.13	4.30	148.3	11.0	37.37	2.17	60.46	3.46
11/18 R3-1	16.10	5.04	0.000	29.0	6.80	1.21	0.00	72.0	14.5	28.12	1.67	70.21	2.32
11/18 R3-2	13.61	4.21	0.006	25.0	6.85	0.12	0.00	46.3	14.5	28.53	1.59	69.88	2.23
11/18 R3-3	17.27	6.57	0.001	31.0	7.04	0.60	0.00	39.7	14.5	28.93	1.52	69.55	2.13
11/18 R3-4	17.82	9.14	0.001	32.0	7.00	1.09	0.00	-4.7	15.0	29.00	1.61	69.39	2.27
11/18 R3-5	16.65	11.20	0.001	31.0	6.95	0.72	2.78	15.7	15.5	29.06	1.70	69.24	2.40
11/18 S1-1	12.23	54.48	0.00	22.0	6.40	3.98	10.62	151.7	16.0	62.71	5.18	32.11	13.88
11/18 S1-2	12.72	50.81	0.00	23.5	6.40	3.14	5.29	93.7	16.8	68.02	6.29	25.69	20.84
11/18 S1-3	12.87	56.58	0.00	23.0	6.19	13.89	7.41	93.7	17.5	73.33	7.41	19.26	27.80
11/18 S1-4	12.48	55.34	0.00	22.5	6.27	11.35	7.03	113.3	17.5	70.13	6.69	23.18	22.92
11/18 S1-5	13.25	50.67	0.01	24.5	6.37	4.35	5.01	76.7	17.5	66.92	5.97	27.11	18.04
11/18 S2-1	11.31	16.63	0.00	20.5	5.83	19.56	3.70	87.0	17.0	70.84	5.60	23.56	19.21
11/18 S2-2	11.93	17.35	0.00	21.0	5.85	18.84	4.14	136.3	17.3	73.09	5.42	21.48	20.24
11/18 S2-3	12.05	13.17	0.00	21.5	5.82	15.94	4.57	201.3	17.5	75.35	5.25	19.41	21.28
11/18 S2-4	11.54	10.76	0.00	21.0	5.89	29.34	3.50	150.3	17.3	75.41	5.91	18.68	24.03
11/18 S2-5	11.54	7.05	0.00	20.5	5.95	11.23	3.90	127.0	17.0	75.47	6.57	17.96	26.79
11/18 S3-1	11.66	8.43	0.238	21.0	6.41	1.57	3.98	-27.3	14.0	76.80	5.93	17.27	25.57
11/18 S3-2	11.57	4.81	0.012	21.0	6.63	1.69	2.51	-11.7	14.5	76.71	5.97	17.32	25.63
11/18 S3-3	12.28	14.04	0.644	23.0	6.45	2.54	4.15	-3.7	15.0	76.63	6.00	17.37	25.69
11/18 S3-4	12.81	15.79	0.001	24.0	6.56	0.00	4.16	77.0	15.0	75.15	5.79	19.06	23.42
11/18 S3-5	11.32	7.77	0.000	20.0	6.52	2.90	3.01	84.7	15.0	73.68	5.57	20.75	21.16
11/18 U1-1	7.13	1.89	0.720	13.0	6.68	20.77	0.19	-62.0	12.0	88.60	6.46	4.94	56.67
11/18 U1-2	7.96	2.61	1.098	15.0	6.90	79.81	1.99	-101.9	12.0	88.96	5.84	5.21	52.74
11/18 U1-3	6.49	2.23	2.003	11.0	6.99	13.04	0.00	248.3	12.0	89.32	5.21	5.47	48.81
11/18 U1-4	6.27	2.64	2.165	11.0	6.82	24.87	0.00	-70.1	12.0	90.32	5.43	4.26	56.88
11/18 U1-5	6.21	1.62	1.827	11.0	6.85	31.75	0.00	-43.8	12.0	91.31	5.64	3.04	64.96
11/18 U2-1	8.41	1.44	0.46	15.0	6.74	14.73	0.00	-64.3	14.0	87.18	5.79	7.03	45.13
11/18 U2-2	8.41	4.18	0.54	15.0	6.82	14.25	0.37	-42.0	14.8	86.68	5.37	7.95	40.50
11/18 U2-3	8.26	2.07	0.67	15.0	6.77	6.28	0.30	14.7	15.5	86.18	4.96	8.86	35.86
11/18 U2-4	8.50	0.73	0.34	15.0	6.84	32.72	0.28	-76.0	15.3	85.86	5.60	8.54	39.54
11/18 U2-5	8.24	3.10	1.17	15.0	7.07	21.73	0.26	-111.3	15.0	85.54	6.25	8.21	43.22
11/18 U3-1	9.26	5.16	1.91	17.0	7.00	16.78	0.39	-91.8	18.0	90.79	5.09	4.12	55.26
11/18 U3-2	12.65	4.70	1.57	22.5	6.71	18.71	0.20	-51.3	18.0	87.89	5.56	6.54	47.75
11/18 U3-3	11.88	5.36	1.65	21.0	6.84	13.52	0.48	-34.0	18.0	85.00	6.04	8.96	40.24
11/18 U3-4	11.17	6.23	1.67	20.5	6.95	20.16	0.20	-66.3	18.0	86.41	6.40	7.20	47.85
11/18 U3-5	11.64	5.32	1.63	20.5	7.00	8.93	0.50	-65.0	18.0	87.82	6.75	5.43	55.45

Appendix E: Relative abundance of microbial communities in marsh sediment.

Table E1. Relative abundance of 25 dominant prokaryote orders in marsh sediment communities based on SSU rDNA, representing 82 % of the overall average

Sample	Methanosarcinales	Methanobacteriales	Anaerolineales	Desulfobacterales	Dehalococcoidales	Chromatiales	Crenarchaeota	Planctomycetales	Desulfuromonadales	Ignavibacteriales	Desulfurococcales	Nitrospirales
W18.R1	0.104	0.045	0.050	0.089	0.013	0.060	0.064	0.046	0.058	0.068	0.020	0.015
W18.R2	0.080	0.056	0.075	0.079	0.028	0.035	0.041	0.035	0.038	0.047	0.042	0.039
W18.R3	0.081	0.024	0.078	0.075	0.040	0.052	0.030	0.026	0.098	0.009	0.036	0.067
W18.S1	0.081	0.071	0.053	0.070	0.059	0.037	0.054	0.072	0.021	0.032	0.055	0.024
W18.S2	0.126	0.049	0.072	0.058	0.014	0.071	0.068	0.031	0.028	0.080	0.033	0.012
W18.S3	0.080	0.036	0.073	0.057	0.047	0.056	0.070	0.029	0.027	0.025	0.034	0.092
W18.U1	0.156	0.156	0.018	0.055	0.062	0.009	0.033	0.067	0.014	0.059	0.039	0.018
W18.U2	0.147	0.164	0.023	0.043	0.036	0.021	0.032	0.048	0.014	0.086	0.043	0.021
W18.U3	0.131	0.160	0.039	0.041	0.068	0.014	0.057	0.051	0.012	0.038	0.058	0.022
Sp18.R1	0.059	0.024	0.099	0.076	0.015	0.071	0.063	0.048	0.076	0.025	0.028	0.032
Sp18.R2	0.083	0.023	0.091	0.079	0.035	0.073	0.027	0.030	0.071	0.011	0.028	0.066
Sp18.R3	0.078	0.028	0.109	0.066	0.031	0.055	0.026	0.027	0.091	0.009	0.021	0.096
Sp18.S1	0.070	0.056	0.054	0.081	0.048	0.052	0.054	0.051	0.031	0.027	0.055	0.025
Sp18.S2	0.103	0.027	0.098	0.047	0.014	0.084	0.040	0.030	0.030	0.047	0.009	0.013
Sp18.S3	0.095	0.062	0.086	0.064	0.032	0.066	0.052	0.033	0.028	0.036	0.033	0.029
Sp18.U1	0.077	0.065	0.058	0.071	0.049	0.046	0.060	0.047	0.026	0.028	0.021	0.015
Sp18.U2	0.075	0.138	0.048	0.064	0.102	0.012	0.057	0.050	0.015	0.029	0.034	0.014
Sp18.U3	0.120	0.134	0.037	0.048	0.062	0.027	0.042	0.040	0.018	0.041	0.035	0.010
Su18.R1	0.095	0.085	0.063	0.070	0.039	0.037	0.053	0.052	0.026	0.031	0.038	0.014
Su18.R2	0.043	0.021	0.117	0.075	0.035	0.083	0.020	0.033	0.061	0.012	0.018	0.070
Su18.R3	0.073	0.021	0.072	0.084	0.043	0.064	0.027	0.032	0.085	0.009	0.031	0.067
Su18.S1	0.045	0.033	0.079	0.077	0.038	0.056	0.035	0.052	0.035	0.019	0.072	0.042
Su18.S2	0.059	0.015	0.102	0.048	0.011	0.084	0.040	0.027	0.037	0.039	0.008	0.013
Su18.S3	0.071	0.034	0.096	0.060	0.033	0.068	0.045	0.032	0.027	0.030	0.030	0.030
Su18.U1	0.118	0.101	0.046	0.061	0.070	0.017	0.045	0.062	0.017	0.027	0.040	0.013
Su18.U2	0.084	0.089	0.054	0.059	0.067	0.036	0.035	0.034	0.021	0.049	0.030	0.015
Su18.U3	0.100	0.106	0.048	0.055	0.072	0.029	0.034	0.038	0.020	0.043	0.032	0.008
F18.R1	0.068	0.076	0.055	0.088	0.058	0.035	0.059	0.053	0.028	0.032	0.031	0.017
F18.R2	0.049	0.021	0.101	0.105	0.033	0.077	0.018	0.029	0.067	0.014	0.017	0.062
F18.R3	0.069	0.042	0.075	0.090	0.078	0.037	0.038	0.040	0.053	0.008	0.053	0.054
F18.S1	0.053	0.045	0.075	0.092	0.043	0.048	0.043	0.049	0.033	0.035	0.041	0.018
F18.S2	0.045	0.010	0.104	0.052	0.013	0.092	0.047	0.036	0.042	0.042	0.010	0.011
F18.S3	0.094	0.064	0.083	0.060	0.032	0.056	0.039	0.037	0.026	0.034	0.027	0.016
F18.U1	0.102	0.121	0.045	0.060	0.098	0.010	0.045	0.061	0.015	0.024	0.040	0.009
F18.U2	0.115	0.099	0.055	0.049	0.074	0.022	0.037	0.047	0.018	0.039	0.029	0.015
F18.U3	0.097	0.120	0.037	0.061	0.105	0.019	0.045	0.052	0.020	0.033	0.032	0.010

Table E1. (continued)

Sample	Acidobacteriales	Syntrophobacterales	Clostridiales	Rhizobiales	Cytophagales	Methanococcales	Spirochaetales	Dehalococcoidia	Bacteroidales	Burkholderiales	Rhodospirillales	Myxococcales	Chloroflexales
W18.R1	0.015	0.023	0.020	0.015	0.018	0.031	0.016	0.007	0.022	0.012	0.016	0.013	0.009
W18.R2	0.023	0.020	0.028	0.006	0.032	0.025	0.018	0.006	0.054	0.004	0.009	0.007	0.015
W18.R3	0.022	0.024	0.034	0.006	0.011	0.008	0.021	0.005	0.022	0.006	0.016	0.013	0.014
W18.S1	0.027	0.023	0.022	0.015	0.016	0.017	0.022	0.018	0.012	0.015	0.009	0.011	0.012
W18.S2	0.024	0.022	0.013	0.015	0.013	0.026	0.010	0.007	0.016	0.013	0.011	0.015	0.005
W18.S3	0.030	0.024	0.011	0.025	0.013	0.015	0.021	0.010	0.007	0.010	0.009	0.015	0.012
W18.U1	0.011	0.019	0.023	0.006	0.027	0.037	0.015	0.025	0.020	0.004	0.003	0.004	0.003
W18.U2	0.012	0.018	0.019	0.008	0.024	0.030	0.017	0.013	0.019	0.008	0.005	0.005	0.005
W18.U3	0.014	0.020	0.019	0.017	0.013	0.021	0.019	0.023	0.009	0.010	0.007	0.005	0.010
Sp18.R1	0.016	0.026	0.017	0.017	0.020	0.014	0.014	0.006	0.022	0.011	0.014	0.016	0.020
Sp18.R2	0.022	0.018	0.025	0.013	0.010	0.011	0.008	0.006	0.006	0.006	0.023	0.014	0.022
Sp18.R3	0.027	0.017	0.022	0.007	0.009	0.010	0.011	0.005	0.012	0.005	0.020	0.013	0.016
Sp18.S1	0.033	0.027	0.021	0.018	0.015	0.016	0.016	0.013	0.011	0.017	0.013	0.014	0.013
Sp18.S2	0.045	0.025	0.016	0.031	0.011	0.024	0.013	0.008	0.012	0.024	0.017	0.023	0.007
Sp18.S3	0.024	0.022	0.015	0.031	0.013	0.014	0.017	0.013	0.008	0.014	0.010	0.018	0.009
Sp18.U1	0.030	0.025	0.021	0.024	0.025	0.017	0.017	0.017	0.014	0.017	0.010	0.014	0.013
Sp18.U2	0.019	0.028	0.023	0.009	0.023	0.017	0.027	0.032	0.011	0.007	0.003	0.007	0.011
Sp18.U3	0.013	0.021	0.018	0.025	0.014	0.020	0.025	0.021	0.009	0.025	0.014	0.008	0.006
Su18.R1	0.019	0.023	0.019	0.022	0.021	0.023	0.016	0.014	0.014	0.024	0.015	0.013	0.010
Su18.R2	0.030	0.013	0.024	0.016	0.011	0.010	0.008	0.006	0.004	0.007	0.026	0.017	0.021
Su18.R3	0.024	0.027	0.031	0.008	0.011	0.010	0.009	0.006	0.015	0.006	0.023	0.011	0.019
Su18.S1	0.031	0.027	0.020	0.027	0.023	0.011	0.015	0.010	0.013	0.017	0.014	0.018	0.016
Su18.S2	0.060	0.026	0.011	0.056	0.008	0.012	0.007	0.009	0.008	0.027	0.032	0.030	0.003
Su18.S3	0.031	0.022	0.017	0.053	0.013	0.012	0.020	0.012	0.008	0.019	0.012	0.022	0.011
Su18.U1	0.020	0.029	0.022	0.014	0.027	0.028	0.027	0.024	0.014	0.011	0.006	0.008	0.007
Su18.U2	0.021	0.029	0.021	0.018	0.022	0.017	0.031	0.019	0.015	0.017	0.007	0.011	0.011
Su18.U3	0.014	0.020	0.019	0.032	0.018	0.015	0.029	0.024	0.010	0.021	0.015	0.009	0.009
F18.R1	0.022	0.030	0.025	0.017	0.017	0.017	0.019	0.019	0.016	0.015	0.012	0.012	0.014
F18.R2	0.025	0.019	0.029	0.014	0.011	0.012	0.007	0.006	0.010	0.008	0.030	0.014	0.023
F18.R3	0.022	0.032	0.028	0.005	0.012	0.008	0.013	0.011	0.009	0.006	0.013	0.009	0.018
F18.S1	0.031	0.028	0.024	0.020	0.019	0.013	0.015	0.011	0.016	0.021	0.014	0.016	0.019
F18.S2	0.043	0.022	0.013	0.039	0.009	0.009	0.008	0.011	0.009	0.028	0.024	0.033	0.005
F18.S3	0.026	0.023	0.015	0.038	0.018	0.018	0.015	0.011	0.013	0.019	0.012	0.021	0.010
F18.U1	0.017	0.025	0.023	0.009	0.028	0.025	0.030	0.035	0.015	0.008	0.004	0.006	0.008
F18.U2	0.019	0.025	0.023	0.018	0.023	0.024	0.025	0.021	0.014	0.014	0.008	0.009	0.010
F18.U3	0.018	0.025	0.024	0.015	0.016	0.020	0.027	0.032	0.010	0.008	0.010	0.009	0.009

Table E2. Relative abundance of 15 dominant sulfate reducing bacteria genera in marsh sediment communities based on *dsr*B DNA, representing 99 % of the overall average

	Desulfatiglans	Desulfotomaculum	Desulfobulbus	Desulfotignum	Desulfosarcina	Syntrophobacter	Desulfovibrio	Desulfacinum	Desulfarculus	Desulfofaba	Desulfonema	Desulfosalsimonas	Desulfomonile	Desulfobacter	Desulfonatronospira
W18.R1	0.173	0.123	0.142	0.295	0.111	0.052	0.034	0.031	0.012	0.003	0.008	0.004	0.001	0.000	0.005
W18.R2	0.176	0.099	0.155	0.266	0.099	0.048	0.043	0.019	0.012	0.009	0.006	0.029	0.007	0.001	0.003
W18.R3	0.081	0.115	0.208	0.159	0.254	0.006	0.030	0.026	0.062	0.002	0.008	0.031	0.005	0.000	0.000
W18.S1	0.221	0.287	0.104	0.168	0.077	0.082	0.012	0.010	0.008	0.009	0.009	0.007	0.001	0.000	0.000
W18.S2	0.136	0.248	0.096	0.196	0.051	0.077	0.022	0.052	0.006	0.009	0.004	0.009	0.001	0.000	0.064
W18.S3	0.225	0.248	0.092	0.083	0.041	0.019	0.055	0.120	0.005	0.018	0.028	0.003	0.001	0.000	0.007
W18.U1	0.350	0.078	0.167	0.209	0.064	0.020	0.012	0.012	0.030	0.020	0.008	0.006	0.001	0.008	0.005
W18.U2	0.283	0.111	0.139	0.286	0.035	0.048	0.013	0.005	0.026	0.014	0.011	0.005	0.001	0.000	0.016
W18.U3	0.304	0.260	0.160	0.070	0.097	0.030	0.036	0.006	0.005	0.022	0.003	0.003	0.000	0.000	0.000
Sp18.R1	0.093	0.174	0.161	0.251	0.114	0.058	0.051	0.052	0.015	0.005	0.004	0.006	0.001	0.000	0.001
Sp18.R2	0.036	0.132	0.270	0.224	0.188	0.012	0.033	0.027	0.026	0.005	0.003	0.020	0.006	0.000	0.001
Sp18.R3	0.055	0.170	0.215	0.141	0.169	0.009	0.053	0.041	0.092	0.003	0.003	0.019	0.005	0.001	0.000
Sp18.S1	0.149	0.232	0.110	0.222	0.119	0.086	0.018	0.018	0.012	0.008	0.008	0.007	0.003	0.000	0.000
Sp18.S2	0.094	0.404	0.073	0.123	0.064	0.069	0.035	0.033	0.006	0.007	0.002	0.005	0.001	0.000	0.058
Sp18.S3	0.198	0.160	0.081	0.235	0.066	0.039	0.051	0.083	0.012	0.023	0.013	0.005	0.004	0.000	0.013
Sp18.U1	0.220	0.132	0.134	0.133	0.242	0.028	0.021	0.015	0.041	0.007	0.012	0.003	0.001	0.000	0.008
Sp18.U2	0.324	0.106	0.153	0.217	0.068	0.039	0.020	0.007	0.028	0.021	0.006	0.005	0.001	0.000	0.002
Sp18.U3	0.246	0.186	0.155	0.167	0.051	0.106	0.024	0.009	0.019	0.023	0.005	0.005	0.000	0.000	0.000
Su18.R1	0.026	0.097	0.145	0.282	0.073	0.047	0.019	0.019	0.017	0.026	0.006	0.005	0.003	0.000	0.003
Su18.R2	0.023	0.146	0.256	0.235	0.179	0.011	0.049	0.028	0.013	0.002	0.002	0.015	0.005	0.000	0.000
Su18.R3	0.053	0.136	0.153	0.187	0.255	0.006	0.031	0.020	0.094	0.008	0.004	0.028	0.006	0.003	0.000
Su18.S1	0.163	0.233	0.148	0.159	0.139	0.062	0.026	0.020	0.013	0.012	0.007	0.007	0.002	0.000	0.000
Su18.S2	0.129	0.372	0.064	0.117	0.074	0.088	0.032	0.034	0.006	0.006	0.002	0.007	0.001	0.000	0.040
Su18.S3	0.205	0.212	0.101	0.198	0.050	0.034	0.043	0.059	0.014	0.023	0.023	0.004	0.003	0.000	0.019
Su18.U1	0.299	0.116	0.133	0.212	0.076	0.034	0.016	0.018	0.061	0.011	0.007	0.004	0.002	0.004	0.005
Su18.U2	0.269	0.155	0.121	0.250	0.048	0.054	0.016	0.006	0.041	0.010	0.012	0.004	0.001	0.000	0.009
Su18.U3	0.248	0.189	0.157	0.187	0.039	0.083	0.028	0.009	0.026	0.023	0.004	0.004	0.000	0.000	0.000
F18.R1	0.222	0.106	0.155	0.279	0.079	0.057	0.020	0.023	0.013	0.011	0.012	0.008	0.002	0.000	0.007
F18.R2	0.030	0.108	0.197	0.230	0.156	0.012	0.056	0.027	0.020	0.003	0.007	0.017	0.008	0.106	0.001
F18.R3	0.087	0.105	0.186	0.165	0.286	0.005	0.023	0.032	0.044	0.003	0.005	0.031	0.007	0.000	0.000
F18.S1	0.117	0.164	0.157	0.263	0.101	0.117	0.019	0.016	0.011	0.004	0.011	0.008	0.003	0.000	0.000
F18.S2	0.079	0.355	0.074	0.132	0.062	0.057	0.052	0.065	0.005	0.004	0.004	0.007	0.003	0.000	0.070
F18.S3	0.196	0.169	0.102	0.217	0.074	0.051	0.048	0.058	0.015	0.020	0.014	0.005	0.003	0.001	0.008
F18.U1	0.312	0.124	0.187	0.174	0.088	0.019	0.012	0.011	0.034	0.020	0.008	0.004	0.001	0.001	0.002
F18.U2	0.285	0.178	0.112	0.203	0.048	0.075	0.016	0.013	0.035	0.011	0.011	0.004	0.001	0.000	0.008
F18.U3	0.319	0.211	0.156	0.123	0.050	0.048	0.035	0.008	0.014	0.024	0.005	0.005	0.000	0.000	0.000

Table E3. Relative abundance of 15 dominant sulfate reducing bacteria genera in marsh sediment communities based on *dsr*B RNA, representing 99 % of the overall average

	Desulfatiglans	Desulfotomaculum	Desulfobulbus	Desulfotignum	Desulfosarcina	Syntrophobacter	Desulfovibrio	Desulfacinum	Desulfarculus	Desulfofaba	Desulfonema	Desulfosalsimonas	Desulfomonile	Desulfobacter	Desulfonatronospira
W18.R1ex	0.218	0.160	0.117	0.116	0.119	0.120	0.039	0.040	0.027	0.001	0.017	0.003	0.005	0.000	0.010
W18.R2ex	0.004	0.135	0.038	0.004	0.149	0.001	0.184	0.005	0.001	0.001	0.001	0.000	0.476	0.000	0.000
W18.R3ex	0.100	0.036	0.376	0.052	0.141	0.002	0.052	0.007	0.012	0.026	0.069	0.080	0.012	0.003	0.000
W18.S1ex	0.238	0.304	0.095	0.116	0.112	0.049	0.017	0.008	0.007	0.012	0.012	0.011	0.002	0.001	0.000
W18.S2ex	0.123	0.325	0.103	0.091	0.089	0.092	0.043	0.049	0.010	0.008	0.006	0.015	0.003	0.000	0.028
W18.S3ex	0.238	0.115	0.119	0.193	0.092	0.033	0.024	0.035	0.012	0.068	0.020	0.028	0.002	0.004	0.010
W18.U1ex	0.443	0.078	0.161	0.055	0.067	0.005	0.010	0.031	0.090	0.010	0.022	0.014	0.006	0.000	0.000
W18.U2ex	0.278	0.163	0.109	0.219	0.040	0.093	0.033	0.041	0.015	0.001	0.001	0.003	0.001	0.000	0.000
W18.U3ex	0.295	0.270	0.148	0.048	0.120	0.022	0.048	0.006	0.011	0.015	0.002	0.010	0.001	0.000	0.000
Sp18.R1ex	0.186	0.126	0.173	0.177	0.114	0.080	0.030	0.049	0.026	0.004	0.010	0.008	0.004	0.002	0.002
Sp18.R2ex	0.040	0.054	0.497	0.059	0.130	0.010	0.017	0.014	0.010	0.023	0.064	0.020	0.013	0.004	0.000
Sp18.R3ex	0.089	0.057	0.192	0.117	0.181	0.027	0.044	0.010	0.008	0.072	0.023	0.080	0.005	0.047	0.000
Sp18.S1ex	0.152	0.215	0.154	0.147	0.108	0.106	0.030	0.018	0.018	0.011	0.014	0.009	0.009	0.001	0.000
Sp18.S2ex	0.106	0.353	0.085	0.081	0.130	0.083	0.040	0.030	0.010	0.007	0.003	0.019	0.002	0.000	0.028
Sp18.S3ex	0.236	0.170	0.097	0.169	0.070	0.039	0.060	0.043	0.023	0.038	0.016	0.009	0.010	0.001	0.003
Sp18.U1ex	0.223	0.139	0.132	0.085	0.215	0.047	0.041	0.021	0.052	0.007	0.018	0.005	0.003	0.003	0.001
Sp18.U2ex	0.343	0.114	0.173	0.160	0.064	0.040	0.037	0.009	0.018	0.026	0.005	0.005	0.001	0.001	0.001
Sp18.U3ex	0.332	0.167	0.156	0.070	0.063	0.082	0.024	0.007	0.023	0.033	0.009	0.022	0.002	0.003	0.000
Su18.R1ex	0.247	0.131	0.155	0.184	0.087	0.070	0.026	0.028	0.029	0.021	0.008	0.004	0.004	0.000	0.002
Su18.R2ex	0.023	0.056	0.378	0.090	0.215	0.006	0.051	0.019	0.004	0.005	0.081	0.020	0.006	0.006	0.000
Su18.R3ex	0.049	0.035	0.456	0.083	0.110	0.016	0.057	0.018	0.011	0.071	0.026	0.014	0.007	0.026	0.000
Su18.S1ex	0.142	0.220	0.222	0.073	0.123	0.098	0.029	0.016	0.009	0.015	0.021	0.013	0.002	0.002	0.000
Su18.S2ex	0.100	0.410	0.068	0.055	0.080	0.098	0.049	0.039	0.009	0.007	0.003	0.011	0.001	0.000	0.031
Su18.S3ex	0.141	0.212	0.107	0.134	0.050	0.053	0.034	0.056	0.006	0.093	0.035	0.014	0.002	0.012	0.015
Su18.U1ex	0.299	0.158	0.123	0.147	0.080	0.038	0.028	0.020	0.068	0.012	0.007	0.005	0.003	0.004	0.003
Su18.U2ex	0.289	0.152	0.141	0.177	0.064	0.055	0.026	0.008	0.029	0.021	0.010	0.006	0.002	0.001	0.005
Su18.U3ex	0.260	0.191	0.163	0.114	0.038	0.104	0.031	0.010	0.036	0.027	0.005	0.007	0.001	0.008	0.001
F18.R1ex	0.226	0.126	0.162	0.189	0.090	0.086	0.023	0.023	0.022	0.011	0.020	0.006	0.004	0.001	0.004
F18.R2ex	0.013	0.029	0.140	0.200	0.112	0.009	0.025	0.014	0.003	0.008	0.104	0.012	0.004	0.291	0.000
F18.R3ex	0.044	0.065	0.491	0.082	0.216	0.002	0.004	0.001	0.003	0.020	0.001	0.041	0.002	0.026	0.000
F18.S1ex	0.139	0.166	0.124	0.196	0.132	0.156	0.021	0.014	0.015	0.004	0.010	0.006	0.007	0.000	0.000
F18.S2ex	0.077	0.279	0.071	0.107	0.097	0.091	0.035	0.143	0.004	0.012	0.005	0.018	0.002	0.001	0.046
F18.S3ex	0.150	0.162	0.142	0.166	0.114	0.039	0.055	0.046	0.019	0.030	0.028	0.007	0.005	0.014	0.005
F18.U1ex	0.304	0.134	0.200	0.110	0.099	0.024	0.020	0.015	0.053	0.015	0.014	0.003	0.002	0.001	0.001
F18.U2ex	0.303	0.152	0.125	0.142	0.050	0.089	0.032	0.014	0.051	0.008	0.012	0.005	0.002	0.001	0.007
F18.U3ex	0.304	0.191	0.185	0.093	0.060	0.048	0.035	0.017	0.012	0.043	0.002	0.005	0.001	0.001	0.000